16 State House Station
Augusta, Maine 04333

MaineDOT

Transportation Research Division

Technical Report 14-01, Phase 2

Development and Evaluation of Pile "High Strain Dynamic Test Database" to Improve Driven Capacity Estimates

Phase 2 Report *January 2014*

Technical Report Documentation Page

1. Report No. ME 14-01 Phase 2	2.	3. Recipient's Accession No.	
4. Title and Subtitle Development and Evaluation of Pile "High Strain Dynamic Test Database" to Improve Driven Capacity Estimates: Phase II Report		5. Report Date January 2014	
		6.	
7. Author(s) Thomas Sandford, PhD, P.E. and Cameron Stuart, EIT		8. Performing Organization Report No.	
9. Performing Organization Name and Address University of Maine, Orono, ME 04469		10. Project/Task/Work Unit No.	
		11. Contract © or Grant (G) No.	
12. Sponsoring Organization Name and Address Maine Department of Transportation		13. Type of Report and Period Covered	
		14. Sponsoring Agency Code	
15. Supplementary Notes			
16. Abstract (Limit 200 words) The Maine Department of Transportation (MaineDOT) has noted poor correlation between predicted pile resistances calculated using commonly accepted design methods and measured pile resistance from dynamic pile load tests (also referred to as high strain dynamic tests) conducted in accordance with ASTM D-4945. The MaineDOT requested that the University of Maine examine and evaluate their current static pile capacity design methodologies using the results from dynamic load tests on piles as a standard. The authors have used the term capacity in this report since the reports for the dynamic load test database used capacity, and most references used capacity. Capacity can be used interchangeably with the term 'resistance' used by AASHTO in LRFD applications. The intent of the final product is to provide MaineDOT with calculation methods that provided the most reliable capacity estimates. More reliable calculation methods will result in more cost efficient designs. The work which went into this report was essentially divided into two phases: the creation of a database which encompassed selected, available project data and comparison of static capacity analysis methods to investigate which combination is most reliable. The second of the two phases is detailed in this report.			
17. Document Analysis/Descriptors		18. Availability Statement	
19. Security Class (this report)	20. Security Class (this page)	21. No. of Pages 136	22. Price

Development and Evaluation of Pile "High Strain Dynamic Test Database" to Improve Driven Pile Capacity Estimates: Phase II Report

Prepared for

Dale Peabody, P.E.

Maine Department of Transportation

16 State House Station

Augusta, ME 04333

Prepared by

Thomas Sandford, PhD, P.E. and Cameron Stuart, EIT

Department of Civil and Environmental Engineering

University of Maine

Orono, ME 04469

10/15/2013

TABLE OF CONTENTS

LIST OF TABLES

LIST OF FIGURES

Chapter 1:

INTRODUCTION

The Maine Department of Transportation (MaineDOT) has noted poor correlation between predicted pile resistances calculated using commonly accepted design methods and measured pile resistance from dynamic pile load tests (also referred to as high strain dynamic tests) conducted in accordance with ASTM D-4945. The MaineDOT requested that the University of Maine examine and evaluate their current static pile capacity design methodologies using the results from dynamic load tests on piles as a standard. The authors have used the term capacity in this report since the reports for the dynamic load test database used capacity, and most references used capacity. Capacity can be used interchangeably with the term 'resistance' used by AASHTO in LRFD applications. The intent of the final product is to provide MaineDOT with calculation methods that provided the most reliable capacity estimates. More reliable calculation methods will result in more cost efficient designs. The work which went into this report was essentially divided into two phases: the creation of a database which encompassed selected, available project data and comparison of static capacity analysis methods to investigate which combination is most reliable. The second of the two phases is detailed in this report.

In Chapter 3 the static pile capacity predictive methods are presented and the methods for obtaining the input parameters are described. The static capacity methods used for analyzing the cohesive soil layers were the α-method and β-method. The Meyerhof Standard Penetration Test (SPT), Meyerhof and Nordlund methods were used to analyze granular soil layers for both side capacities and end bearing in glacial till (till).

However, the majority of piles were bearing on rock so the Canadian Geotechnical Society method (CGS) and the proposed Intact Rock method (IRM) were also investigated.

Chapter 4 presents the dynamic test data provided by the MaineDOT. The methods by which the data is obtained were explained, and a summary of the types of piles and soil layers encounters in all the tests. All pile capacities by dynamic field measurements per ASTM D-4945 were obtained from analysis of the output by the Case Pile Wave Equation Analysis Program (CAPWAP®) from GRL Engineering, Inc. CAPWAP® test capacities were analyzed for trends with depth, soil and pile types. These measurements typically conducted only at the end of driving (EOD) with some project requiring analysis at a later time at the beginning of restrike (BOR) and/or at the end of redriving (EORD). When EOD and BOR data were both provided for a pile, they were analyzed for time dependant capacity changes in both side and end bearing capacities.

To compare the measured CAPWAP® capacities at EOD and BOR setup factors were required to compare to the ultimate capacities calculated from the static analysis methods. The process for obtaining these factors is described in Chapter 5. These factors were calculated with the Skov and Denver (1988) analysis and both the MaineDOT provided data and the Fore River Bridge Project data (FHWA 1990). This chapter also describes the derivation of parameters for use in the Skov and Denver (1988) relationship as well as the justification for using them in design.

Chapter 6 compares the measured CAPWAP® capacities factored to the ultimate state with the capacities calculated from the static analysis equations. These comparisons

were conducted for each combination of side capacity methods as well as each of the end bearing methods. The comparisons were then analyzed for outliers to see if there was cause for removal. The final comparisons of the methods were conducted using the data with the justified outliers removed. This chapter also discusses the cause of the scatter in the data.

The final two chapters of this report summarize the research and provide the recommended predictions respectively. The recommendations include the best predictive methods for side capacity, end bearing on rock and end bearing in till. Additionally, recommendations for obtaining soil strength parameters and dynamic pile measurements are presented in Chapter 8.

Chapter 2:

OVERVIEW OF PILE LOAD TESTING

2.1. Static Load Testing

Static test piles are commonly loaded to twice the design load or failure. Loading is commonly applied with a jack against a supported weight or against a cross beam attached to anchor piles. The pile is then unloaded incrementally. The increment of loading and monitoring time and procedure depend upon the type of load test. Hannigan et al (2006b) recommends the quick load test method of ASTM D1143, "Standard Test Method for Piles Under Static Axial Load." AASHTO (2002) recommends that the design capacity be evaluated by the Davisson criteria (Davisson 1972). This criterion defines the pile failure to occur at the intersection of the pile top displacement and a line offset to the elastic deformation portion of the pile loading. This line is described by the following equation (Bradshaw and Baxter 2006):

$$d_T = \frac{QL}{EA} + (0.15 + 0.008D) \qquad [2.1]$$

Where:

d_T = displacement of the top of the pile (inches)

Q = applied test load (lbs)

E = modulus of elasticity of the pile (psi)

A = cross sectional area of the pile (in^2)

L = length of the pile (inches)

D = diameter of the pile (inches)

The high cost of testing is the main deterrent to static load testing. It also does not provide information on the quality of the installation or driving efficiency (Bradshaw and Baxter 2006).

2.2. Dynamic Load Testing

High strain dynamic load testing as specified in ASTM D-4945 is a more cost effective option to static load testing, and it does verify proper installation. The test can be administered at any point during the installation, so the pile can be tested if there is suspected damage or misalignment during driving. The test is also helpful in deciding if the appropriate hammer is being used for the driving, and if the fuel setting and hammer stroke are appropriate. The high strain dynamic load tests in this study use the Pile Driving Analyzer (PDA®) from Pile Dynamics, Inc. (PDI) to collect data during striking, and the data is refined using a computer program, such as the CAPWAP® of Pile Dynamics, Inc (PDI), to estimate in situ capacities. The CAPWAP® software conducts a post-driving numerical evaluation of the raw field data obtained from the dynamic pile test. High strain dynamic test methods as available with PDI's PDA® equipment were used in all the tests covered by this report, so PDA® tests will be referenced.

2.3. Limitations of CAPWAP® Analyses

The study by Lai and Kou (1994) investigated the reliability of using PDA® and CAPWAP® predictions to validate in situ pile capacities. They concluded that the CAPWAP® predicted capacities are more reliable than the PDA® predictions alone because the CAPWAP® analysis refines the Smith damping factor used in the predictions. However, when the CAPWAP® predictions were compared to a static capacity analysis using Davisson failure criteria, it was observed that the CAPWAP® analysis could over

predicted the static capacity by up to a factor of 1.15. Additionally, it was observed that CAPWAP® analysis compared to static testing could under predict by a factor down to 0.4 from hammer limitations or from soil disturbance.

Long et al (1999) investigated the effectiveness of dynamic measurements at predicting the measured static capacity determined using the Davisson criteria. The paper compared the Engineering News, Gates, WEAP, Measured Energy, PDA®, and CAPWAP® methods by calculating the wasted capacity index (WCI) for each method. The WCI is an indication of the uncertainty associated with each method, and it essentially compares the amount of addition capacity required to ensure that the pile meets a certain level of certainty. A lower WCI is an indication of a better prediction. The comparison in this paper was for a 99% reliability of prediction, and the WCI values reflect this reliability. The results of this study showed that when using the CAPWAP® analysis at the end of driving (EOD) (WCI = 4.4) it performed the second worst to the Engineering News method (WCI=5.7). The best method at EOD was the Gates formula (WCI = 2.1). However, the same comparisons at the beginning of restrike (BOR) indicated that the CAPWAP® method had a reduction in WCI by a factor 2.4. This indicated that the CAPWAP® analysis with BOR data had the most reliable predictions (WCI = 1.8); however, the time at which the BOR tests were conducted was not reported.

Chapter 3:

METHODS

In order to estimate the capacities of the piles included in the database the properties and strength parameters of the soil must first be determined. The Nordlund method is recommended by the Federal Highway Administration (Hannigan et al, 2006a) for calculating the capacities of piles driven through granular soils. However, this method does not provide a limiting value for side capacity and can provide erratic estimates for piles driven to great depths or through very dense soils.

The FHWA lists both the α-method and the β-method as acceptable methods for determining the ultimate skin friction of piles driven through cohesive materials. However, most of the piles included in this study were only tested at end of driving (EOD) with testing at the beginning of restrike (BOR) for some, so most measured capacities will be for the cohesive soils in a remolded state. The strength gain with time (setup) will be applied to measured capacities for comparison to both the undrained α-method calculation and the drained β-method calculation.

The method currently used by MaineDOT designers for determining the end capacity in bedrock was developed by the Canadian Geotechnical Society (CGS) in 1985. This method requires information about the rock quality and the fracture planes contained within to make an estimate of the end bearing capacity. Typical rock sampling for the bridge projects does not go further than providing basic information collected from boring logs. They do not include much (if any) information about the fractures. This causes the engineer to have to estimate the parameters, which results in inaccurate estimates of the end capacity. More extensive sampling of the bedrock would be needed

for the design equations to perform properly. The following sections detail the methods used to determine these parameters for granular and cohesive soils, till and bedrock.

3.1. Obtaining Strength Parameters for Granular Soils

The boring logs provided in the geotechnical report for each project provided standard penetration test (SPT) numbers as the strength parameter for granular soils. These values were averaged over the designated layers to obtain a representative strength value. The SPT numbers were corrected for field conditions and effective overburden pressure using Equation 3.1 (Das 2010).

$$(N1)_{60} = \frac{N\eta_H\eta_B\eta_S\eta_R}{60} \times C_N \quad [3.1]$$

Where:

N = standard penetration test (SPT) number in field

η_H = hammer efficiency (%)

η_B = correction for borehole diameter

η_S = sampler correction

η_R = rod length correction

C_N = correction factor

The correction factor (C_N) was calculated using the relationship proposed by Liao and Whitman (1986). This relationship is shown in Equation 3.2.

$$C_N = \left[\frac{1}{\sigma'_v / p_a}\right]^{0.5} \quad [3.2]$$

Where:

σ'_v = vertical effective stress (psf)

p_a = atmospheric pressure (2000 psf)

The relative density (D_r) and Unified Soil Classification System description of the soil were used to aid in estimating the effective friction angle, dry density, and void ratio of the soil. The Naval Facilities Engineering Command (1986) published a design chart for determining these parameters and is shown in Figure 3-1.

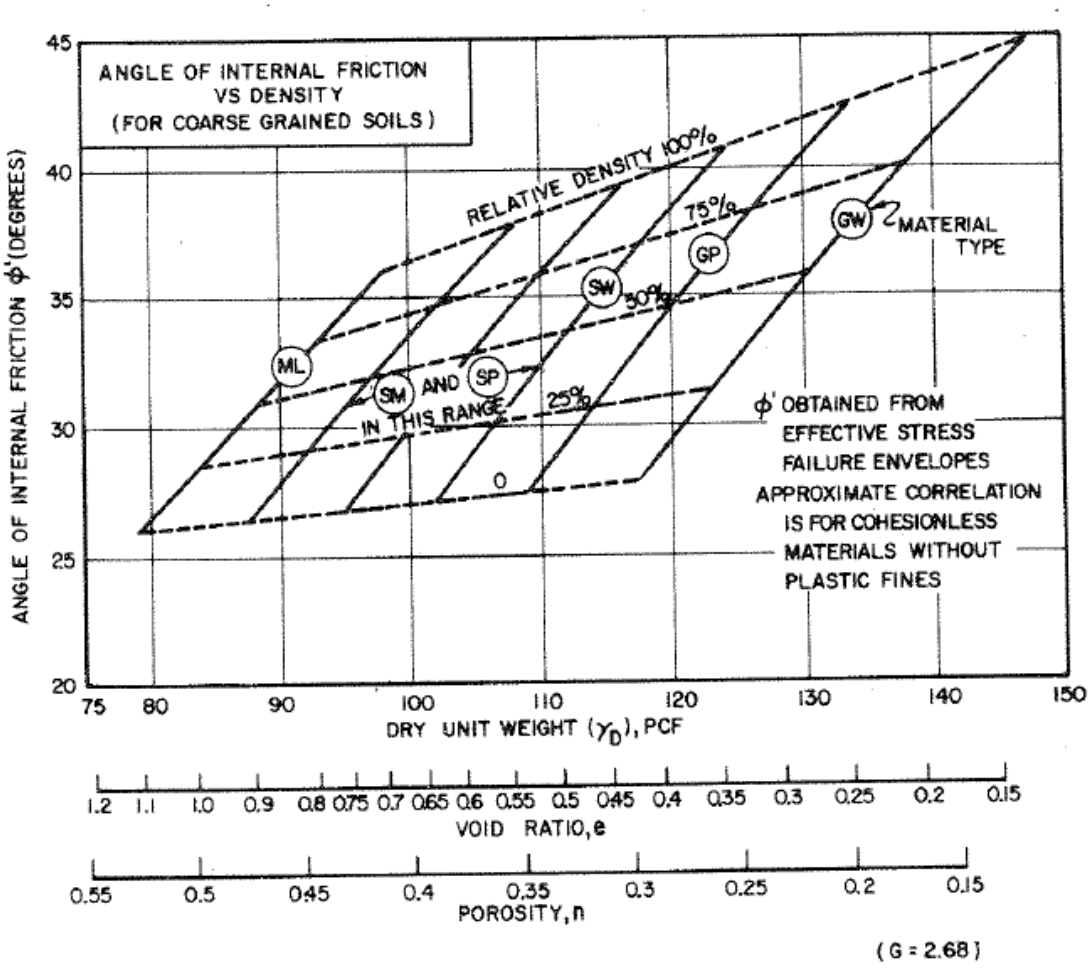

Figure 3-1: Granular Soil Strength Parameters (from NavFAC 1986)

The relative density (Dr) of the soil for use in Figure 3-1 was correlated from the field corrected SPT (N_{60}) using the relationship proposed by Meyerhof (1957). This relationship is shown below.

$$D_R = \left[\frac{N_{60}}{17 + 24\left(\frac{\sigma'_v}{p_a}\right)}\right]^{0.5} \quad [3.3]$$

Where:

N_{60} = field corrected standard penetration test (SPT) number

The total unit weight (γ_T) and water content of the soil were not always specifically quantified in the project documents. In the cases where water content was not available a representative value was obtained from the following relationship.

$$w = \frac{Se}{G_s} \quad [3.4]$$

Where:

S = degree of saturation

e = void ratio

G_s= specific gravity of the solids

In this calculation due to a lack of information the degree of saturation was assumed to be 1.0 (saturated) and the specific gravity of the soil solids was assumed to be 2.68 to stay consistent with the assumptions in Figure 3-1 (NavFAC 1986). The void ratio was obtained from Figure 3-1. After determining the water content of the soil, the total unit weight (γ_T) of the layer could be determined from the following equation.

$$\gamma_T = \gamma_D[1 + w] \quad [3.5]$$

Where:

γ_D = dry unit weight

The dry unit weight of the soil is determined from the correlation presented in Figure 3-1.

3.2. Obtaining Strength Parameters for Cohesive Soils

The unit weights (γT) of the cohesive layers were determined based on the average in situ water content for the soil layer. The following relationships from Holtz and Kovacs (1981) were used to determine an appropriate value.

$$e = \frac{w \times G_s}{S} \quad [3.6]$$

Where:

w = water content

G_s = specific gravity of solids

S = saturation percentage

$$\gamma_T = G_s \gamma_w \frac{1 + w}{1 + e} \quad [3.7]$$

Where:

G_s = specific gravity of solids

γ_w = unit weight of water

w = water content

e = void ratio

To obtain the total unit weight of the cohesive soil, the void ratio of the layer needed to be determined. Equation 3.6 was used to determine the void ratio (e) by

assuming the specific gravity of solids was 2.75 and the saturation percentage (S) was 100%. Equation 3.7 was then used to evaluate the total soil density. The unit weights determined from this procedure were used in calculations of skin friction of clay layers using the β-method.

The undrained shear strengths of the soils for both the undisturbed and remolded soil states were obtained from the geotechnical reports and boring logs where applicable. The values used in calculations were taken as the average strength for the layer. However, the undrained shear strengths were not always available from the project documents. In the cases when the measured undrained shear strengths were not available representative values were estimated through correlations with the field corrected STP number (N_{60}). These correlations were provided by Terzaghi, Peck, and Mesri (1996) and are shown in Table 3-1. The undrained shear strength used in calculations was linearly interpolated from the ranges provided in the table. The strength valuations in parentheses are those used by MaineDOT and are 4.4% more conservative than those used in the calculations.

Table 3-1: Correlations of N_{60} to Undrained Shear Strength (Terzaghi et al,1996)

Soil Description	Very Soft	Soft	Medium	Stiff	Very Stiff	Hard
N_{60}	<2	2-4	5-8	9-15	16-30	>30
S_u (psf)	<261 (<250)	261-522 (250-500)	522-1044 (500-1000)	1044-2089 (1000-2000)	2089-4177 (2000-4000)	>4177 (>4000)

3.3. Determination of Side Capacities

The side capacity of each pile was determined by calculating the shear resistance along the pile in each of the subsurface soil layers as defined in the preceding database. The side capacity is then taken as the sum of the resistances in each soil layer. The following sections will describe the methods for calculating the capacities in granular and cohesive soils. In granular soils The Nordlund method (Hannigan et al 2006), Meyerhof's Standard Penetration Test (SPT) method (Hannigan et al 2006), and Meyerhof's method (Meyerhof 1976) were considered. In cohesive soils the α-method (Hannigan et al 2006) and β-method (Hannigan et al 2006) were considered.

3.3.1. Nordlund Method for Granular Soils

The Nordlund method (Nordlund 1963) is useful for cohesionless soils of sand size or smaller. The first step in this method is to determine the friction angle of the soil against the pile (δ) for the layer being analyzed. Nordlund provided ratios of soil-pile friction angle to soil friction angle (ϕ) as shown in Figure 3-2.

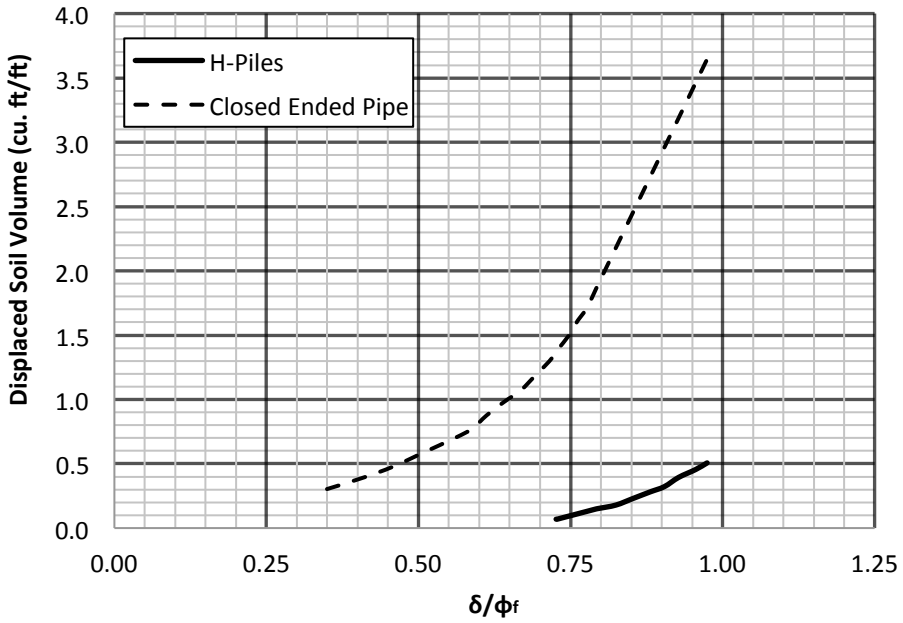

Figure 3-2: Friction Angle at Soil Pile Interface (after AASHTO 2010)

This ratio is obtained by entering the figure with the volume of displaced soil and in situ friction angle and finding the curve related to the correct pile type. The volume of displaced soil is quantified by cubic feet of soil displaced per linear foot of driving. This is effectively the cross-sectional area of the pile. Nordlund provided curves for H-piles and closed end pipe piles, but did not provide one for open end pipe piles. To cope with this issue, it was assumed that there would be some plugging to some extent within the pile that would provide a closed end condition and the closed end curve could be used. After the ratio is pulled from the figure, it is multiplied by the in situ soil friction angle to obtain the soil-pile friction angle.

Table 3-2 presents the design values for the lateral earth pressure coefficient (K_δ) for use in Equation 3.8. The values are determined from the amount of soil displaced by

the pile and the friction angle of the soil. Hannigan et al (2006) recommends that a linear interpolation be used to find values that fall between the rows of the table, and log linear interpolation is used to obtain values that fall between the columns. The values displayed in the table are for piles with no taper, such as the piles included as a part of this database. The volume of soil displaced by the pile can then be used along with the failure angle of the soil and the pile type to find the soil-pile friction angle.

If it is determined that the soil-pile friction angle differs from the failure angle in the soil, a correction factor (CF) needs to be factored into the capacity calculation. The factor is used to correct the K_δ value, and can be obtained from Figure 3-3.

Table 3-2: K_δ Coefficient for $\omega = 0$ and V=0.1 ft^3/ft to 1.0 ft^3/ft (Hannigan et al 2006)

ϕ	Displaced Volume -V, m^3/m, (ft^3/ft)									
	0.0093 (0.10)	0.0186 (0.20)	0.0279 (0.30)	0.0372 (0.40)	0.0465 (0.50)	0.0558 (0.60)	0.0651 (0.70)	0.0744 (0.80)	0.0837 (0.90)	0.0930 (1.00)
25	0.70	0.75	0.77	0.79	0.80	0.82	0.83	0.84	0.84	0.85
26	0.73	0.78	0.82	0.84	0.86	0.87	0.88	0.89	0.90	0.91
27	0.76	0.82	0.86	0.89	0.91	0.92	0.94	0.95	0.96	0.97
28	0.79	0.86	0.90	0.93	0.96	0.98	0.99	1.01	1.02	1.03
29	0.82	0.90	0.95	0.98	1.01	1.03	1.05	1.06	1.08	1.09
30	0.85	0.94	0.99	1.03	1.06	1.08	1.10	1.12	1.14	1.15
31	0.91	1.02	1.08	1.13	1.16	1.19	1.21	1.24	1.25	1.27
32	0.97	1.10	1.17	1.22	1.26	1.30	1.32	1.35	1.37	1.39
33	1.03	1.17	1.26	1.32	1.37	1.40	1.44	1.46	1.49	1.51
34	1.09	1.25	1.35	1.42	1.47	1.51	1.55	1.58	1.61	1.63
35	1.15	1.33	1.44	1.51	1.57	1.62	1.66	1.69	1.72	1.75
36	1.26	1.48	1.61	1.71	1.78	1.84	1.89	1.93	1.97	2.00
37	1.37	1.63	1.79	1.90	1.99	2.05	2.11	2.16	2.21	2.25
38	1.48	1.79	1.97	2.09	2.19	2.27	2.34	2.40	2.45	2.50
39	1.59	1.94	2.14	2.29	2.40	2.49	2.57	2.64	2.70	2.75
40	1.70	2.09	2.32	2.48	2.61	2.71	2.80	2.87	2.94	3.0

Table 3-3: K_δ Coefficient for $\omega = 0$ and V=1.0 ft3/ft to 10.0 ft3/ft (Hannigan et al 2006)

ϕ	Displaced Volume -V, m^3/m (ft^3/ft)									
	0.093 (1.0)	0.186 (2.0)	0.279 (3.0)	0.372 (4.0)	0.465 (5.0)	0.558 (6.0)	0.651 (7.0)	0.744 (8.0)	0.837 (9.0)	0.930 (10.0)
25	0.85	0.90	0.92	0.94	0.95	0.97	0.98	0.99	0.99	1.00
26	0.91	0.96	1.00	1.02	1.04	1.05	1.06	1.07	1.08	1.09
27	0.97	1.03	1.07	1.10	1.12	1.13	1.15	1.16	1.17	1.18
28	1.03	1.10	1.14	1.17	1.20	1.22	1.23	1.25	1.26	1.27
29	1.09	1.17	1.22	1.25	1.28	1.30	1.32	1.33	1.35	1.36
30	1.15	1.24	1.29	1.33	1.36	1.38	1.40	1.42	1.44	1.45
31	1.27	1.38	1.44	1.49	1.52	1.55	1.57	1.60	1.61	1.63
32	1.39	1.52	1.59	1.64	1.68	1.72	1.74	1.77	1.79	1.81
33	1.51	1.65	1.74	1.80	1.85	1.88	1.92	1.94	1.97	1.99
34	1.63	1.79	1.89	1.96	2.01	2.05	2.09	2.12	2.15	2.17
35	1.75	1.93	2.04	2.11	2.17	2.22	2.26	2.29	2.32	2.35
36	2.00	2.22	2.35	2.45	2.52	2.58	2.63	2.67	2.71	2.74
37	2.25	2.51	2.67	2.78	2.87	2.93	2.99	3.04	3.09	3.13
38	2.50	2.81	2.99	3.11	3.21	3.29	3.36	3.42	3.47	3.52
39	2.75	3.10	3.30	3.45	3.56	3.65	3.73	3.80	3.86	3.91
40	3.00	3.39	3.62	3.78	3.91	4.01	4.10	4.17	4.24	4.30

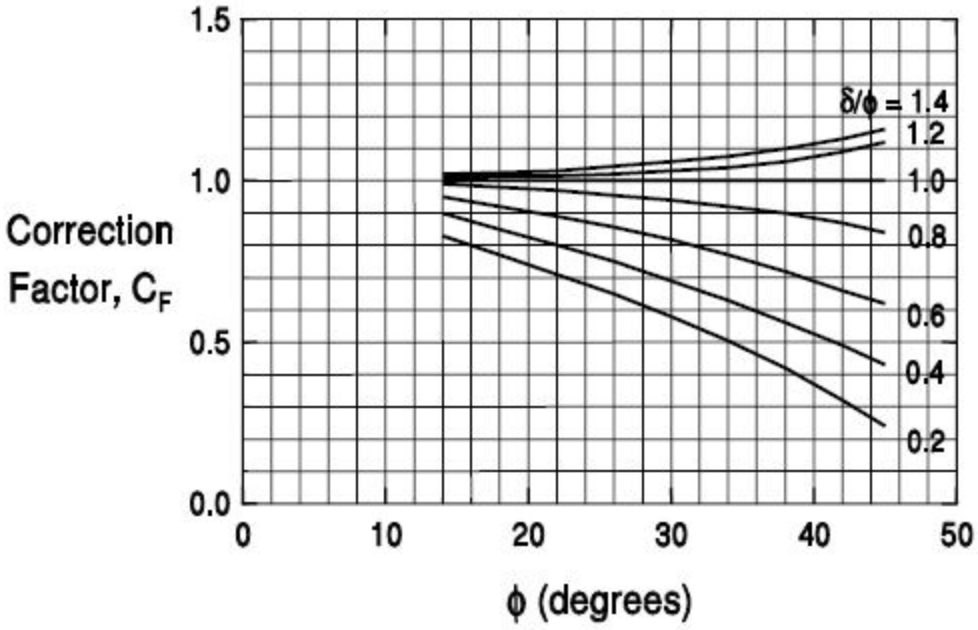

Figure 3-3: Correction Factor for Lateral Earth Pressure Factor (Hannigan et al 2006)

Once all of the parameters have been determined, the side capacity can be estimated using the equation provided below:

$$q_s = K_\delta C_F \sigma'_v \frac{\sin(\delta + \omega)}{\cos \omega} \quad [3.8]$$

Where:

σ'_v = vertical effective stress (ksf)

ω = pile taper (equal to 0 for all piles in this study)

Equation 3.8 calculates the unit skin resistance of the pile in a granular soil layer. To obtain the total capacity of the pile, the unit resistance must be multiplied by the surface area of the pile. The surface area is calculated as the product of the pile perimeter and the embedded length of the pile in the layer. For H-piles a box perimeter was

assumed. For displacement needed in Figure 3-2, Table 3-2, and Table 3-3, the steel cross-sectional area is used. The Nordlund method does not use a limiting shear stress after a given depth.

Nordlund's method creates some problems without a limiting value for overburden stress with depth. In a report published by the FHWA (1990), static pile capacity estimates were compared to the results of static and dynamic load testing in Portland, Maine. The study was conducted on the Fore River Bridge replacement which connects Portland to South Portland. The subsurface profile on the project is shown in Figure 3-4. It shows that there is a significant amount of granular material on the site with significant amounts of till encountered in Boring B17 & B23.

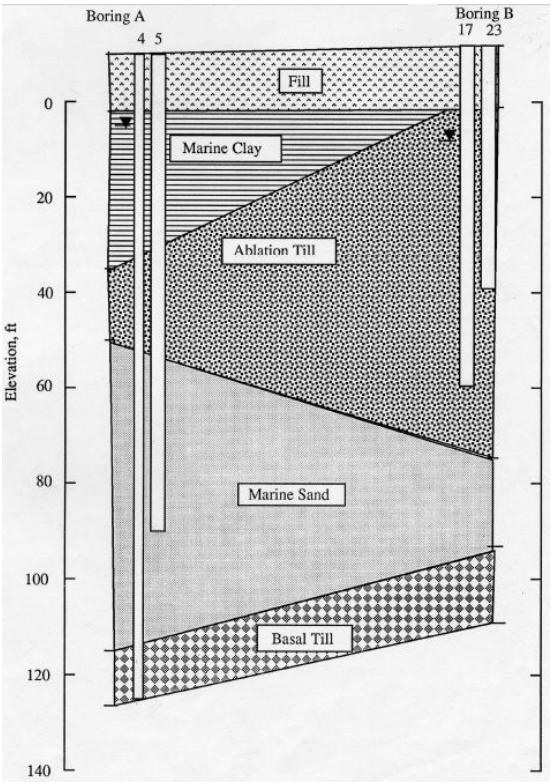

Figure 3-4: Soils at Fore River Bridge (FHWA 1990)

After the piles were installed, some piles were tested dynamically at EOD and BOR and 4 piles were tested with a static load test. The results of the testing as well as the Nordlund predicted capacity are shown in Table 3-4. The limitations of Nordlund's method are easily visible upon analysis of the test results. It proves to be under-conservative for all piles except for the HP 14x117 piles. In some cases it over predicted the measured pile capacities by over 300 tons.

Table 3-4: Predicted to Measured Pile Capacities at Fore River Bridge (FHWA 1990)

		Nordlund	CAPWAP®			Static Load Test
Pile	Length (ft)	(kips)	EOD (kips)	BOR (kips)	Restrike Time (days)	(kips)
18" C.E.P	79.1	610	336	414	1	N/A
18" C.E.P	99.9	858	346	500	2	440
18" C.E.P	71.3	1040	424	526	1	400
18" C.E.P	50.8	720	N/A	N/A	N/A	N/A
18" C.E.P	71.1	1040	416	436	3	N/A
18" C.E.P	50.8	720	322	340	6	350
HP 14x89	131.0	806	564	286	3	N/A
HP 14x89	114.7	806	N/A	238	N/A	N/A
HP 14x89	115.0	1476	278	328	5	N/A
HP 14x89	114.7	1476	296	306	5	N/A
HP 14x117	135.5	966	732	1104	8	900 (Did Not Fail)
HP 14x117	133.8	966	1010	770	1	N/A

3.3.2. Standard Penetration Test (SPT) Based Method for Granular Soils

In 1976 Meyerhof proposed a method for correlating the side capacity of pile in granular soils to the standard penetration test (SPT). Hannigan et al (2006) built off of his research and suggest that the side capacity of the pile is directly proportional to the

modified SPT readings, however, the equation changes slightly for high displacement and low displacement piles. The equation for both scenarios is detailed below:

$$q_s = C(N_1)_{60} \leq 2ksf \quad [3.9]$$

Where:

$(N_1)_{60}$ = average corrected SPT value for the layer for overburden pressure

C = constant, equals 1/25 for displacement piles, equals 1/50 for low displacement piles

To obtain the total capacity of the pile the unit resistance must be multiplied by the surface area of the pile. The surface area is calculated as the product of the pile perimeter and the embedded length of the pile in the layer. For H-piles a box perimeter was assumed.

3.3.3. Meyerhof Method for Granular Soils

Meyerhof proposed another method in 1976 that was based on soil strength parameters. This method related the unit shaft resistance to the horizontal effective stress (σ'_h) to the soil-pile friction angle (δ). NavFAC (1986) suggested δ value of 20° for steel piles was used in the calculation. The σ'_h is related to the vertical effective stress (σ'_v) by an effective earth pressure coefficient (K_h). The proposed equation is shown below in Equation 3.10.

$$q_s = K_h \sigma'_v \tan\delta \quad [3.10]$$

The K_h value was estimated based on recommendations by NavFAC (1986). They recommend that for a single driven steel H-pile a K_h value between 0.5-1.0 and for a single displacement pile K_h values between 1.0-1.5. It was desired to relate K_h to the coefficient of earth pressure at rest (K_o). The K_o value was determined from the relationships found by Kulhawy and Mayne (1990) shown in Figure 3-5.

The friction angles used in the figure were determined as described in Section 3.1. However, for the friction angles of till this method may lead to unrealistic values since there is a substantial amount of fines. To address this, a limiting value of 38° was used as measured by Linell and Shea (1960) for New England tills.

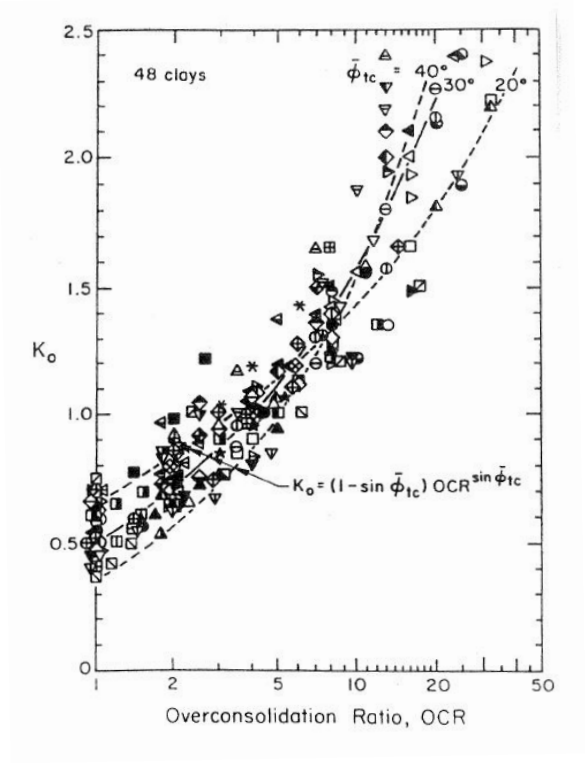

Figure 3-5: Relationship Between OCR and Ko (Kulhawy and Mayne 1990)

The benefit of using the Meyerhof method is that there is a limiting stress with depth that is applied to the calculation to prevent erratic values with depth. Sowers (1979)

using Vesic (1967) recommends that for D_r>70% the effective overburden stress should be calculated to be constant for a depth greater than 20 times the pile diameter and for D_r<30% the effective overburden stress should be calculated to be constant for a depth greater than 10 times the pile diameter. These depths are referred to as critical depths (L′), and were determined for homogenous sands. However, the soil layers are often not homogeneous along the length of the pile. In the cases where the soil layers above L′ did not have a homogeneous D_r, L′ was calculated as 15 times the pile diameter. To obtain the total capacity of the pile the unit resistance must be multiplied by the surface area of the pile. The surface area is calculated as the product of the pile perimeter and the embedded length of the pile in the layer. For H-piles a box perimeter was assumed.

3.3.4. Meyerhof Method Adjustments for Basal Till Layers

Basal till is extremely dense as it was deposited beneath continental glaciers with a thickness of more than a mile. Since the glaciers subsequently melted, the basal till deposits are highly consolidated with a corresponding high K value. Meyerhof's method was derived for sands as described previously, so some K correction factor is needed to account for basal till's overconsolidated state.

The passive earth pressure of the soil is the maximum pressure that can be exerted on to the soil. By calculating the passive pressure coefficient, the limiting value for horizontal earth pressure coefficient (K_h) will be known. This passive pressure coefficient is well under the K resulting from the removal of more than one mile depth of ice overburden. The passive pressure coefficient (K_p) was calculated using the method outlined by NavFAC 7.02 (1986). The design chart for this method is shown in Figure 3-6. The friction angle for till was taken to be 38° for the reasons described previously.

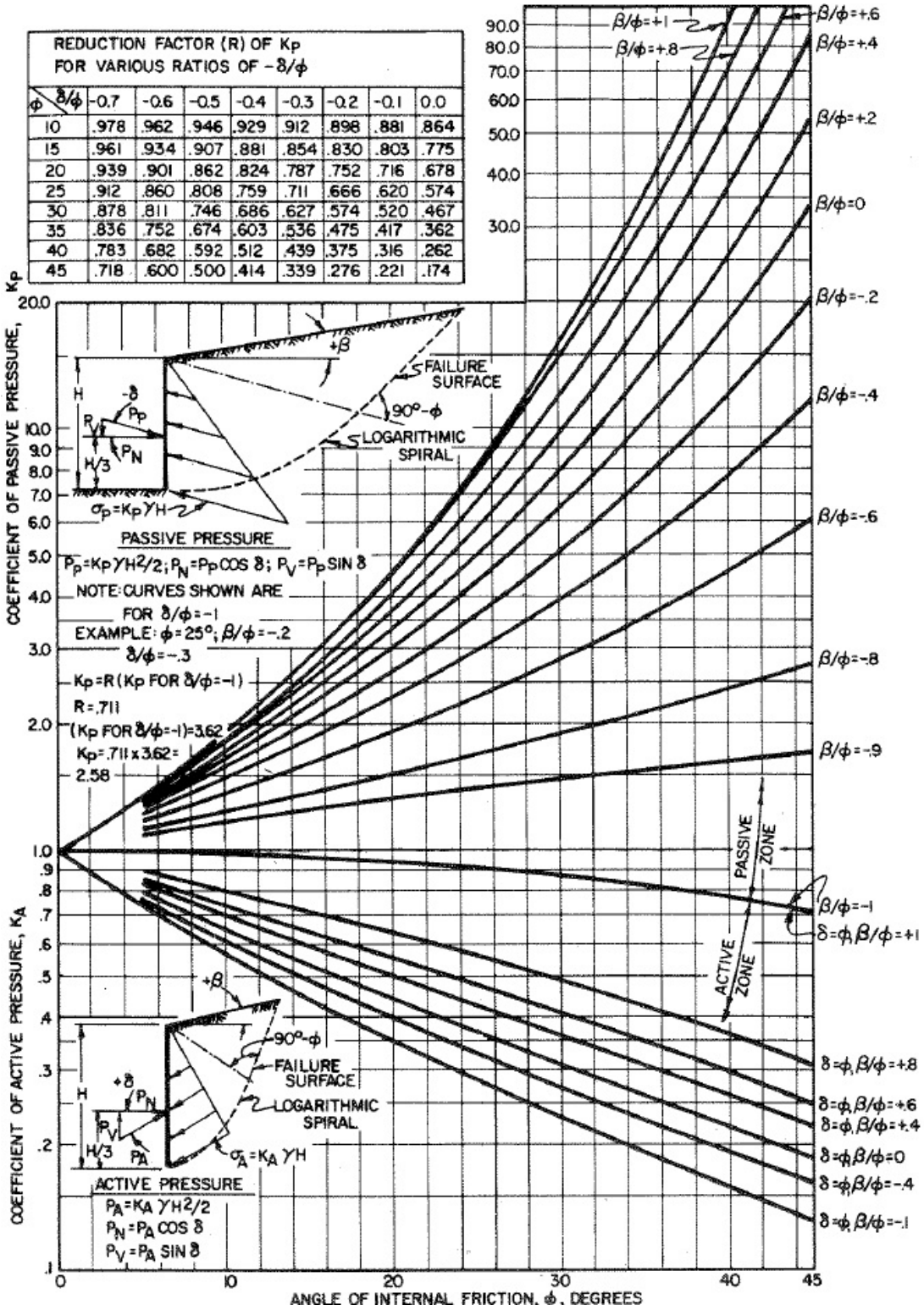

Figure 3-6: Passive Pressure Coefficient Determination (NavFAC 1986)

For a horizontal soil surface with β equal to 0°, the K_p is equal to 14.0. For planar failure with release of overburden ice pressure, it is equivalent to the friction angle between the soil and the wall (δ) being 0°. A reduction factor (R) of 0.302 is applied to K_p resulting in an adjusted K_p of 4.2. Alternatively, this describes the Rankine passive condition where:

$$K_p = \tan^2\left(45 + {}^{\phi}/_{2}\right) \qquad [3.11]$$

For a $\phi = 38°$, $K_p = 4.20$ by this equation.

Using a K=4.2 for a displacement pile in basal till, it would be anticipated that an H-Pile will have a lower K. The same ratio of K (0.75/1.25) is maintained in the basal till as in the normally consolidated granular material. This gives a working $K = 4.2 \times \frac{0.75}{1.25} = 2.52$ (call 2.5) for the H-pile.

3.3.5. α – Method for Cohesive Soils

The α-method (Tomlinson 1957) for pile support in cohesive soils uses the undrained strength of the clay to obtain capacity. This method presumes that an undrained failure is the critical shear for piles in cohesive material. The American Association of State Highway and Transportation Officials' (AASHTO) LRFD Bridge Design Specifications (2010) provides the α-method as one method for determining the side capacity of piles through various cohesive soil materials. In the α-method, the adhesion at the pile-soil interface is formed by applying a factor to the undrained shear strength. The side capacity is the summation of the adhesion over the perimeter area of the sides of the pile. The α-method is described below:

$$q_s = \alpha S_u \quad [3.12]$$

Where:

α = adhesion factor determined from design charts

S_u = undrained shear strength (ksf)

The design charts below provide the α adhesion factors to use for clays overlain by different soil types. The α factors are determined by entering the design charts with the undrained shear strength and depth of embedment into the layer to pile width ratio. The undrained shear strengths and remolded undrained shear strengths are determined through the methods described in Section 3.2. The ultimate resistance for the clay layer is calculated using the adhesion determined from the undisturbed undrained shear strength and the corresponding α factor. The adhesion resistance at EOD, which is representative of most the piles included in this study, is calculated using the remolded undrained shear strengths and the corresponding α factor. To obtain the total capacity of the pile the adhesion resistance must be multiplied by the surface area of the pile. The surface area is calculated as the product of the pile perimeter and the embedded length of the pile in the layer. For H-piles a box perimeter was assumed.

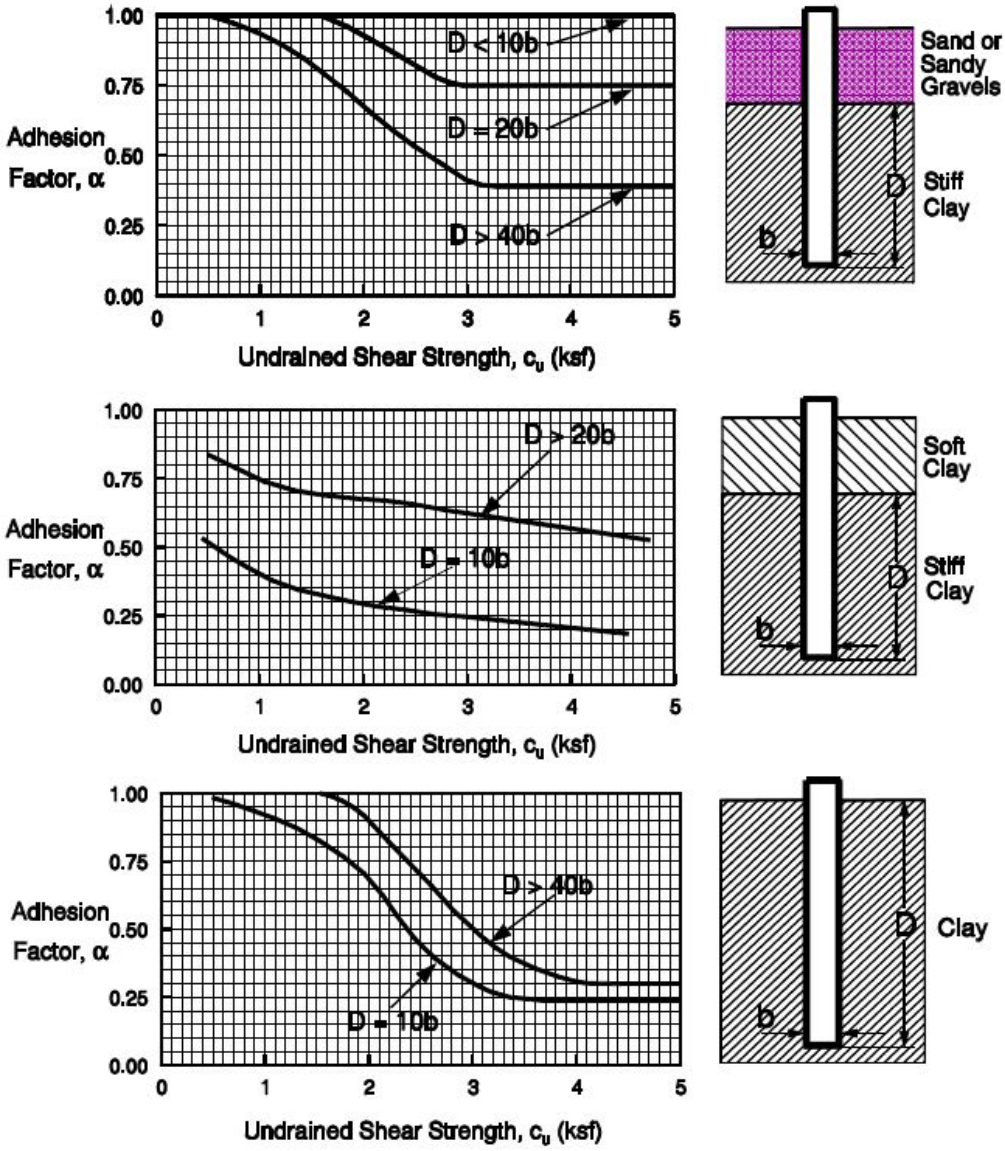

Figure 3-7: Adhesion Factors for The α – Method (Hannigan et al 2006)

3.3.6. β – Method For Cohesive Soils

The β-method is an effective stress method for cohesive soil. This method presumes that the critical failure will be a drained failure. This β-method for cohesive soils is similar to the Meyerhof method for granular soils. However, it combines the

$K_h \tan(\delta)$ term of the Meyerhof method into a single factor, β. This method estimates side capacity by finding the side shear with a directly proportionate relationship to vertical effective stress. The vertical effective stress is multiplied by a factor that represents the ratio of the soil's shear strength to vertical effective stress. The equation for the β-method is shown below (Hannigan et al 2006):

$$q_s = \beta \sigma'_v \quad [3.13]$$

Where:

β = a factor determined from Figure 3-8

σ'_v = vertical effective stress (ksf)

The FHWA recommended method for finding the β factor is shown in Figure 3-8. They have correlated the β factor to the effective drained friction angle and soil type. However, the drained friction angle for cohesive materials is rarely measured in practice. To circumvent this, a typical friction angle was assumed for the entire Presumpscot Formation. Sandford and Amos (1987) reported an effective friction angle of 35° for the Presumpscot Formation in a 1987 report on a landslide in Gorham, Maine. This value was used to obtain a β factor. The β method gives strengths after all pore pressures from driving have dissipated. To obtain the total capacity of the pile at EOD the unit resistance at EOD must be multiplied by the surface area of the pile. For the full capacity of the pile after dissipation, the strength with full setup is used. The surface area is calculated as the product of the pile perimeter and the embedded length of the pile in the layer. For H-piles a box perimeter was assumed.

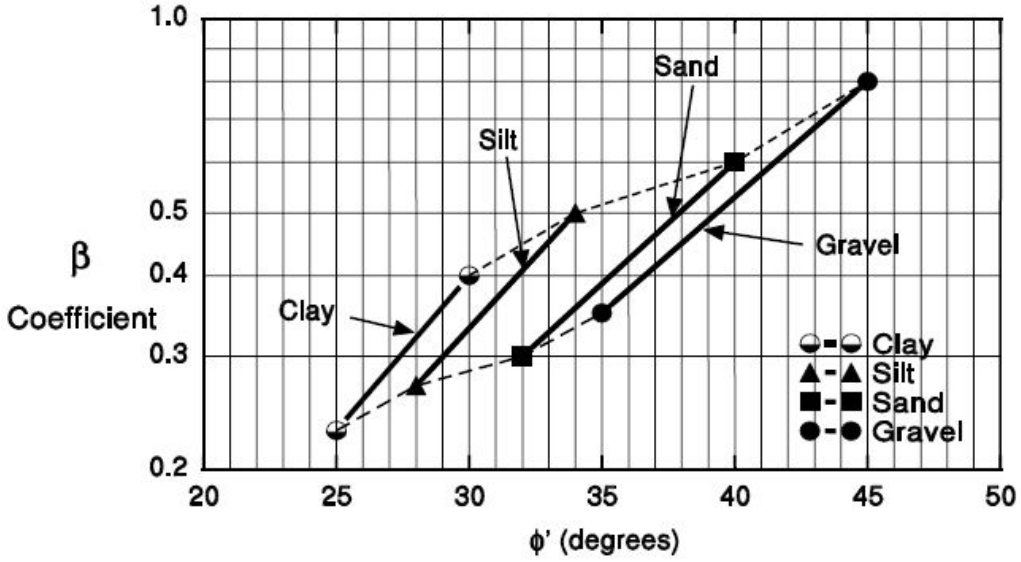

Figure 3-8: β Factor Determination (Hannigan et al 2006)

3.4. End Bearing on Bedrock

End bearing capacity in rock can be difficult to determine. These values are not necessary for all types of piles because some piles, especially concrete, will fail in compression before the bedrock. In most applications in Maine steel piles are used, so the end bearing on rock becomes relevant. Typical capacity values for different bedrock materials can be found in literature; however, it is intuitive that these values will not provide reliable values for every site. Bedrock can be weathered, highly fractured, or more poorly formed than anticipated from the literature. To get an idea of the type and quality of rock at a project site the borings should sample past refusal and collect some bedrock. There are two different methods that were studied to determine the bearing capacity of bedrock. However, first the cross sectional area of the piles must be adjusted for pile tip protectors which increase the bearing area of the pile on bedrock.

To find the pile tip area the dimensions of the protective driving shoe needed to be obtained. MaineDOT (Krusinski 2012) reported that the two typical H-pile driving tips used on bridge projects in the State are the APF HP 77600-B and the APF HP 77750-B. The dimensions on these pile tips were found on the R.W. Conklin Steel Supply website, and are shown in Appendix A. A request for information submitted to Associated Pile & Fitting (2012) provided tip protection dimensions for both conical (for closed end pipe piles) and cutting shoe (for open end pipe piles). The dimensioned drawings they provided can be found in Appendix A.

3.4.1. Canadian Geotechnical Society Method For End Bearing in Rock

In 1985 the Canadian Geotechnical Society (CGS) proposed a method in which bearing capacity is determined from measurements of the fractures in the bedrock. The method is described in the following equation (Turner 2006):

$$q_{ult} = 3q_u \frac{3 + \frac{s_v}{B}}{10\sqrt{1 + 300\frac{t_d}{s_v}}}\left(1 + 0.4\frac{L_s}{B}\right) \quad [3.14]$$

Where:

q_u = unconfined compressive strength of bedrock

s_v = vertical distance between fractures

t_d = thickness of fracture

B = diameter of boring in bedrock

L_s = depth of penetration into bedrock

The unconfined compressive strengths (q_u) were obtained from the geotechnical reports for each project. The MaineDOT rarely perform unconfined compression testing

on bridge projects and assume q_u from correlations provided in AASHTO *Standard Specifications for Highway Bridges* 17th ed. (2002). In the cases where q_u was unavailable from the reports a value was assumed based on the rock type and q_u for those rock types on similar projects. When the calculations for the CGS method were provided in the geotechnical design reports, they were used in this study. However, for projects that did not include the calculation a procedure was needed to evaluate the input parameters without the bedrock samples.

The piles installed on the bridge projects included in this study were rarely socketed into bedrock, so the depth of penetration into bedrock (L_s) was set equal to zero. Although there was no specified driving of the pile into bedrock, the equation would not function properly if B was set equal to zero. Therefore B was set to 1 foot (approximate width of the piles) for calculations. The thickness of fractures (t_d) in the bedrock and the vertical spacing between fractures (s_v) were interpreted from the bedrock descriptions in the boring logs. The boring logs provide bedrock core descriptions including rock type, dip, spacing, tightness and infilling of the discontinuities. MaineDOT (Krusinski 2012) indicated that from the rock samples examined, the s_v can range from inches to feet and the fractures range from 1/64-inch for tight joints/bedding to <1/4 for open/healed joints. To determine the total capacity, the value calculated in the CGS method must be multiplied by the cross sectional area of the pile on bedrock.

3.4.2. Proposed Intact Rock Method For End Bearing

The proposed Intact Rock Method (IRM) for end bearing is equivalent to the Rowe and Armitage (1987) equation (cited by Turner, 2006) that relates the ultimate

bearing capacity of intact rock to the compressive strength of the bedrock. The equation is presented below:

$$q_p = 2.5q_u \quad [3.15]$$

Where:

q_p = end bearing capacity of the bedrock

q_u = unconfined compressive strength of the bedrock

3.5. Tip Capacity for Piles Bearing in Till

There are a few piles included in the study that were designed to obtain support from soils without bearing on bedrock. There are also some piles that fetched up in the till or other overlying strata. There were not any piles that experienced end bearing in cohesive strata, so tip capacity in cohesive soils will not be considered in this report. The methods for determining end bearing on piles above bedrock are described in this section.

3.5.1. Nordlund Method

The Nordlund method (Nordlund 1963) comprised a bearing capacity relation from Berezantzes et al (1961) which did not have a limiting value. Since the Nordlund (1963) paper, the bearing capacity relation has been changed and a limiting value from Meyerhof (1976) has been added by Hannigan et al (2006a) based on Bowles (1977). Subsequent editions (Bowles 1982; Bowles 1988) do not use this method. The end bearing capacity of the soil now associated with the Nordlund method is detailed below (Hannigan et al, 2006a):

$$q_p = \alpha_t N'_q \sigma'_v \leq q_L \quad [3.16]$$

Where:

α_t = coefficient determined from Figure 3-9.

N'_q = bearing capacity factor determined from Figure 3-10.

σ'_v = vertical effective stress (ksf)

q_L = maximum end bearing (ksf) from Figure 3-11 (Meyerhof 1976).

To obtain the ultimate capacity, the calculated q_p is multiplied by the pile tip area which is the area of the protective driving tips and cutting shoes attached to the piles.

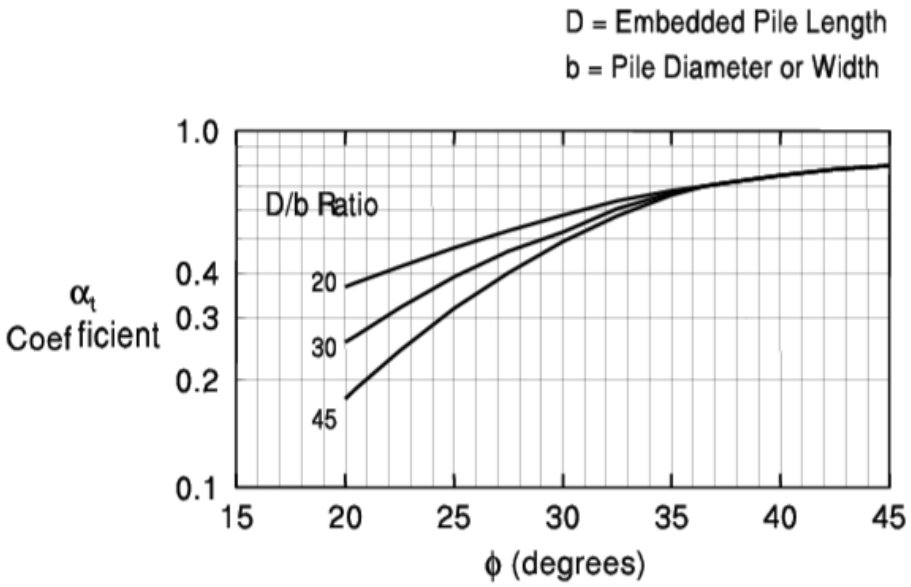

Figure 3-9: α_t Value for Use with Nordlund Method (Hannigan et al, 2006a)

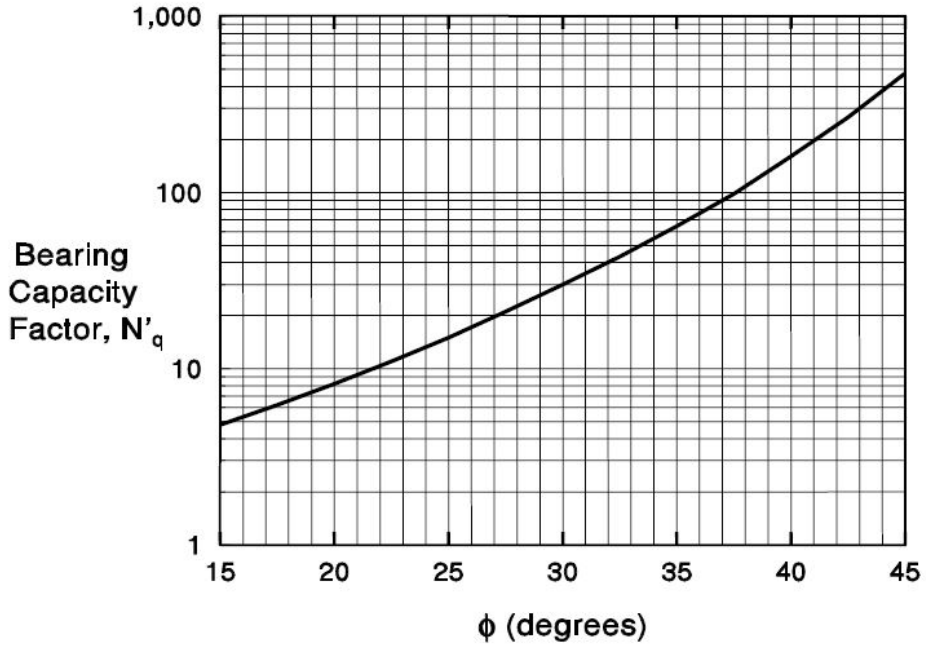

Figure 3-10: Bearing Capacity Factor for Use with Nordlund Method (Hannigan et al, 2006a)

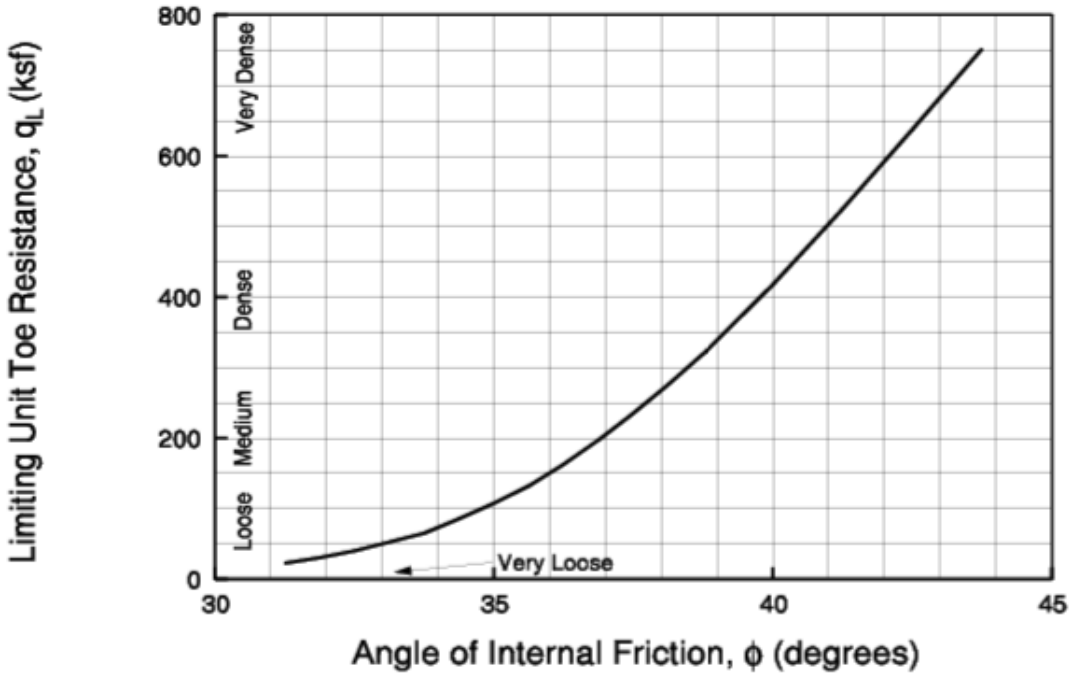

Figure 3-11: Ultimate Unit Base Capacity Based on Soil Friction Angle (Hannigan et al, 2006a)

3.5.2. Meyerhof Standard Penetration Test (SPT) Method

The Standard Penetration Test Method (SPT) method proposed by Meyerhof (1976) is another method for determining the bearing capacity of piles in cohesionless soils. It uses SPT and modified SPT values to determine the capacity values. The end bearing capacity is determined using the following equation:

$$q_p = \frac{0.8 \times (N_1)_{60} \times D}{d} \leq q_L \qquad [3.17]$$

Where:

$(N_1)_{60}$ = corrected SPT value of the bearing strata

D = driven depth of pile (feet)

d = pile diameter (feet)

q_L = maximum end bearing from design tables (ksf)

The maximum end bearing value (q_L) for this equation is eight times the modified SPT value ($8(N_1)_{60}$) for sands (AASHTO 2010). To obtain the ultimate capacity, the calculated q_p is multiplied by the pile tip area which is the area of the protective driving tips and cutting shoes attached to the piles.

3.5.3. Meyerhof Method

The Meyerhof method (1976) for determining point capacity uses a generalized formula that relates the pile capacity to the overburden pressure and self weight of the soil at the pile tip. This method is not specified in AASHTO (2010), but the limiting value for the Nordlund method in AASHTO (10) has been derived from the Meyerhof method. For piles with lengths beyond about 15 ft, the limiting value typically controls the capacity. In the full formula the cohesion at the tip is considered, however, none of

the pile tips were located in a cohesive bearing stratum. Ignoring the cohesive term, pile tip capacity is calculated as:

$$Q_p = A_p \sigma'_v N_q \leq A_p q_L \quad [3.18]$$

Where:

N_q = bearing capacity factors

σ_v' = overburden stress at pile tip (ksf)

A_p = cross sectional area of pile tip (ft^2)

q_l = limiting bearing stress (ksf) = $0.5 p_a N_q \tan\phi$

p_a = atmospheric pressure (2.0 ksf)

The bearing capacity factor (N_q) is taken from design charts from Meyerhof (1976). N_q' is determined using the friction angle of the soil in the bearing stratum, the length to width ratio of the pile, and the N_q' curve from Figure 3-12.

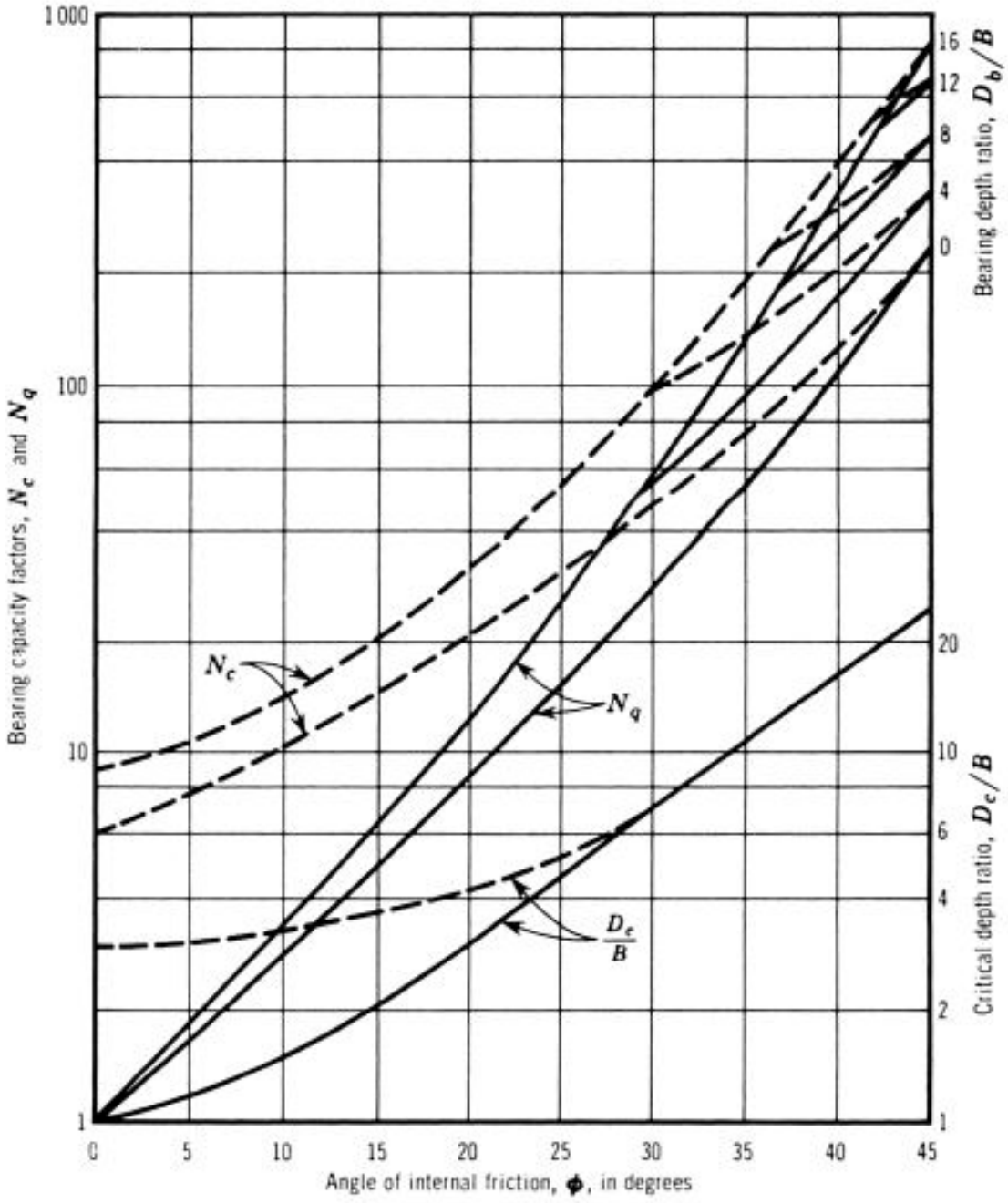

Figure 3-12: Determination of Nq' for Meyerhof's Tip Capacity Equation (Meyerhof 1976)

Chapter 4:

DESCRIPTION OF AVAILABLE DATA

4.1. Process of Test Data Collection

The MaineDOT uses the dynamic pile load test following the procedures in ASTM D-4945 to determine the in situ capacity for piles installed on bridge projects in the State. In this method, pile driving waves generated by the blow of a pile driving hammer are monitored in the field. These dynamic field measurements are entered to a pile-soil software model that yields an estimate of pile side and end capacity at the moment of the hammer blows. The Pile Dynamic Inc. (PDI) software, PDA® and CAPWAP® are routinely employed by pile testing subcontractors on MaineDOT projects.

Typically one pile from each group was selected as a representative of the group to test its capacity. The piles are normally tested at the end of driving (EOD). Sometimes piles are subjected to additional load testing at a later time to assess the time dependent change of pile capacity. Pile capacity information from dynamic testing was provided with the project documents and was used to gauge the effectiveness of the capacity estimates provided by design methods.

Pore pressures generated during pile driving affect the capacity measured at the EOD. Capacities in clay at the EOD can be significantly less than capacities measured after pore pressure dissipation, while capacities in granular soils are less affected with time. Thus CAPWAP® estimates of capacity at EOD generally underestimate the long term capacity.

4.2. Descriptions of Test Piles and Soil Profiles

4.2.1. General

The data provided by MaineDOT included the majority of the dynamic tests conducted from the fall of 1994 through the spring of 2012. During this period, there were 80 different bridge projects with 258 piles selected for dynamic capacity testing using a high strain dynamic testing per ASTM D4945 withCAPWAP® analyses on measured field data. Of these piles 90% were end bearing on bedrock while 10% were bearing in till strata. The data consisted predominantly of low displacement piles (H-piles and open end pipe piles) with only 11% of all tests being conducted on closed end pipe piles. A tabulation of the pile types tested is shown in Table 4-1. The side capacities versus penetration depth were analyzed to look for trends with pile type.

Table 4-1: Distribution of Pile Types Included in Project Data

Type of Pile	# of Piles
12" H-piles	24
14" H-piles	158
30" Pipe Open	2
26" Pipe Open	3
24" Pipe Open	23
22" Pipe Open	17
20" Pipe Open	1
30" Pipe Closed	2
26" Pipe Closed	1
24" Pipe Closed	19
20" Pipe Closed	8
Total # of piles	258

4.2.2. Total Capacities

The total capacity measured of each pile was plotted against penetration depth in Figure 4-1. This included both piles on bedrock and till and was organized by pile type. The piles had penetration depths ranging from 3 feet to 162 feet with an average penetration depth of 60 feet. The total capacities showed significant scatter with depth and no general trend with depth was observed. The closed end pipe piles, open end pipe piles, and H-piles had total capacities ranging from 490 kips to 1490 kips, 498 kips to 1810 kips, and 240 kips to 1379 kips respectively. H-piles with penetration depths greater than 117 feet showed a decrease in capacity with increasing depth. Additionally, some open end pipe piles had significantly larger capacities at shallower depths than other piles.

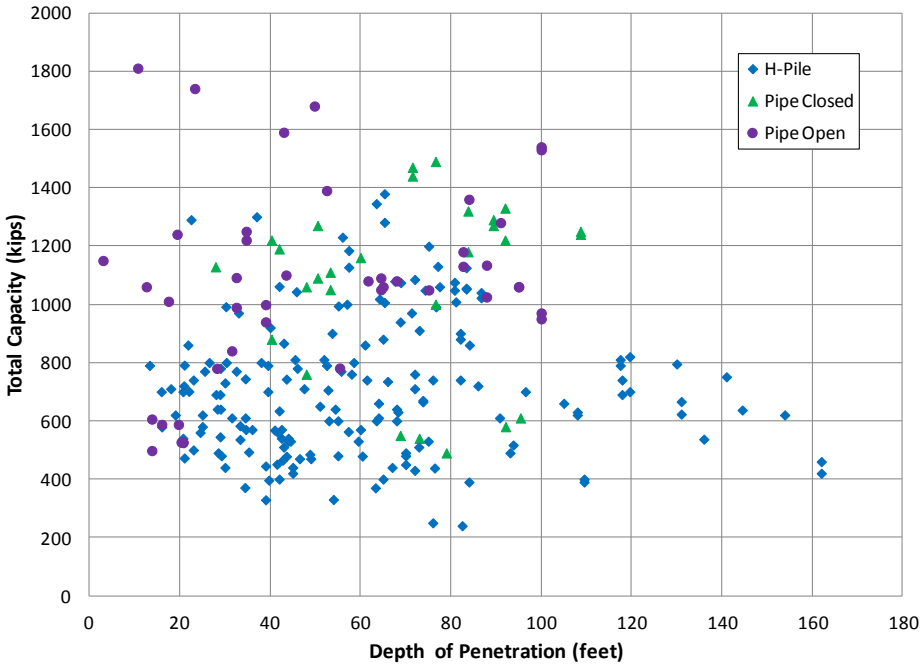

Figure 4-1: Total Pile Capacities with Depth

4.2.3. Side Capacities

The piles were also plotted with side capacity versus depth in Figure 4-2. The data showed that 52% of the pile lengths were driven into cohesive strata. These piles were then grouped by the percentage of their total lengths penetrating cohesive strata.

- > 0-20% - 40 piles
- 20-40% - 38 piles
- 40-60% - 21 piles
- 60-80% - 20 piles
- 80-100% - 14 piles

These categories of cohesive percentages are helpful in the prediction of behavior for each pile because clay along the side of the pile lowers the capacity at EOD. The data indicated that at EOD the piles with lengths 80-100% cohesive had an average side capacity of 56 kips; lengths 60-80% cohesive had an average side capacity of 78 kips; and lengths 40-60% cohesive had an average side capacity of 22 kips. The piles with >0-20% and 20-40% of their total length in cohesive strata had average side capacities of 213 kips and 141 kips respectively.

The side capacities of the piles were observed to generally increase with depth for piles with less than 40% of its length in cohesive soil. However, the side capacities of piles with greater than 40% of its length in cohesive soil appear to be more susceptible to the sensitivity of its cohesive layer(s). There were also a considerable amount of piles that exhibited lower capacities than their depth of penetration would indicate.

Additionally, the data indicated that there were some piles which had side capacities significantly larger than the majority of the other piles.

Approximately 70% of the 258 piles were driven through a till layer (not considered cohesive). These piles are grouped below by the percentage of their total lengths within till strata.

- > 0-20% - 41 piles
- 20-40% - 50 piles
- 40-60% - 42 piles
- 60-80% - 15 piles
- 80-100% - 31 piles

`

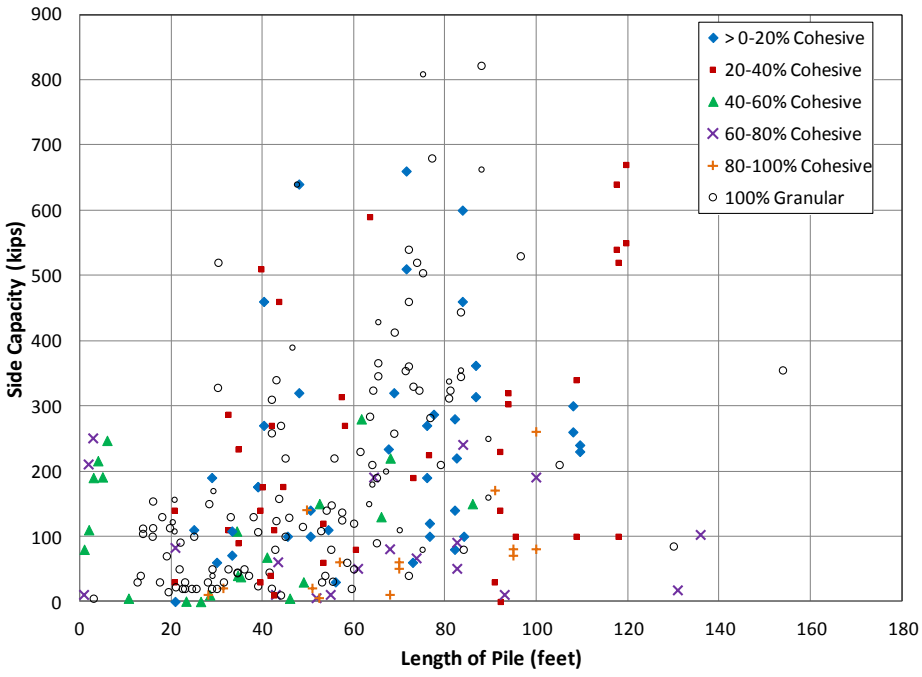

Figure 4-2: Side Capacities with Depth

4.3. Setup Characteristics of Test Data

Figure 4-3 presents the side and end bearing capacities of piles with both beginning of restrike (BOR) and EOD test data. The BOR tests were typically tested at one day after initial drive. The data indicated that approximately 78% of side capacities increased with time albeit only one day after driving. This time dependent capacity increase can cause piles to exhibit significantly larger strengths than the measured capacities at EOD or even one day BOR would indicate. However, the data also indicated that approximately 70% of the end bearing capacities decreased within the first day after driving. The figure also had several data points which appear to be abnormal and upon further inspection it was evident that these data points corresponded to two unique projects in Canaan and Falmouth.

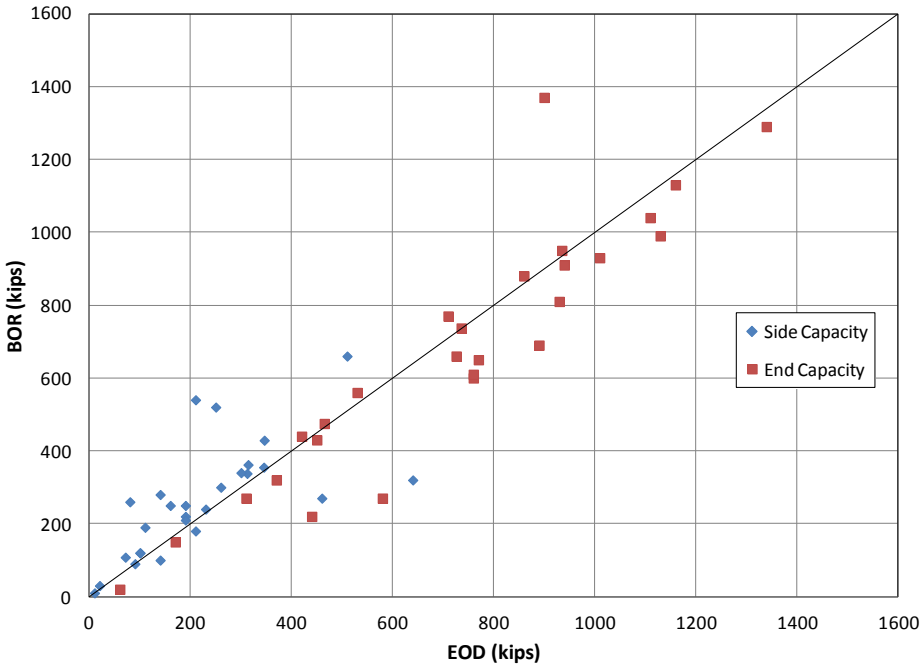

Figure 4-3: BOR versus EOD Pile Capacities

It was expected that the side capacity would increase with depth, but there were not any trends by pile type observed. Another observation was that in general the open end pipe piles had the largest tip capacities in both bedrock and till. This is counterintuitive to the expectation that the closed end pipe piles would have the largest pile capacity because they have the largest cross sectional area.

It is expected that the tested piles included in the study will experience time dependent changes in capacity. However, only 27 piles in this study were tested at EOD and BOR with each test providing a side and end bearing capacity estimate. Those that were tested for time dependent changes in capacity are listed in Table 4-3. The table provides EOD and BOR information for both side and end bearing capacity, the percentage of clay along the length of the pile, and water content of the clay layer (where applicable).

Setup values could be determined for the piles close to one day after driving, since most piles (23) had the restrike BOR the day after the EOD measurement, with 3 piles on the second day and one pile at one hour after the EOD. The first step was to determine the setup for piles in granular soils. There were 5 piles which had only granular soils along their entire length. Four of these piles were H-piles which had an average setup of 1.07; the other pile was a closed end pipe pile which had a setup of 1.51. These values were then used to back-calculate setup factors for the cohesive layers for piles driven through mixed soil strata. When combined with the percentage of cohesive and granular soil along the side of the pile and the overall BOR/EOD ratio, the setup of the cohesive layers could be determined. On average the raw setup for H-piles was 2.08, for

open end pipe piles was 1.92, and for closed end pipe pile 2.31 based on 6, 4, and 3 piles respectively. In general, these setup values correspond to a time equal to about one day.

Additionally, the setup factors for piles listed in Table 4-3 were calculated and sorted by water content in the cohesive soil layers. These setup factors for side capacity are shown in Table 4-2. It is evident that the closed end pipe piles experience greater setup than low displacement piles albeit a small sample size. This occurrence is likely due to the larger cross section of closed end pipe piles disturbing more soil during driving than other types of piles.

Table 4-2: Setup Factors for Side Capacity in Cohesive Soil for MaineDOT Test Data

Water Content	Pile Type	Setup Factor	# of Piles
< 26%	H-Pile	N/A	0
	Pipe Open	0.69	2
	Pipe Closed	2.06	1
26-35%	H-Pile	2.62	2
	Pipe Open	N/A	0
	Pipe Closed	2.67	1
35-40%	H-Pile	1.28	2
	Pipe Open	1.39	1
	Pipe Closed	2.25	2
> 40%	H-Pile	2.92	4
	Pipe Open	3.52	1
	Pipe Closed	N/A	0

Table 4-3: List of Piles Tested at EOD and BOR

						Side (kips)		End (kips)			
Project ID	Location	Structure	Pile ID	Pile Type	BOR # of Days	EOD	BOR	EOD	BOR	% Length in Clay	w %
6900.00	Norridgewock	Abutment 1	20	HP 14x73 Grade 50	1/24	210	180	450	430	0.0	N/A
7965.00	Verona Island	Prospect Verona Bridge	A-20	HP 14x117	2	345	355	710	769.9	0.0	N/A
7965.00	Verona Island	Prospect Verona Bridge	B-1	HP 14x117	1	314	362	726	660	3.5	Unknown
7965.00	Verona Island	Prospect Verona Bridge	B-14	HP 14x117	2	312	338	736	737	0.0	N/A
7965.00	Verona Island	Prospect Verona Bridge	Q-15	HP 14x117	2	346	429	935	950	0.0	N/A
15094.00	Falmouth	Pier 1	14	HP 14x73 Grade 50	1	140	280	760	600	16.1	40.3
15094.00	Falmouth	Abutment 2	11	HP 14x73 Grade 50	1	110	190	310	270	47.3	42.8
15094.00	Falmouth	Pier 2	27	HP 14x73 Grade 50	1	260	300	370	320	17.6	36.6
15094.00	Falmouth	Pier 2	30	HP 14x73 Grade 50	1	230	240	170	150	17.4	36.6
15094.00	Falmouth	Pier 3	2	HP 14x73 Grade 50	1	210	540	580	270	38.4	40.3
15094.00	Falmouth	Pier 3	9	HP 14x73 Grade 50	1	250	520	440	220	38.3	40.3
15094.00	Falmouth	Abutment 1	1	HP 14x73 Grade 50	1	190	220	60	20	16.8	36.6
15106.00	Portland	Pier 3 West	2	22" Pipe Open	1	80	260	890	690	89.0	42.9
15106.00	Portland	Abutment 1	3	22" Pipe Open	1	90	90	1160	1130	21.6	25.2
15106.00	Portland	Pier 1	3	HP 12x53 Grade 50	1	10	10	530	560	23.5	36
15106.00	Portland	Pier 1 East	11	22" Pipe Open	1	190	250	1340	1290	77.0	36.4
15106.00	Portland	Pier 3 North	6	HP 14x89 Grade 50	1	20	30	770	650	21.5	29.6
15106.00	Portland	Pier 5 West	14	22" Pipe Open	1	190	210	860	880	71.3	22.3
15110.00	York	Pier 1	3	20" Pipe Closed	1	300	340	940	910	26.7	35.5
15110.00	York	Pier 3	2	20" Pipe Closed	1	160	250	1110	1040	0.0	N/A
15110.00	York	Pier 4	3	20" Pipe Closed	1	100	120	900	1370	13.1	24
15110.00	York	Pier 5	3	24" Pipe Closed	1	510	660	930	810	14.0	31.55
15618.00	Canaan	East Abut.	4	HP 14X89 Grade 50	1	71	108	465	475	19.5	32
15618.00	Canaan	Pier 2	2	24" Pipe Closed	1	100	120	1010	930	26.5	38.7
15618.00	Canaan	Pier 7	2	24" Pipe Closed	1	460	270	760	610	19.1	38.7
15618.00	Canaan	Pier 8	3	24" Pipe Closed	1	640	320	420	440	16.0	38.7
15618.00	Canaan	Pier 9	3	24" Pipe Closed	1	140	100	1130	990	7.5	38.7

As piles have more end bearing on rock (higher capacities), the end bearing shows progressively less loss in the first days after driving as shown in Table 4-4 for H-piles. More than one-half of end bearing restrike capacity data was from H-piles that covered 5 projects. The setup data shows that H-piles lose end capacity for the first days (setup is 0.93) when the end capacity is less than 500 k, where it is expected that most pile ends are founded on till. For H-pile capacities of 500-800 k, where mostly rock end bearing is anticipated, there is a slight loss of capacity (setup is 0.97). While for end bearing greater than 800 k, where it is expected that all piles are founded on rock, there is a slight gain of H-pile end capacity (setup is 1.02). In contrast to H-piles, pipe piles with closed end for capacities greater than 800 k show a drop in capacity (setup is 0.91), while open pipes having a greater than 800 k end capacity have a between setup of 0.94.

Table 4-4: End Bearing Setup Factors for MaineDOT Test Data

End Bearing Capacity	Pile Type	Setup Factor	# of Piles
< 500 kips	H-Pile	0.93	6
	Pipe Open	N/A	0
	Pipe Closed	1.05	1
500-800 kips	H-Pile	0.97	5
	Pipe Open	N/A	0
	Pipe Closed	0.80	1
> 800 kips	H-Pile	1.02	2
	Pipe Open	0.94	4
	Pipe Closed	0.91	5

4.4. Dynamic Test Data at Fore River Bridge

To supplement the findings in the data provided by the MaineDOT, test data from the State Highway 77 Fore River Bridge Replacement (FHWA 1990) was analyzed.

Table 4-5 summarizes the Fore River Bridge test data. There were 9 piles on the project that were tested at EOD and BOR. Four of these piles were driven through clay while all of the piles were driven through ablation till. However, none of the piles were driven to bedrock. Table 4-6 displays the setup factors for the piles on this project.

Table 4-5: EOD and BOR Data for Piles Driven at Fore River Bridge (after FHWA 1990)

				Side Capacity (kips)		End Capacity (kips)			
Pile ID	Depth (ft)	Pile Type	BOR # of Days	EOD	BOR	EOD	BOR	% Length in Clay	% Length in Ablation Till
A10	79	18" Pipe Closed	1	141	202	195	212	41.8	19.0
B17	71	18" Pipe Closed	1	267	380	157	146	0.0	81.7
B23	51	18" Pipe Closed	6	63	120	260	220	0.0	74.5
B22	71	18" Pipe Closed	3	221	297	196	139	0.0	81.7
A5	99	18" Pipe Closed	2	143	318	203	181	33.3	15.2
B14	115	HP 14x89	5	188	259	91	70	0.0	63.5
A8	115	HP 14x89	N/A	N/A	225	N/A	12	28.7	13.0
A6	115	HP 14x89	N/A	N/A	212	N/A	53	28.7	0.0
	131		N/A	236	N/A	321	N/A	25.2	0.0
B21	115	HP 14x89	5	215	218	82	89	0.0	63.0
A4	136	HP 14x117	8	141	251	590	853	24.3	11.0
A9	134	HP 14x117	1	214	418	649	465	24.6	11.2

Table 4-6: Setup for Piles Driven at Fore River Bridge (after FHWA 1990)

	Pile Type	Setup Factor	# of Piles
Side Capacity			
Ablation Till	H-pile	1.27	2
	Pipe Closed	1.59	3
Cohesive Soils	H-pile	4.24	2
	Pipe Closed	2.46	2
End Bearing Capacity			
< 500 kips	H-Pile	0.92	2
	Pipe Open	N/A	0
	Pipe Closed	0.89	5
500-800 kips	H-Pile	1.06	2
	Pipe Open	N/A	0
	Pipe Closed	N/A	0

The average setup factor of 0.92 for end bearing of H-piles for capacities less than 500 k was similar to the average factor of 0.93 for the previous MaineDOT projects. With a larger average time of 4 days from EOD to BOR compared to close to 1 day for MaineDOT data, this indicates that there is practically no capacity change beyond 1 day. The average setup factor of 1.06 for end bearing capacities of 500 - 800 k of H-piles compared to 0.97 of the previous MaineDOT data indicates that the combined factor is close to 1.0.

The average setup factor of 0.89 for 5 closed end pipe piles with capacities below 500 k was lower than the setup factor of 1.05 for 1 closed end pipe in the MaineDOT data. This setup factor of 0.89 reflects similar behavior to the H-pile at this load level.

The closed end pipe piles experienced side capacity setup in granular soils of 1.59 similar to the 1.51 in the previous database. The side capacity setup of H-piles in granular soils on the Fore River Bridge project was about 20% larger than the setup factor on the other MaineDOT projects. Additionally, the side capacities of piles in cohesive soils were also larger on the Fore River Bridge project. However, these piles were typically tested after longer periods of time, so the larger setup factors indicate that the piles are continuing to gain capacity after one day. It is interesting to note that the side capacity setup of H-piles in cohesive soils was significantly larger than the closed end pipe piles, but again the H-piles had greater setup times than the closed end pipe piles which could account for the difference.

Chapter 5:

SETUP FOR END OF DRIVING CAPACITIES

5.1. Pile Setup

Piles are generally designed based on peak strength states of the soils along the sides and end of the pile. However, MaineDOT typically uses end of driving (EOD) capacity measurements using dynamic tests to check that the piles have obtained the required capacity. The EOD capacities will be conservative especially in cohesive soils, since the pile is supported by lower remolded strength at EOD. In general, the piles will gain capacity with time as the pore pressures from driving dissipate. To assess the reliability of the calculated ultimate capacities using peak strengths, the calculated capacities need to be compared to a measured pile capacity at ultimate strength. The most effective comparison is to conduct a load test after pore pressures have fully dissipated and compare to the predicted ultimate capacity. Setup is the ratio of the capacity after driving pore pressures have dissipated compared to EOD capacity. To determine how much setup would ultimately be experienced by each pile after EOD, the beginning of restrike (BOR) measurement at full dissipation can be compared to the EOD measured capacity. The setup with time can be determined by conducting restrike tests at various times after EOD. However, due to a lack of time dependent capacity measurements, a method for estimating capacity with time based on the MaineDOT pile database is presented in this chapter.

5.1.1. Setup for Cohesive Soils

When piles are driven through cohesive soil, then the piles cause remolding of the cohesive soil close to the pile with accompanying high pore pressures. The remolded

strength of the Presumpscot Formation and other sensitive soils is often significantly lower than the peak strength. However, with time after driving, the excess pore pressures from driving will dissipate, and the remolded clay will regain its original strength. The measured sensitivity of the cohesive soil (ratio of peak strength to remolded strength) has been taken as the setup in the past (see Hannigan et al, 2006 p.16-20).

Bjerrum (1954) has found that the sensitivity of Norwegian clay is related to the liquidity index (LI) of the clay.

$$LI = \frac{w_n - PL}{LL - PL} \qquad [5.1]$$

Where:

LI = Liquidity index

w_n = Natural water content

PL = Plastic limit

LL = Liquid limit

Norwegian clays have a similar geologic history and similar properties to the Presumpscot. Typically the Atterberg limits of the Presumpscot do not vary greatly, and thus it would be expected that the clay sensitivity (and thus setup) would be primarily related to the water content of the clay.

With the piles that had CAPWAP® data at EOD and BOR a plot was generated that showed the ratio of BOR to EOD against water content. This plot is shown in Figure 5-1 with a line of best fit. This best fit line indicated that the magnitude of setup in

cohesive soil was related to water content of the clay. It should be mentioned that the assumption with this figure is that all pile setup occurs within the cohesive layer.

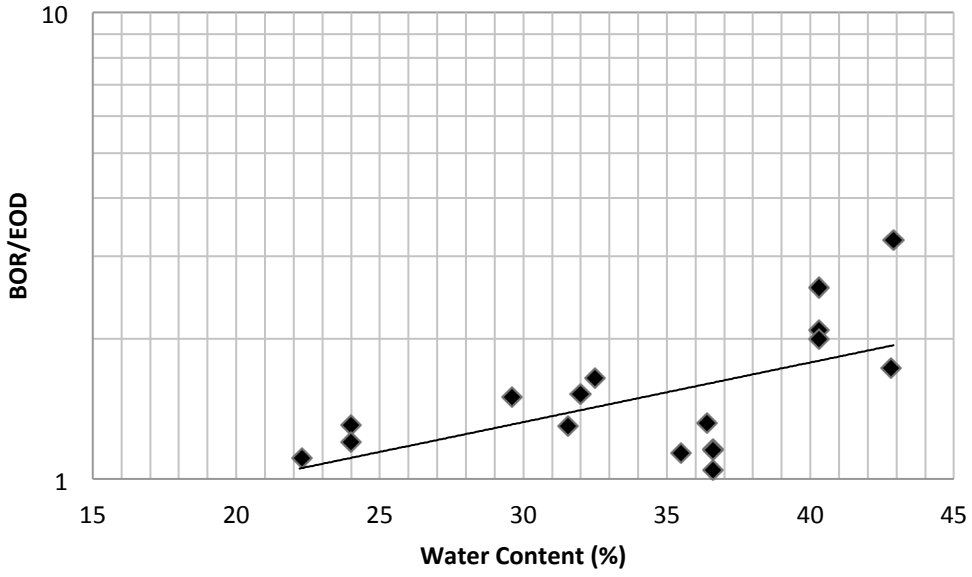

Figure 5-1: Pile Setup Factor as a Function of Cohesive Soil Water Content (MaineDOT Data)

Attwooll et al (1999) presented some data that showed the significance of accounting for setup in pile design. Figure 5-2 shows that the EOD measured side capacity had very little variation in the unit skin friction with depth. However, the BOR measured side capacity at 93 days after pile installation had significant changes in unit skin friction with depth. Additionally, Figure 5-3 indicated the amount of setup that could be expected with time. The percentages are all based off of the measured static capacity at 38 to 43 days after initial drive. The piles were dynamically tested at EOD and at 20 days after the static tests (58 to 63 days after initial drive). The second set of dynamic tests indicated that the piles were still gaining capacity.

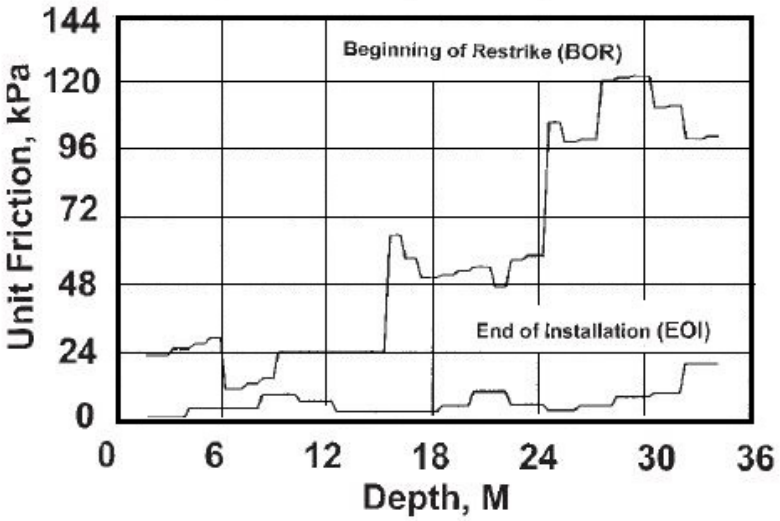

Figure 5-2: Changes in Unit Skin Friction with Depth (Attwooll et al 1999)

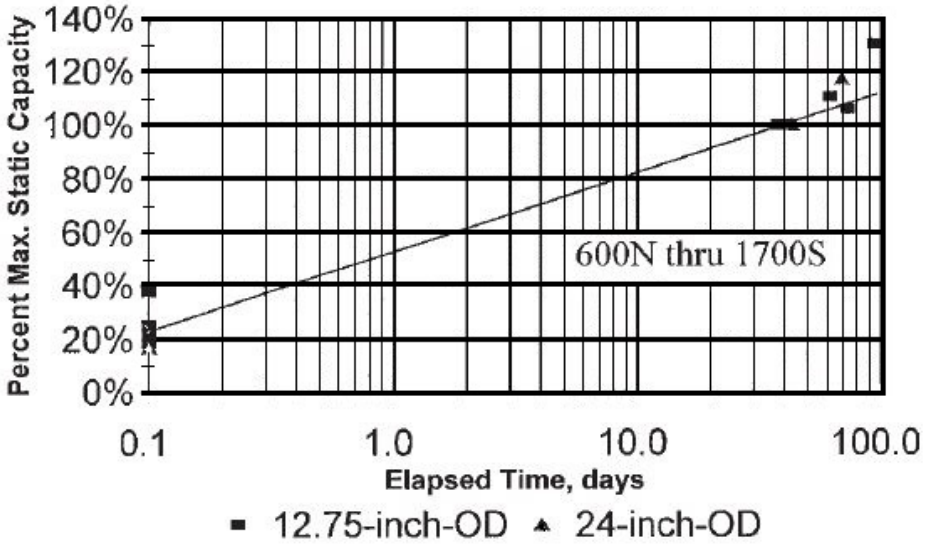

Figure 5-3: Setup in Clay (Attwooll et al 1999)

Long, Kerrigan, and Wysockey (1999) also examined the amount of setup experienced by piles in cohesive soils. Their data suggested that pile capacity will increase rapidly with time for up to 100 days after initial driving at which point the rate

of setup becomes smaller. Additionally, their data suggested that these piles can increase from 1 to 6 times their measured EOD capacities.

5.1.2. Setup for Granular Soils

There is also some time dependent increase in capacity from granular soil layers albeit significantly less than the setup of the cohesive soils. Long, Kerrigan, and Wysockey (1999) conducted an analysis of dynamic load tests which substantiated this claim. As Figure 5-4 shows, their analysis indicated that the final capacities of piles driven in sand can range from 1.3 to 2 times the EOD measurement. The data used to demonstrate this relationship was for almost entirely loose to medium dense sands. Their analysis also indicated that the capacities of piles driven in sand can continue to increase up to 500 days after initial drive.

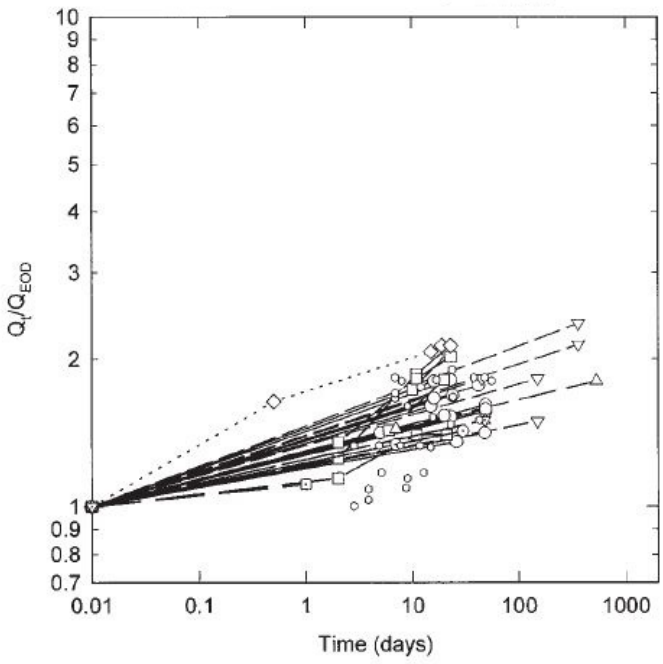

Figure 5-4: Setup for Piles in Granular Soil (Long, Kerrigan, and Wysockey 1999)

5.1.3. Setup for End Bearing

Based on results of MaineDOT and Fore River restrike tests on H-piles for end bearing capacity less than 500 k, there is a loss of end bearing capacity for 1 day restrikes, but the capacity does not continue to change beyond day one. This behavior indicates relatively rapid pore pressure dissipation or particle adjustment after EOD.

For end bearing capacities of H-piles greater than 500 k at the sites investigated herein, it does not appear that on average there is loss of capacity from EOD to BOR even up to 8 days after EOD. However, these test values may not be representative of the behavior of some shales or other weaker bedrocks that may occur in Maine.

Although the loss of bearing capacity for closed end pipe piles was similar to H-piles for capacity levels less than 500 k, the closed end pipe pile capacity also showed restrike loss for capacities greater than 800 k. For open pipe piles, there was not enough data to develop separate behavior, and thus the end bearing behavior was taken to be the same as H-pile behavior.

5.1.4. Skov and Denver Method (1988)

The most widely used method for calculating pile setup as a function of time in soil is the method proposed by Skov and Denver (1988). The Skov and Denver method allows for the capacity to be calculated at any time after installation. This method is shown below:

$$\frac{Q_t}{Q_0} = 1 + A \log\left(\frac{t}{t_0}\right) \qquad [5.2]$$

Where:

Q_t = Pile capacity at time t

Q_0 = Pile capacity at time t_0

A = Dimensionless coefficient

t = Time of interest

t_0 = Elapsed time after driving for initial capacity

The Skov and Denver method (1988) was used by both Camp and Parmar (1999) and Long, Kerrigan, and Wysockey (1999) to analyze pile setup with time. However, there does not appear to be a steadfast method for determining the t_o and A parameters for use in the equation. The appropriate values vary among users. Long, Kerrigan, and Wysockey (1999) reported that the reference time that they used was 0.5 day and 1.0 day for sands and clays respectively. The reference time used by Camp and Parmar (1999) was 2 days. The t_o value chosen for use in the design equations has a significant effect on the A parameter. Additionally, the A parameter will change based on the type of soil being analyzed.

5.1.5. Determination of Setup Factors for Design

The MaineDOT test data (Table 4-3) combined with the Fore River Bridge data (Table 4-5) were used to estimate pile setup with time. The setup values at one day for each of the H-piles entirely in granular soil (4 piles) from Table 4-3 were averaged to calculate a typical setup BOR/EOD ratio. Using this value, an A parameter for granular soil can be calculated using Skov and Denver's (1988) relationship (Equation 5.2). The A

parameters suggested in the literature review did not come with any recommendations for identifying which types of cohesive soils correspond to each parameter. The elapsed time from EOD to the measurement for use in the equation was assumed to be 20 minutes (0.014 days) (Hannigan et al 2006). The dynamic test reports generally report that the BOR test was conducted the following calendar day from the EOD. The elapsed time was taken to be 19 hours rather than 24 hours. It was considered that the pile was likely tested at EOD in the afternoon (the office of the testing company is 3 to 5 hours from most Maine locations. The technician came back in the morning to conduct the BOR test and returned to his office (3-5 hours) following the test. This analysis produced an A parameter of 0.042 for granular material.

A similar procedure was used to calculate the A parameters for closed end pipe piles in granular soils and for all piles in cohesive soils. However, due to a lack of reliable time dependent test for closed end pipe piles the test data from the Fore River Bridge project was used. This resulted in an A parameter of 0.29. There was not sufficient data to determine trends in cohesive setup by pile type. Instead, these A parameters were calculated for various water contents. From the available MaineDOT test data and the setup trend shown in Figure 5-1, it was determined that the A parameters would be calculated for three ranges of water content: water contents < 26%, water contents 27-39%, and water contents > 40%. The resulting A parameters were 0.061, 0.38, and 1.42 respectively.

Using the Skov and Denver (1988) relationship and the calculated A parameters, setup factors were calculated at 0.8 days (1 day BOR), 1 day, 2 days, 3 days, 5 days, 6 days, 8 days, 14 days, 90 days, and 270 days. The 270 days as suggested by Orrje and

Broms (1967) for Swedish glacial clays was assumed to be the time at which the pore pressure had fully dissipated and reached the ultimate strength state. This time was confirmed for Maine clays through a time rate of consolidation analysis using the following equation (Poulos and Davis 1980).

$$T = \frac{tC_h}{a^2} \qquad [5.3]$$

Where:

T = time factor

a = pile radius (feet)

C_h = coefficient of horizontal consolidation (ft^2/day)

The time factor can be found from the above equation for various elapsed times. A C_h value of 0.15 ft^2/day was used and was obtained from a C_v average of 0.10 ft^2/day (Andrews 1987) with a $C_h/C_v = 1.5$ (Poulos and Davis 1980). The relation between time factor T and percent consolidation was used to find the consolidation for each time. It was determined that at 289 days the pore pressure was 96% dissipated. This indicated that the Orrje and Broms (1967) suggestion was reasonable. The resulting setup factors from the Skov and Denver analysis are shown in Table 5-1 for various elapsed times.

The MaineDOT test data indicated that some piles will experience a reduction in end bearing capacity from EOD to the 1 day BOR analysis as shown in Figure 4-3. These reduction factors are shown in

Table **5-2**. It should be noted that these factors were based only on the MaineDOT test data which did not have any data beyond 1 day BOR for comparison. However, it is assumed that these end setups did not change further with time.

Table 5-1: Final Time Dependent Side Capacity Setup Factors

	Cohesive Factors			**Granular Factors**	
	w > 40%	w = 26-39%	w < 26 %	HP & Open Pipe	Closed End Pipe
Time (days)	Qt/Qo	Qt/Qo	Qt/Qo	Qt/Qo	Qt/Qo
0.8	3.49	1.67	1.11	1.07	1.51
1	3.63	1.70	1.11	1.08	1.54
2	4.06	1.82	1.13	1.09	1.62
3	4.31	1.89	1.14	1.10	1.68
5	4.63	1.97	1.16	1.11	1.74
6	4.74	2.00	1.16	1.11	1.76
8	4.91	2.05	1.17	1.12	1.80
14	5.26	2.14	1.18	1.13	1.87
90	6.41	2.45	1.23	1.16	2.10
270	7.09	2.63	1.26	1.18	2.24

Table 5-2: Final Bearing Capacity Setup Factors

	H-Pile and Open Pipe Pile	**Closed End Pipe Piles**
EOD Bearing Capacity	Q_{BOR}/Q_{EOD}	Q_{BOR}/Q_{EOD}
< 500 kips	0.92	0.92
500-800 kips	1.00	0.91
> 800 kips	1.00	0.91

Chapter 6:

PRESENTATION OF RESULTS

There were 250 pile load tests selected for analysis. For piles to be included in this study, they must have been tested dynamically and analyzed using CAPWAP® and have enough associated information available to create a representative subsurface profile for the project area. Some of these loads tests were on the same pile (i.e. piles tested at the end of driving (EOD) and beginning of restrike (BOR)), but each of these tests were treated as an individual pile analysis (e.g. a pile tested at EOD and BOR counts as 2 piles in this analysis). There were 30 piles that pertain to this annotation. The tip capacities of the piles are categorized as follows: 216 piles founded on bedrock (26 of which are closed end pipe piles) and 26 piles that have fetched up in granular soil.

The analyses are separated into side capacity and end bearing capacity. Each combination of design equations is examined to demonstrate the effectiveness of the equations at predicting the total pile capacity. For the side, three methods (Meyerhof, SPT and Nordlund) for granular and two methods (α and β) were examined. For the end, there were two methods for rock (proposed Intact Rock method (IRM) per Rowe and Armitage (1987) and the Canadian Geotechnical Society method (CGS)) and three methods for till (Nordlund, Meyerhof and SPT). This could perhaps provide some insight to the effectiveness of CAPWAP® in separating end bearing and side capacities at EOD and BOR.

6.1. Back-Calculated Unconfined Compressive Strengths of Bedrock

The measured unconfined compressive strength (q_u) of the bedrock was not available as described in Section 3.4.1. The q_u of the rock was needed for bearing

capacity calculations and thus without onsite values, these values need to be assumed from a published range. It was desired to obtain a back-calculated q_u value for specific rock types. This value was obtained by setting Q_p equal to the CAPWAP® measured end bearing capacity and finding q_u from Equation 3.15. The bedrock was categorized into three types: igneous, metamorphic, and sedimentary rock. A weighted average of each bedrock subtype provided a q_u value for each rock type. A summary of how the rocks were categorized and the resulting averages is shown in Table 6-1 through Table 6-3. The average values for each rock type were then used to make an estimate of the end bearing capacity using Equation 3.15.

Table 6-1: Back-Calculated Unconfined Compressive Strength For Igneous Bedrock

Igneous				
Rock Type	Number of Piles	Ave (ksi)	Max (ksi)	Min (ksi)
ANORTHOSITE	3	5.9	7.3	4.7
DIORITE	2	8.4	10.5	6.3
GABBRO	5	6.7	7.4	6.1
GRANITE	33	5.0	8.1	2.3
SYENITE	2	3.6	3.8	3.3
All Igneous Rock Types	**45**	**5.4**	**10.5**	**2.3**

Table 6-2: Back-Calculated Unconfined Compressive Strength, Metamorphic Bedrock

Metamorphic				
Rock Type	Number of Piles	Ave (ksi)	Max (ksi)	Min (ksi)
GNEISS	14	4.5	6.6	1.5
GRANOFELS	2	8.2	11.1	5.3
GREENSCHIST	6	4.6	5.3	4.0
HORNFELS	2	5.1	5.9	4.3
PHYLLITE	24	6.0	9.3	2.7
QUARTZITE	1	3.9	3.9	3.9
SCHIST	55	4.8	8.1	1.3
SLATE	4	7.8	9.3	5.4
All Metamorphic Rock Types	**108**	**5.2**	**11.1**	**1.3**

Table 6-3: Back-Calculated Unconfined Compressive Strength For Sedimentary Bedrock

Sedimentary				
Rock Type	Number of Piles	Ave (ksi)	Max (ksi)	Min (ksi)
LIMESTONE	4	2.2	2.8	1.9
LIMONITE	3	1.2	1.5	0.9
METASILTSTONE	8	4.1	6.1	2.3
MUDSTONE	1	1.5	1.5	1.5
SANDSTONE	15	5.6	11.3	2.8
SHALE	5	5.5	6.9	4.4
SILTSTONE	4	4.0	5.3	2.5
All Sedimentary Rock Types	**40**	**4.4**	**11.3**	**1.0**

A random sample of piles was selected to analyze the effects of rock quality designation (RQD) on the back-calculated q_u values. The results of this analysis are tabulated in Table 6-4. This selection of piles did not indicate any trend in the data with RQD. This indicates that the best recommendation of the q_u value for any site is based solely on the type of bedrock underlying the pile.

Table 6-4: Back-Calculated q_u with Measured RQD

Rock Type	RQD	q_u (ksi)	Rock Type	RQD	q_u (ksi)
Gabbro	68	6.4	*Granite*	90	4.7
Gabbro	97	6.1	*Granite*	83	4.7
Gabbro	77	7.4	*Granite*	43	4.5
Gneiss	97	3.1	*Granite*	28	5.5
Gneiss	68	6.3	*Granite*	33	4.2
Gneiss	37	3.9	*Schist*	80	6.6
Sandstone	98	4.5	*Schist*	57	3.1
Sandstone	76	2.8	*Schist*	87	5.5
Sandstone	38	11.3	*Schist*	35	4.9
Metasiltstone	100	2.3	*Phyllite*	54	4.2
Metasiltstone	26	5.1	*Phyllite*	28	5.9
Metasiltstone	99	6.1	*Phyllite*	47	2.7

6.2. Comparison of Measured and Calculated Side Capacities

Out of the 250 piles included in the side capacity analysis, there were 2 piles that had CAPWAP® measured side capacities of 0 kip. These piles were not included in the presentation of results because the division by zero causes the predicted to measured ratio to become infinite. In the side capacity calculations for open pipe piles, the soil plug was assumed to go to the top of the pile when in reality the plugging will not completely fill the pipe. This will likely cause an over prediction of the side capacity. The dynamically measured side capacities from CAPWAP® analyses were factored to the 270 day ultimate capacities using the values in Table 5-1 &

Table **5-2**. These factored measured values were then compared to the calculated ultimate side capacities from static design methods that used peak strengths. The results of these comparisons are shown in

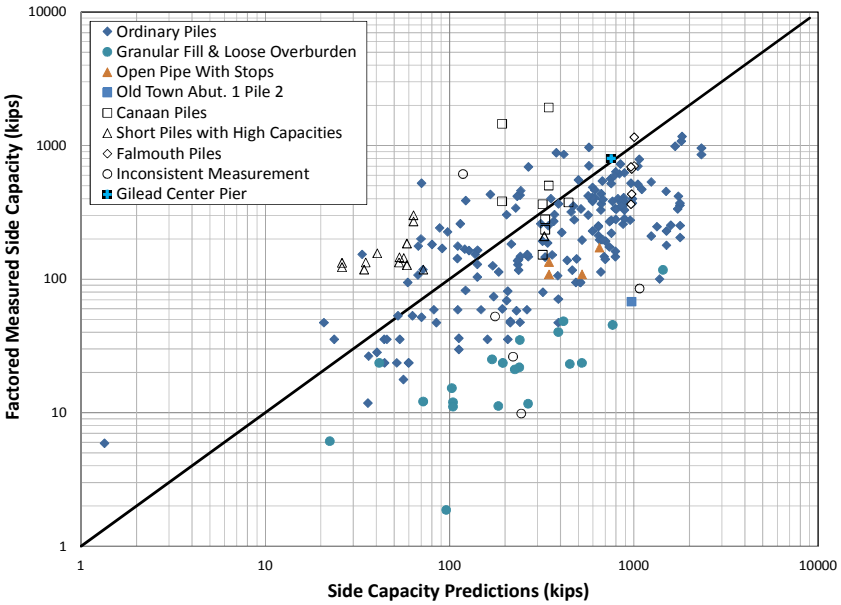

Figure **6-1** through Figure 6-6. These figures each have a line which indicates equality. Each figure has unique cases plotted separately from the typical pile behavior.

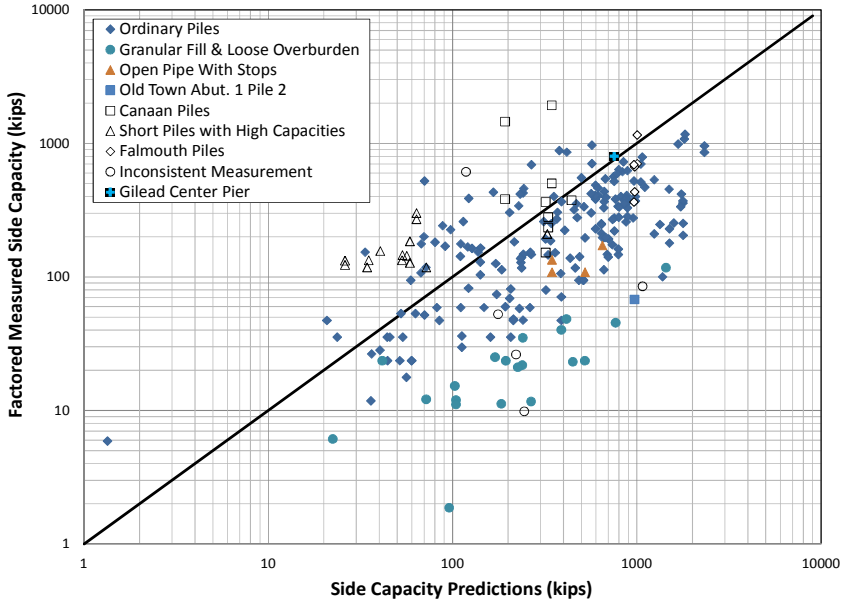

Figure 6-1: Nordlund and **α** Methods Side Predictions

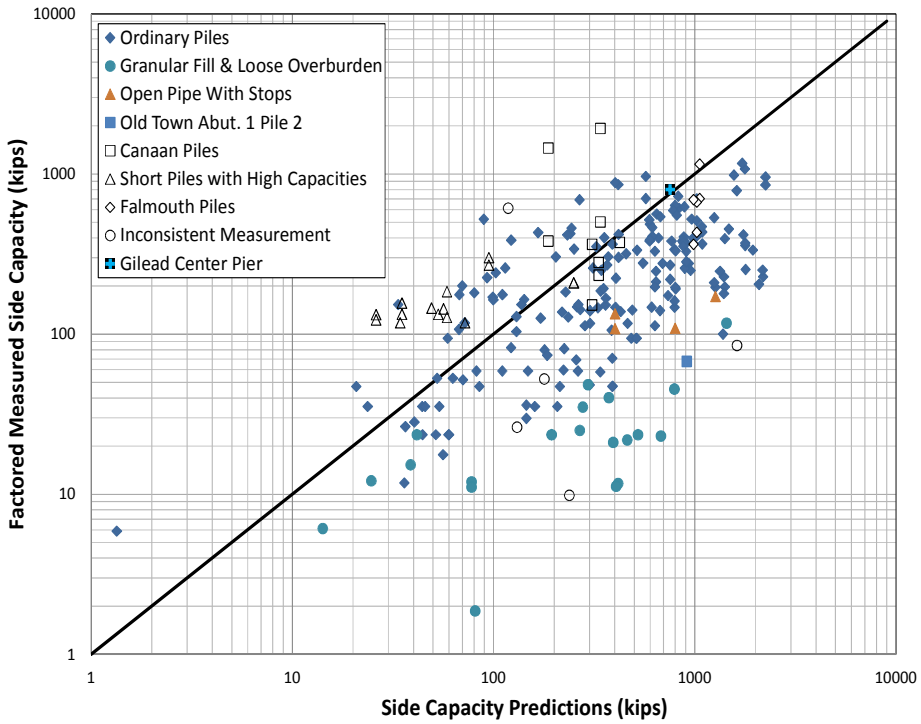

Figure 6-2: Nordlund Method and **β**-Method Side Predictions

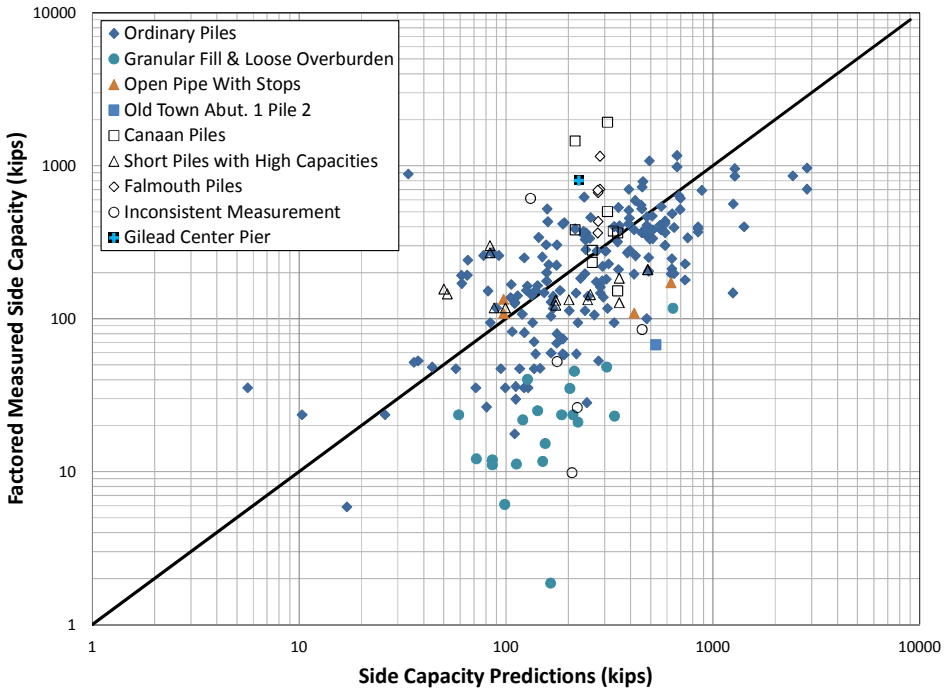

Figure 6-3: Meyerhof SPT Method and **α**-Method Side Predictions

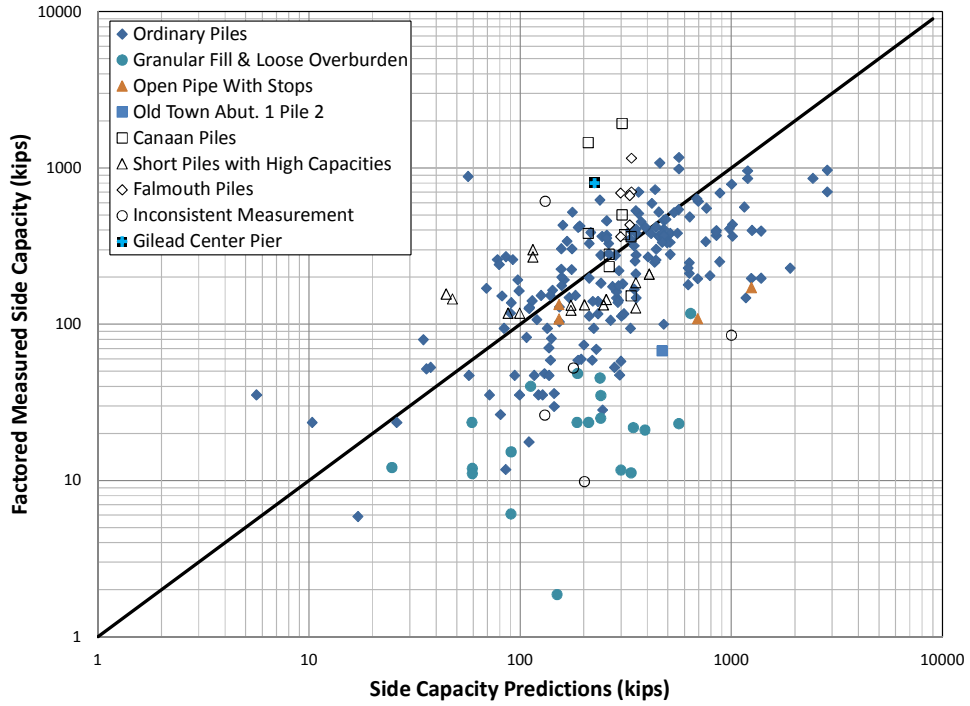

Figure 6-4: Meyerhof SPT Method and **β**-Method Side Predictions

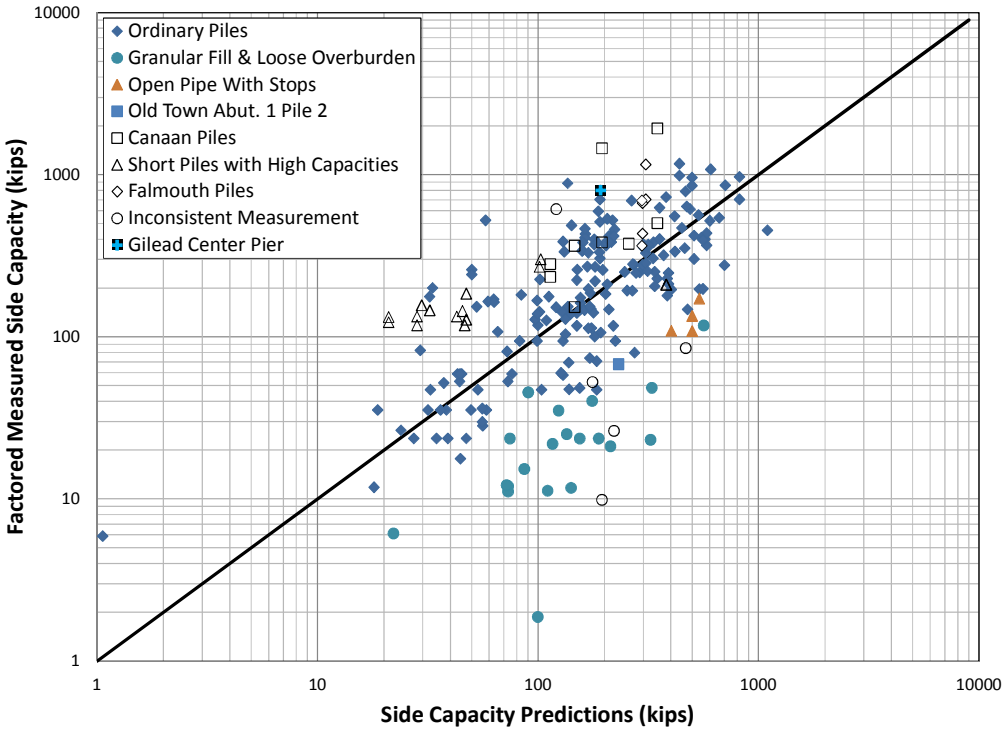

Figure 6-5: Meyerhof Method and **α**-Method Side Predictions

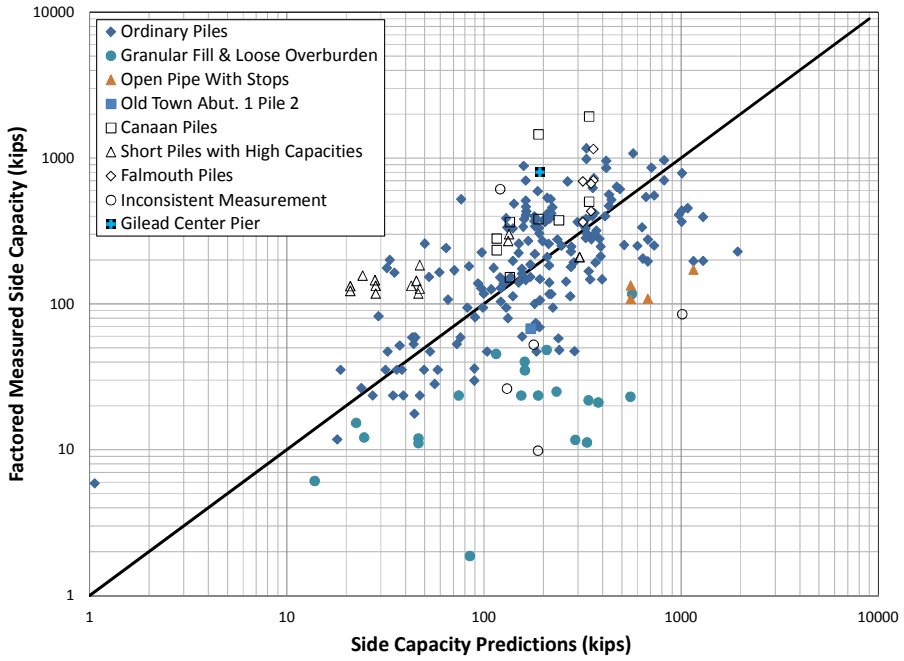

Figure 6-6: Meyerhof Method and **β**-Method Side Predictions

6.2.1. Description of Outliers

The outliers occurring in comparisons of dynamic test capacities (with setup applied) to calculated capacities in the figures were scrutinized to determine possible special conditions that may not have been considered in the comparisons. Special conditions included possible specific recurring soil profiles, abnormal construction conditions, results from the dynamic tests that were questionable, and changed soil profiles. The special cases found were:

1. Granular fill over soft cohesive and loose overburden over soft cohesive
2. Open pipe with stops
3. Short piles with high capacities
4. Specific project anomalies

6.2.1.1. Granular Fill Over Soft Cohesive and Loose Overburden

Some long piles had unusually low EOD measured side capacities (see Figure 4-2). Most of these low capacities appear to occur when piles are driven through granular fill material or natural granular soils which overlie soft cohesive layers. Even when setup was applied to the measured side capacities, the measured capacity was unusually low.

A study conducted on a test pile at the Biddeford Connector by Sandford (1989) for the Maine Department of Transportation is relevant to the interpretation of these low values. The Biddeford Connector is off Alfred St in Biddeford (location of a case history in this study) and over the railroad. The test H-pile at the Biddeford Connector was monitored with instrumentation and driven through 35 feet of sand fill over 77 feet of clay with 5 feet of sand and gravel beneath the clay and bedrock below. The instrumentation indicated that the 35 feet of sand fill did not contribute any downdrag stress on the pile despite settling in excess of two feet relative to the pile during the monitoring period. The monitoring indicated that during the driving of the pile through the sand fill above the soft clay, a hole was created around the pile within the sand (a hole was observed at the top of the fill). This hole stayed open by arching of the sand for the full monitoring period of 260 days.

A study on downdrag conditions using instrumentation monitoring by Dixon (1998) at Brunswick was done on one of the piles tested by dynamic loading for this study (pile #6 at Rte 196, Abutment 1, Ramp B, called V2C by Dixon). The instrumentation showed that there was no downdrag through the fill (22 ft) or in the organic cohesive layer (10 ft) beneath the fill at the time of the dynamic test. A hole was observed around the pile at the surface of the fill. This test together with the Biddeford

Connector test shows that fill can provide no frictional support. This can be part of the explanation for the low values of side shear measured by the dynamic test on piles driven through fill overlying soft cohesive. In the calculations, all layers were considered to be contributing to the support of the pile. However, all pile driving does not create a hole through the fill, so the fill layer over cohesive can not be deleted from calculations to be comparable to the layers measured by the dynamic test.

Dixon monitored other piles besides the one that was monitored with a dynamic test. The uncoated piles (the dynamically tested one had a bitumen coating) had side shear stress through the fill at the time that the dynamic test was done on the other pile. But the pile at Biddeford Connector was uncoated without showing any stress caused by the fill. The coated pile at Brunswick continued to be monitored for 390 days. At the end of the 390 days, there were 12 kips of downdrag indicating that the hole in the fill was closing with time. A drop hammer started the pile at Biddeford with a continuation by a diesel driver, while at Brunswick a vibratory hammer started the pile with a diesel driver used to continue driving. The type of starter hammer may affect the development of the hole in the fill around the pile.

At the Biddeford Connector, the profile was essentially fill and cohesive over bedrock, but the profile at Brunswick was different. At Brunswick, below the fill and organic clay there was marine sand (20 ft) and marine clay (33 ft) below the marine sand. Following the end of driving at Brunswick, downdrag was measured in the marine sand and in the marine clay. Thus the hole around the pile in the fill and low strength in the soft cohesive did not extend below the first cohesive layer. The total downdrag at Brunswick measured at the bottom of the marine clay layer after the end of driving was

267 kN (60 kips). This is a significant downdrag indicating the different behavior of the lower two layers.

The piles in the loose overburden over soft cohesive or granular fill over soft cohesive were separated from the rest of the piles, as a result of the questions raised above about arching in the fill and low strength in the cohesive. The piles that satisfied the filter are displayed in Figure 6-7 with the factored ultimate measured capacities on the y-axis and the Meyerhof and α-method predicted capacities along the x-axis. The resistance from the granular fill layer and cohesive and loose overburden and cohesive were then removed from the calculations and compared to the factored measured capacities. The adjusted side predictions are shown in Figure 6-8.

The results suggest that when a loose overburden or fill layer above soft clay exists there is little contribution from the granular and also from the soft clay to the measured side capacities. These piles were treated separately from the remaining piles.

6.2.1.2. Open Pipe with Stops

There were also some open end pipe piles that caused over predictions of the ultimate pile side capacities. These piles were used on the Pan Am Railroad and Veteran's Memorial Bridges in Portland. Though the dynamic testing reports never explicitly reported issues with the testing, the piles were unique enough to warrant erratic predictions. These piles had stop plates welded inside the open pipe at approximately 50 feet from the tip which may have caused issues with drivability and hammer performance. It appears that the function of these stop plates was to provide a clean upper

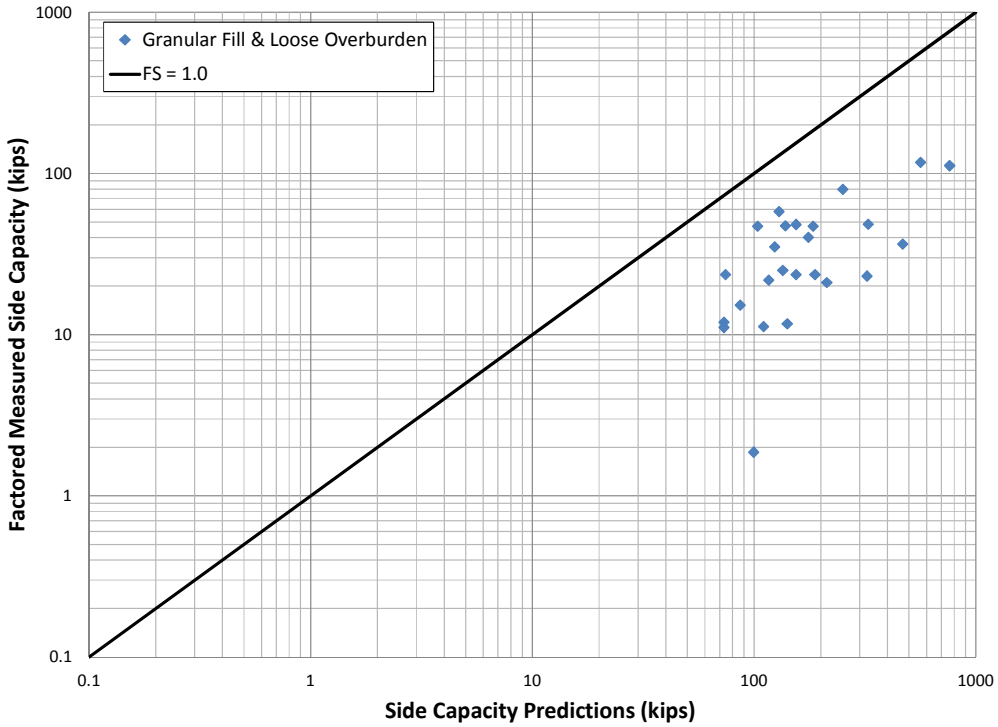

Figure 6-7: Piles in Granular Fill and Loose Overburden

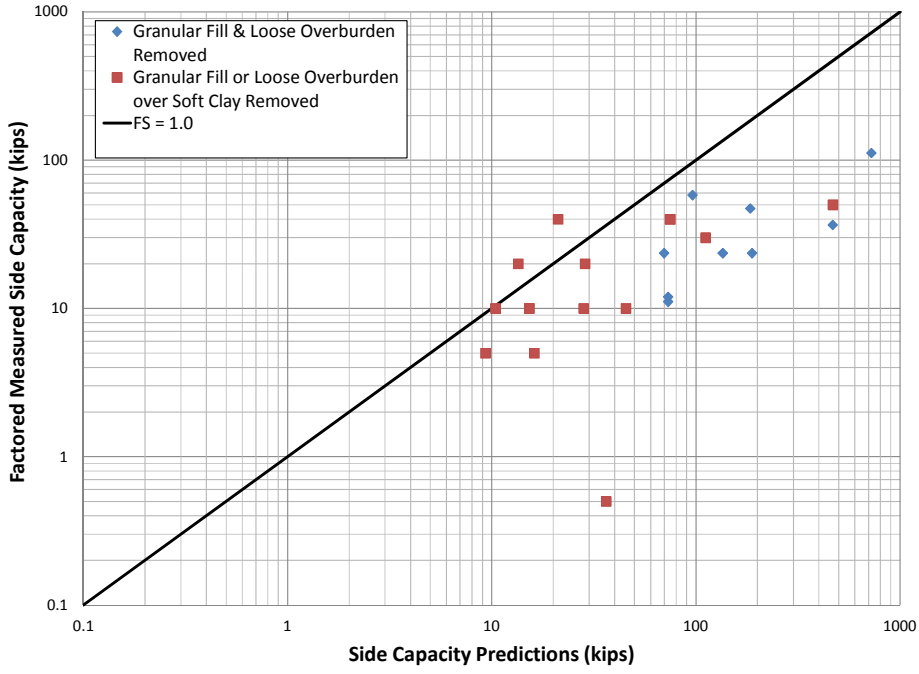

Figure 6-8: Adjusted Predictions for Piles in Granular Fill and Loose Overburden

section to receive concrete for additional lateral stability. The additional resistance generated with this plate prevented the specified hammer from effectively driving the pile and required a switching of hammers during the test. As a result of the somewhat erratic capacity of this type of pile, they were removed from the correlations.

6.2.1.3. Short Piles

Another set of piles which resulted in conservative predictions by some methods were short piles with unexpectedly high side capacities at Georgetown, Fryeburg and Auburn. The Nordlund and Meyerhof methods significantly under predicted the measured side capacities. These piles were generally less than 20 or 30 feet long with measured capacities greater than 100 kips of skin friction measured by the CAPWAP® analysis. Additionally, the boring logs for these piles indicated that they were generally driven through soft/loose silts and/or loose to medium dense sands that typically will not result in these large capacities. Perhaps there are limitations in predicting side capacity with CAPWAP® when piles are short with high end bearing on competent bedrock.

6.2.1.4. Specific Case Anomalies

A case of over prediction is the Irving Bridge in Old Town. The pile was located in the Abutment 1 substructure, and the analysis significantly over predicted the pile capacity. According to the boring the pile was driven through a dense till layer, but it would appear that the measured capacity does not reflect that resistance. The tested pile in the Abutment 2 substructure was approximately 18 feet shorter than the Abutment 1 pile and according to the boring was not driven through till. However, it had a capacity twice as large as the Abutment 1 pile.

The Boothbay Knickerbocker Bridge alignment was located downstream of the provided subsurface investigation alignment. There were some conflicting elevations reported in the geotechnical report as compared to the dynamic testing reports at the bridge alignment. The conflicting elevations greatly affected which soil layers would contribute to the side resistance because there were highly sloping bedrock and dense sand layers.

On the project in Grand Lake Stream there were two piles tested at each of the abutment structures which were driven through similar subsurface profiles. One pile was 22.5 feet long and measured 20 kips of skin friction at EOD, the other pile was 30.3 feet long and measured 520 kips at EOD. A difference of 500 kips in skin friction measurement for 8 feet difference in pile length is counterintuitive. The same situation was observed at the MCRR Bridge in Yarmouth. There were also some piles on the Bartlett Bridge and Center Street Bridge in New Portland and Auburn respectively which exhibited little to no side capacity.

Some of the figures also show some data which indicate some very conservative predictions. One of these projects is the Sibley Pond Bridge in Canaan. This project had a few piles that had significant drops in side capacity from EOD to 1 day BOR. The dynamic test report indicated that after the pile was allowed setup, the hammer may not have been able to activate the total side resistance which likely led to the under predicted capacities upon restrike.

The Falmouth Railroad Crossing Bridge over Presumpscot River Bridge produced erratic results. The reported results claimed that the side capacity of the piles had

increased by 200-300 kips and the end bearing capacities had decreased by 200-300 kips overnight. This drastic change indicates unnatural soil behavior and an error in the analysis or presentation of the data. One possible cause was that when some of the first piles driven on the site were not achieving the required capacity, it was decided to change to a larger hammer to redrive the piles.

On the Wild River Bridge project in Gilead, one of the piles located in the Center Pier substructure had an odd distribution of skin friction along the side of the pile. The dynamic test for the pile reported that 550 kips developed along the bottom 7 feet of the pile in a very dense till stratum. The density of this layer was considered in design; however, the predicted skin friction due to the dense till was far below the measured amount. The boring logs indicated the presence of cobbles which required drilling during the subsurface exploration. Perhaps the pile was wedged between some cobbles along the bottom of the pile. The pile was reported to be caught up on bedrock at an elevation 10 feet above the reported bedrock elevation in the corresponding boring log. The reported end bearing capacity of 450 kips is also lower than other piles which were claimed to be resting on bedrock.

6.2.2. Analysis of Predictions with Outliers Removed

6.2.2.1. Presentation of Results

The previously discussed outliers in side shear capacity were removed from the measured test data for use in the method comparison. The predicted side shear capacities by equations were compared to the dynamic test results. A best fit trend line was put through each data set, and a standard error from the best fit was determined to describe the quality of the fit. Additionally to compare the effectiveness of each prediction, the standard deviation of the data from the line representing equality between predicted and measured was determined for each data set. The plots used in comparing the effectiveness of each method are shown in Figure 6-9 through Figure 6-14.

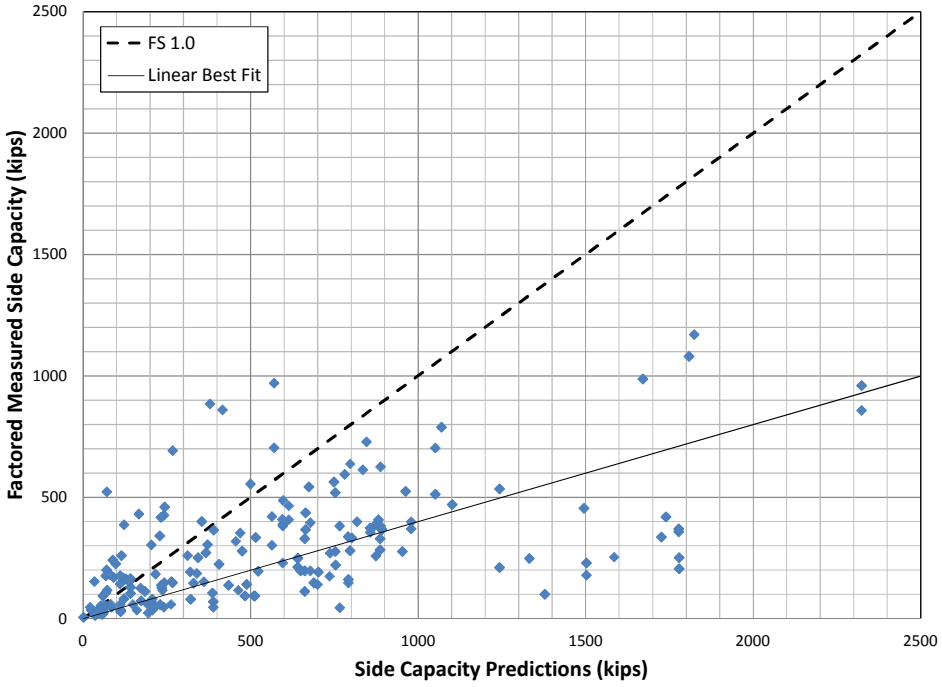

Figure 6-9: Nordlund Method and **α**-Method Combined Side Capacity Predictions with Outliers Removed

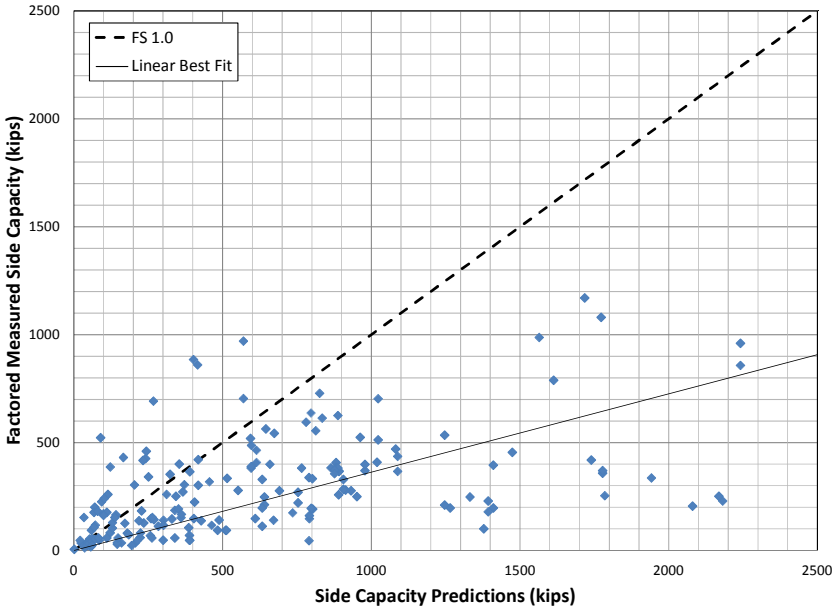

Figure 6-10: Nordlund Method and **β**-Method Combined Side Capacity Predictions with Outliers Removed

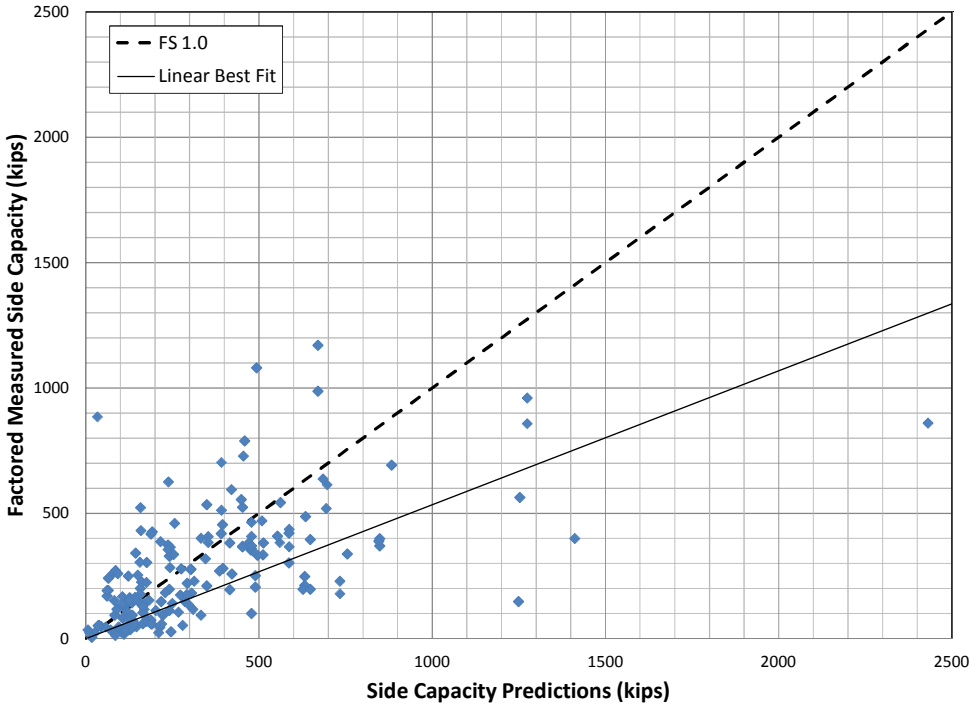

Figure 6-11: Meyerhof SPT Method and **α**-Method Combined Side Capacity Predictions with Outliers Removed

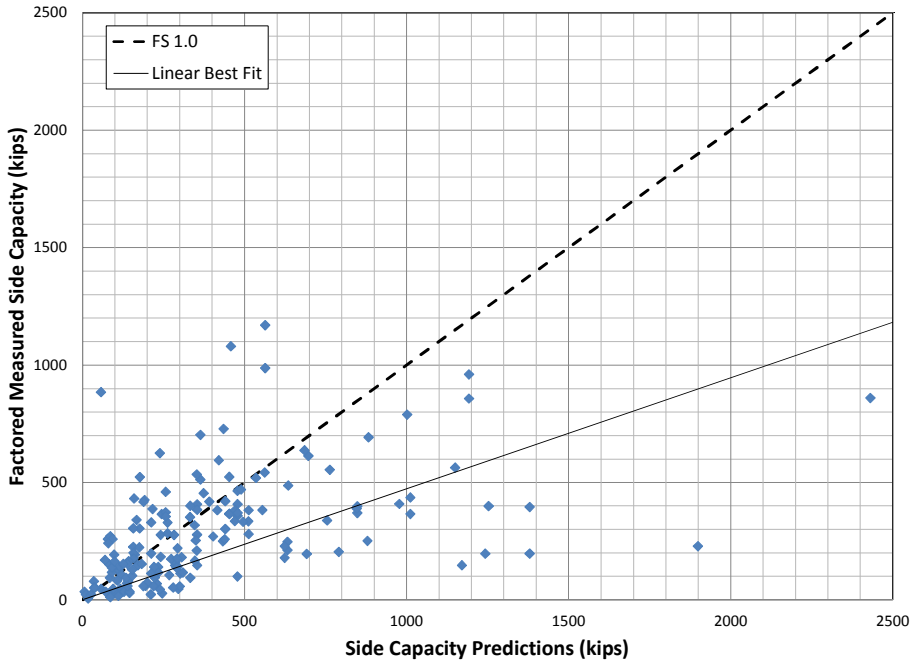

Figure 6-12: Meyerhof SPT Method and **β**-Method Combined Side Capacity Predictions with Outliers Removed

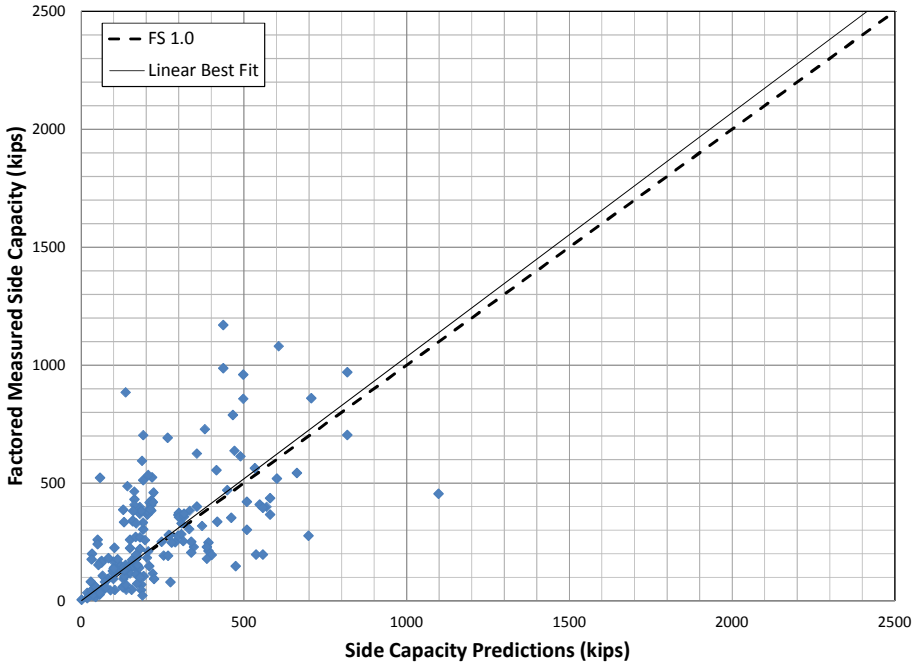

Figure 6-13: Meyerhof Method and **α**-Method Combined Side Capacity Predictions with Outliers Removed

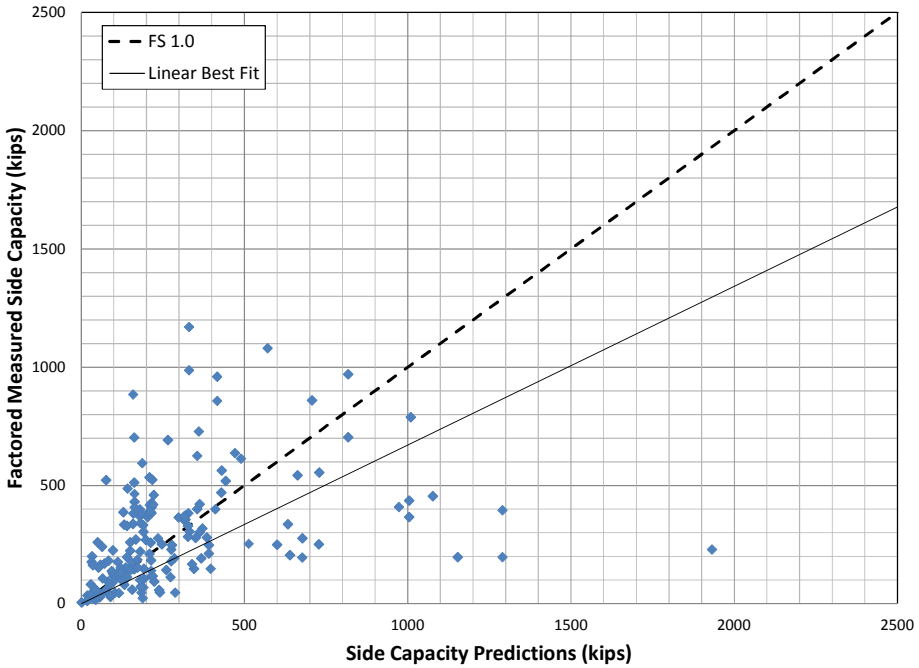

Figure 6-14: Meyerhof Method and **β**-Method Combined Side Capacity Predictions with Outliers Removed

The quality of each best fit line is presented in Table 6-5. It is immediately evident that the Meyerhof method coupled with the α-method for cohesive soils had the most reliable best fit line. The slope of the best fit line for the Meyerhof and α-method was 1.04 which is close to the line of equality having a slope of 1.0. The slopes of the best fit lines for the other methods showed that on average the other methods overestimated the side capacity of the pile by 1.5-2.8 times. The slope of the best fit lines for methods containing the α-method for cohesive were always closer to the equality line than those methods containing the β-method for cohesive. Likewise the slope for the best fit lines for methods containing the Meyerhof method for granular were closer to the equality line than either the Standard Penetration Test (SPT) or the Nordlund method, with the Nordlund method being further away than the SPT method.

Table 6-5: Description of Best Fit Line for Side Capacity Prediction Method

	Nordlund + α	Nordlund + β	Meyerhof SPT + α	Meyerhof SPT + β	Meyerhof + α	Meyerhof + β
Slope	0.40	0.36	0.53	0.47	1.04	0.67
Std. Error of Regression (kips)	203.17	214.23	220.43	231.51	188.18	249.10
R^2	0.68	0.65	0.64	0.60	0.73	0.52

Even the scatter around the best fit line for the Meyerhof and α-method was the least of all best fit lines. The line had the smallest standard error and coefficient of determination R^2 value that was closest to 1.0. However, the data around the best fit line still showed significant scatter with a relative standard error of 33% (standard error/mean). It was also interesting to note that the scatter around the best fit lines for the Meyerhof SPT based methods were worse than the best fit lines for the Nordlund method.

The effectiveness of each prediction method was evaluated by comparing the standard error of each method's data to the line of equality rather than the best fit line. The standard error relative to the line of equality for each prediction method is displayed in Table 6-6. The Meyerhof method + α-method was determined to have predictions closest to the line of equality. This method had a standard error from the line of equality that was approximately 100 kips closer than any of the other prediction methods. The data also indicated that the comparisons using the α-method on average had prediction errors approximately 70 kips less than the β-method predictions using corresponding prediction methods for granular material. Furthermore, it was readily evident that the Meyerhof based predictions had the smallest error and the Nordlund based predictions had the largest error. The Nordlund based errors were on the order of 2.25 larger than the

Meyerhof based errors. The strength of the Meyerhof method is that it has a limiting stress value with depth which is not applied to the Nordlund method. The Meyerhof, Nordlund and α-method predictions will likely improve as the quality of the soil properties increase while the SPT method and β-method will not. These predictions used soil properties for granular soils correlated from SPT N-values, but if the properties were measured directly the predictions would likely improve.

The relative standard error is an indicator of the precision of the estimates made by each combination of methods. The analysis of each method's predictions versus the equality line indicated that none of the methods showed much precision, but when compared to each other it was evident that the Meyerhof method and α-method combination was most precise. It was the only method with less than 100% relative standard error. This statistic also indicated that the β-method for cohesive soil and Nordlund method for granular soil were least precise. The relative standard error could be important for determining an appropriate factor of safety to be applied to each method's prediction.

Table 6-6: Standard Error in Side Capacity Estimates Relative to Line of Equality

	Nordlund + α	Nordlund + β	Meyerhof SPT + α	Meyerhof SPT + β	Meyerhof + α	Meyerhof + β
Std Error from Equality Line	488 kips	549 kips	338 kips	393 kips	189 kips	280 kips
Rel. Std Error from Equality Line, %	175	197	122	142	68	101

6.2.2.2. Discussion of Causes of Scatter

The scatter of the data can be divided into two divisions. One is the systematic differences of a method as indicated by the slope of the best fit line relative to the line of equality. This highlights differences of the methods. The second major division of scatter relates to scatter around the best fit line. Some of this pertains to a particular method, but in general this type of scatter affects all methods and has different sources than the method related differences. In this category also are possible shortcomings of the predictions.

The parameters for the β-method for cohesive soils are obtained from correlations to material descriptions in published literature. They assume an effective stress limiting value for side shear. For piles that are placed in soft clay, it is difficult to accept that a limiting value of shear will occur as a drained failure rather than an undrained failure. The better performance of the undrained α-method may be indicative of this difference of failure mode. This better performance of the α-method may be related to the availability of undrained shear strength tests onsite, while strength data is obtained historically for the β-method.

The Nordlund method was developed for piles with lengths of 25 to 40 ft and thus does not show a limiting shear stress with depth. For deep piles, the limiting stress with depth as used by the Meyerhof method is quite important. Although the Nordlund method has a correction for pile displacement, there were few H-piles in its development. The Nordlund method may not reflect the low displacement nature of H-piles as well as the Meyerhof method. The SPT method is subject to limitations of the SPT Test. In glacial tills, where gravel and cobbles exist, the SPT can give misleading results when the gravel

and cobble particles are bigger than the split spoon opening. Different kinds of split spoons and hammers used in the SPT can affect the ability of the measurements to produce consistent and repeatable correlations.

For scatter around the best fit lines, there are a number of possible limitations of the properties or methods to obtain property values that can cause scatter. The horizontal earth pressure (K_h) used in the Meyerhof method and also in the Nordlund method were taken from typical ranges and were not measured. This is especially relevant for basal till where the K_h value may be quite high and where much side support is found. The peak drained friction angle for each granular layer was obtained from correlations to SPT. The above noted limitations to SPT will affect obtaining a representative friction angle from SPT. The values of pile-soil interface friction angle were taken from historical values which are given in ranges. It is not known where in the range that Maine soils may be. A constant of friction angle for glacial till (obtained from the literature) was used. Variations in this friction angle will affect the side capacity.

The setup factors applied to the CAPWAP® measured values were developed from limited EOD/BOR data where most of the BOR values were taken the day following the EOD. Although the extrapolations to an anticipated 95% consolidation setup at 270 days appears reasonable, differences in consolidation rate can change the number of days to 95% setup. Although the change with time of setup by Skov and Denver is used by others and appears reasonable in the literature, it is still an extrapolation based on limited data to obtain the A factor.

In general, one boring was conducted per abutment. This soil profile was applied to all piles for that abutment. When more than one pile was dynamically tested at an abutment, sometimes quite different capacities were measured between the piles. This indicated the presence of a variation in subsurface profile across the abutment. When only one pile for an abutment was tested, then it is not known how much the profile at the pile is different from the subsurface profile at the boring.

There were anomalies in the dynamic testing that were noticed. These included large increases or decreases in the side shear with corresponding decreases or increases in end bearing from EOD to BOR. Sometimes with increased side capacity at BOR, the hammer in insufficient to create a bearing failure at the tip (thus the tip capacity shows to be lower). This may have contributed some scatter.

6.3. Comparison of Measured and Ultimate Bearing Capacities

The dynamically measured end capacities from CAPWAP® analyses were factored to the 270 day ultimate capacities using the values in

Table **5-2**. These factored measured values were then compared to the calculated ultimate bearing capacities from static design methods. The results of the comparisons on bedrock are shown in Figure 6-15 through Figure 6-16 and piles in till are shown in Figure 6-20 through Figure 6-22. The comparisons are separated by pile type to show the effectiveness of each static analysis equation at predicting the measured capacity.

There were a total of 216 piles resting on bedrock and 26 piles that fetched up during driving above bedrock in granular soil layers. There are 8 piles located in Georgetown which were not included in the bedrock analyses, because the piles were

founded on highly sloping bedrock. This indicated that they would not achieve the full bearing area on bedrock. There were only 179 piles included in the end bearing analysis using the CGS method. The pile deficit is due to a lack of information about the bedrock joints in the project documents provided by MaineDOT. Without this information predictions about the capacity of the pile could not be determined.

6.3.1. Comparison for Piles Bearing on Bedrock

The factored measured end bearing capacities for piles resting on bedrock were compared to predicted pile capacities using the CGS and proposed IRM. The results of the comparisons are shown in Figure 6-15 and Figure 6-16. The piles were plotted separately for closed end pipe piles, H-piles and open end pipe piles to investigate the effects of bearing area on the predicted capacities.

Upon inspection of the capacity comparison plots, it was evident that the proposed IRM, per Rowe and Armitage (1987), produced the better predictions. In the proposed IRM, an average rock effective unconfined strength based upon rock type (sedimentary, metamorphic, or igneous) is used to find the bearing capacity of the rock. This effective average unconfined strength was derived from the existing database of dynamic end bearing measurements. Therefore the average calculated bearing for each rock type should be close to the line of equality, but the variability around the mean is important for this simplified method. However, when the variability of the proposed IRM is compared to the variability of the CGS method, there is greater variability in the CGS method despite the CGS method considering more variables than the proposed IRM. There are too many unknowns with the CGS method to make reliable predictions. Estimations about parameters for the rock mass need to be made from small rock cores or

in the case of this report from bedrock descriptions in the boring logs. Some of the parameters, such as discontinuity opening, are not found with traditional subsurface investigations. Additionally, the unconfined compressive strengths of the bedrock are taken from published ranges.

There are some conflicting trends shown in the results of each method. The proposed IRM indicated that open end pipe piles achieved larger bearing capacities on bedrock than closed end pipe piles and H-piles, but the CGS method predicted that the closed end pipe piles would have much larger pile capacities. The CGS trend is the most sensible because closed end pipe piles have the largest cross sectional area. However, the open end pipe piles generally had the highest measured bearing capacities as shown in the proposed IRM predictions. It is intuitive that the open end pipe piles have larger measured capacities than the H-piles because the cross sectional area of steel is larger for the open end pipe piles. The lower closed end pipe pile capacities may be counterintuitive, but are likely due to the fact that a reduction factor of 9.3 was applied to the proposed IRM predictions as explained in Section 3.4.1. The reduction factor was used to ensure that the closed end pipe piles could use the same back-calculated q_u values as for low displacement piles. It was assumed that the pile tip fully penetrated the bedrock, so the full cross section of the pipe was used as the bearing area of the pile.

Some of the scatter of both methods may be caused by some piles fetching up in till while they were calculated to bearing on rock. The dividing line between a pile that ends in till and one that ends on rock is not well defined. Some of the lower measured rock values may have actually been terminated in till.

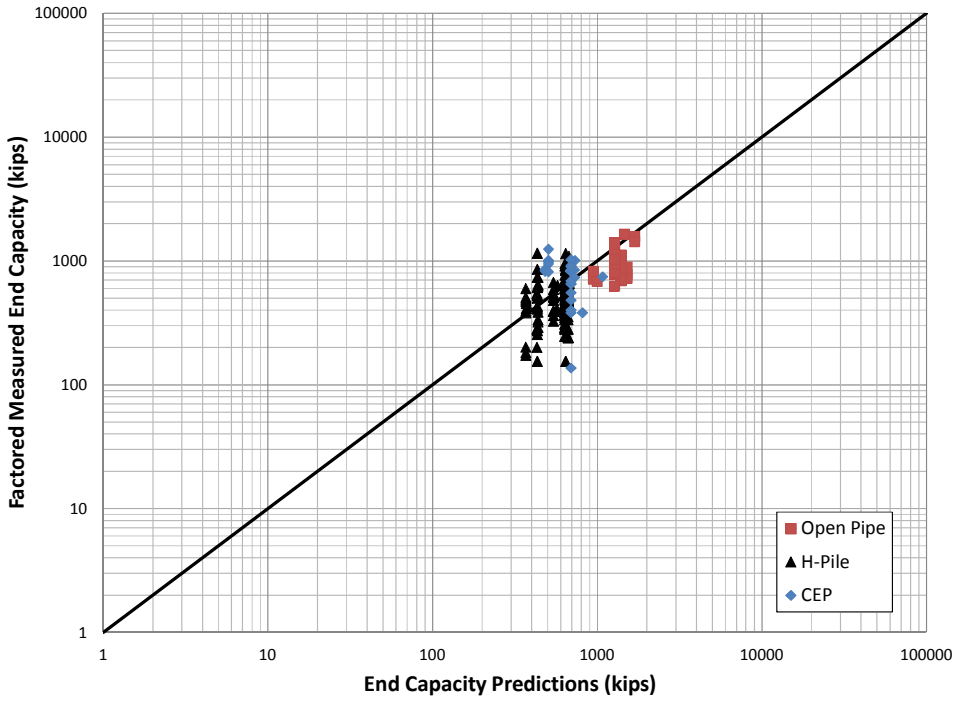

Figure 6-15: Proposed Intact Rock Method Predictions for Bearing Capacity on Rock

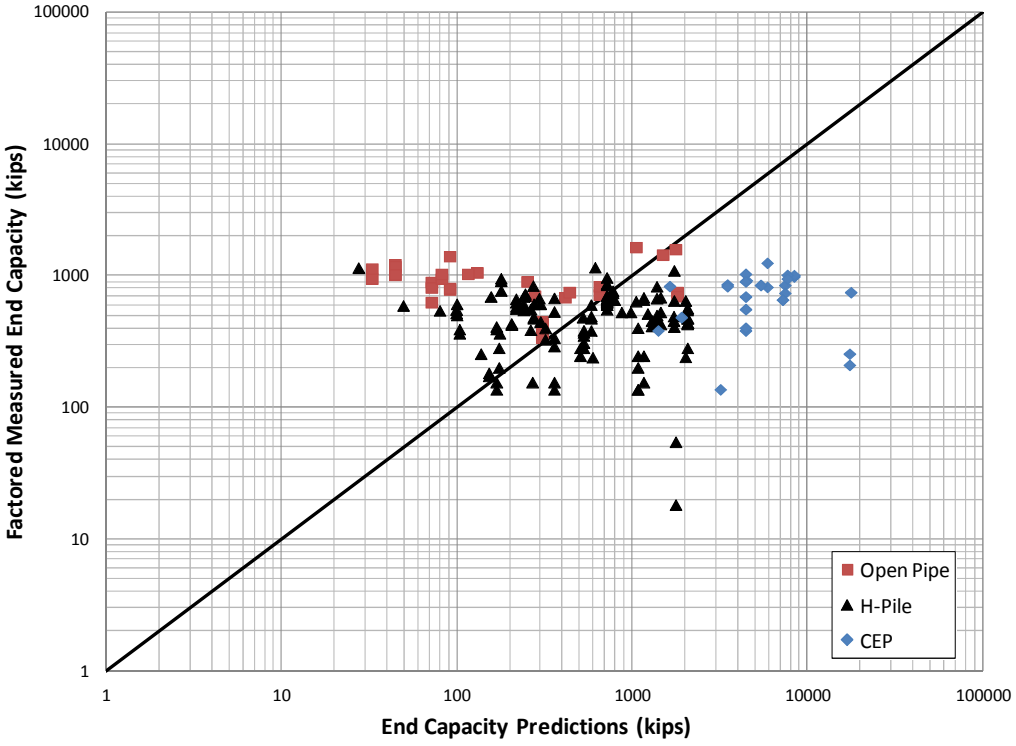

Figure 6-16: CGS Method Predictions for Bearing Capacity on Rock

6.3.2. Comparison for Piles Bearing in Till

A difference in the pile bearing capacities existed depending on the type of materials in the bearing strata. This led to an analysis on the effect of the pile bearing area and soil composition on predicting the measured capacities. The results of these analyses are shown in Figure 6-17 through Figure 6-19. The data suggested that generally the coarse grained till material (which sometimes included cobbles) had better predictions of the measured capacity when a box perimeter (H-piles) or closed pipe area (open end pipe piles) was used as the bearing area. The cross sectional area of the steel provided the best prediction for fine grained tills such as dense clayey, silty, or fine sandy material. These respective areas were used for the comparisons. If strength tests confirm a difference of friction angle for these two tills, then this correction must be reexamined. There were not any changes made to the bearing area for the closed end pipe piles because there is no chance of plugging like there is with the low displacement piles.

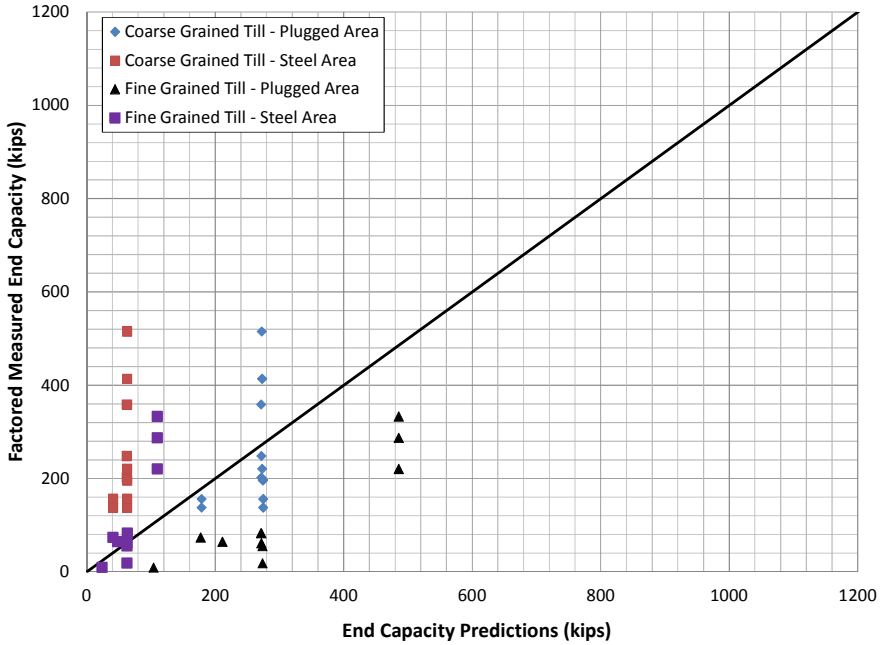

Figure 6-17: Effect of Grain Size on Meyerhof Bearing Predictions in Till

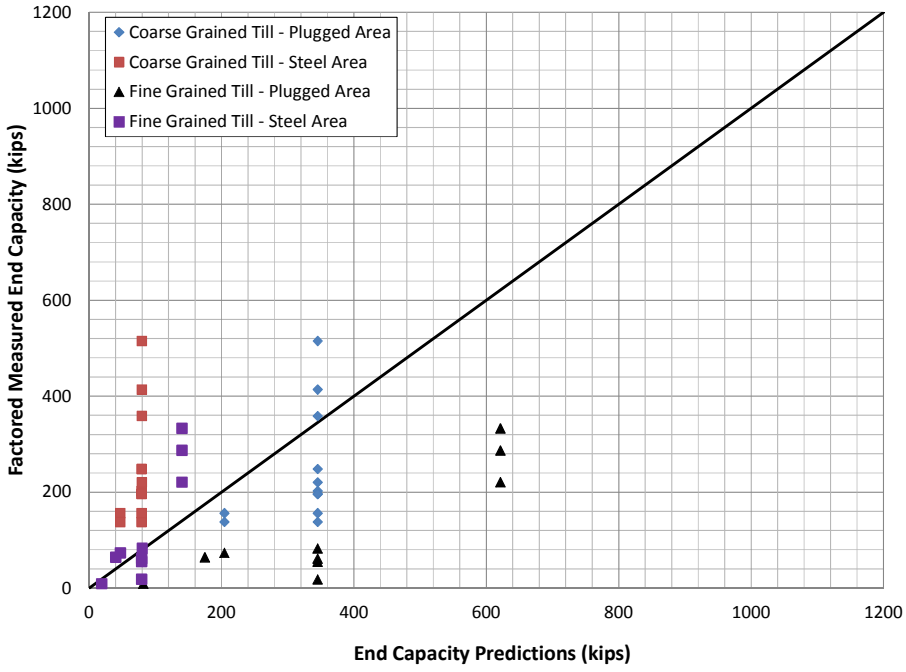

Figure 6-18: Effect of Grain Size on Nordlund Bearing Predictions in Till

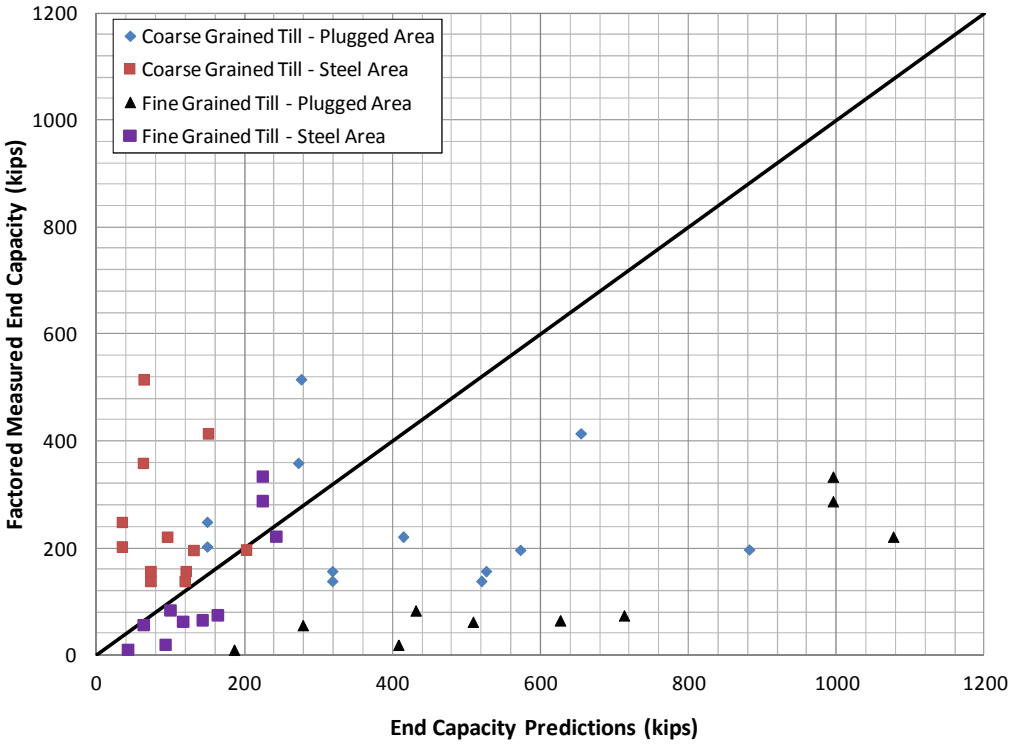

Figure 6-19: Effect of Grain Size on Meyerhof SPT Bearing Predictions in Till

The ultimate pile tip capacities in till were predicted using the Meyerhof, Nordlund, and Meyerhof SPT analyses and compared to the dynamically measured capacity at 270 days using the setup factors presented in Section 5.1.5. The results of the till comparisons are shown in Figure 6-20 through Figure 6-22. The Meyerhof and Nordlund methods provided very similar comparisons, while the SPT based method showed some more scatter in its predictions. The similarities of the Meyerhof and Nordlund methods are not coincidental. The assumed friction angle of 38° for dense to very dense tills and the limiting values allow for little deviation in the predictions. The limiting criterion used in recent versions of Nordlund's method is the same as for the Meyerhof method. The SPT based analysis shows more scatter in its predictions due to the variability of the SPT readings from pile to pile. The use of a constant friction angles within the till layers eliminates the scatter from the Nordlund and Meyerhof predictions, however, this does not necessarily mean that these values are more reliable.

The bearing capacity predictions for the open end pipe piles are a little low. This may be related to using the steel area as the bearing area. There is likely some resistance due to the soil plug which has formed inside the pile. Not considering the plug for bearing potentially under predicts the end bearing capacity. The plug in the pile should pick up some of the bearing load.

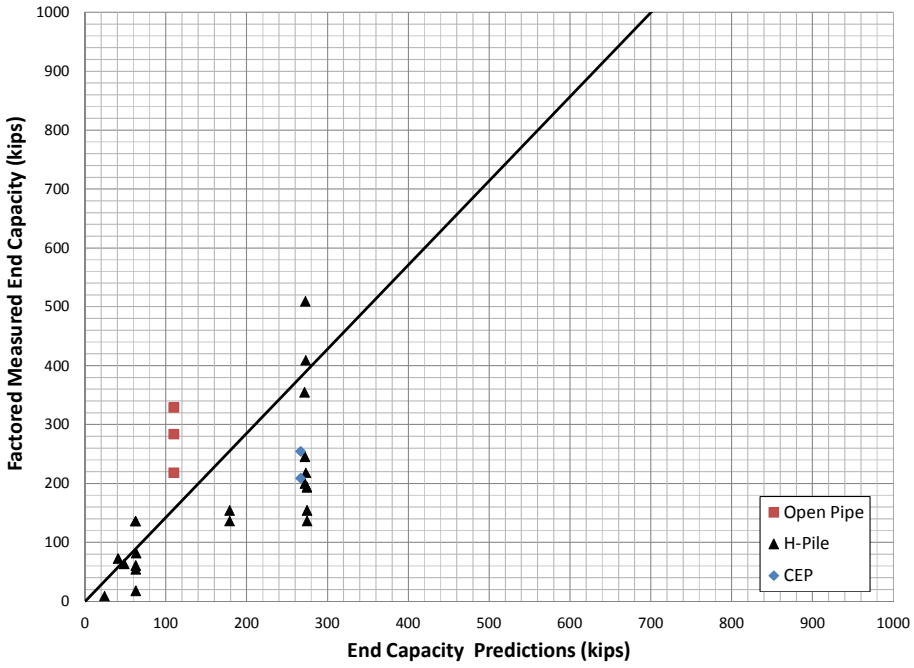

Figure 6-20: Meyerhof Method Bearing Predictions for Till

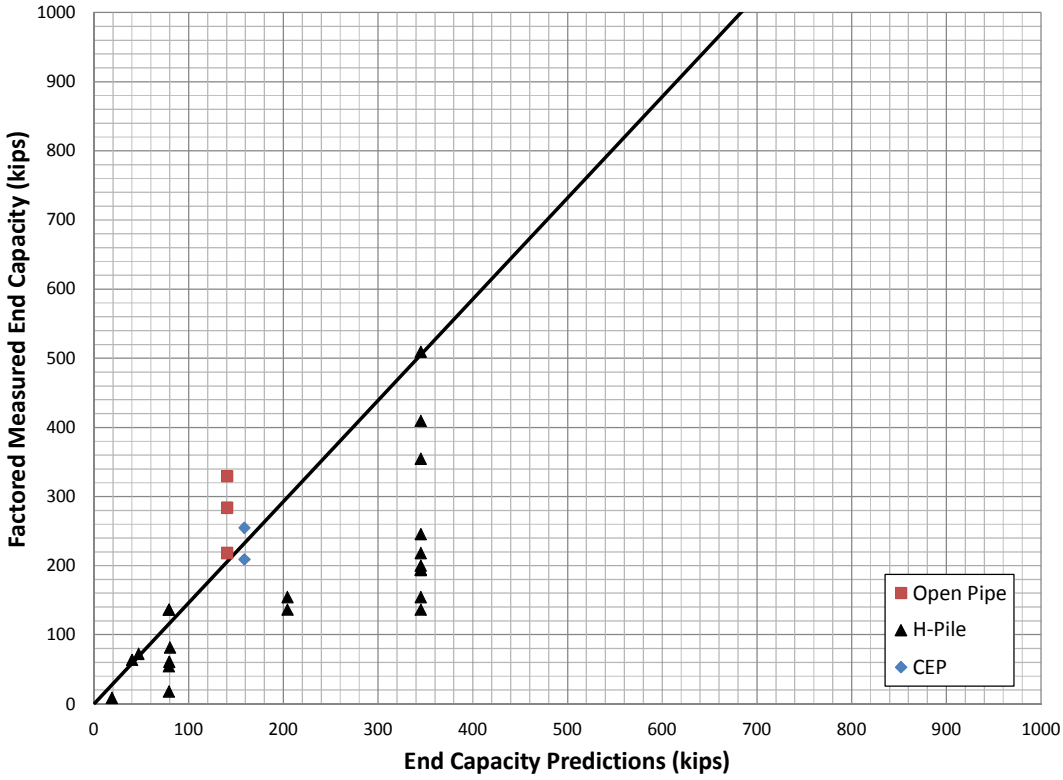

Figure 6-21: Nordlund Method Bearing Predictions in Till

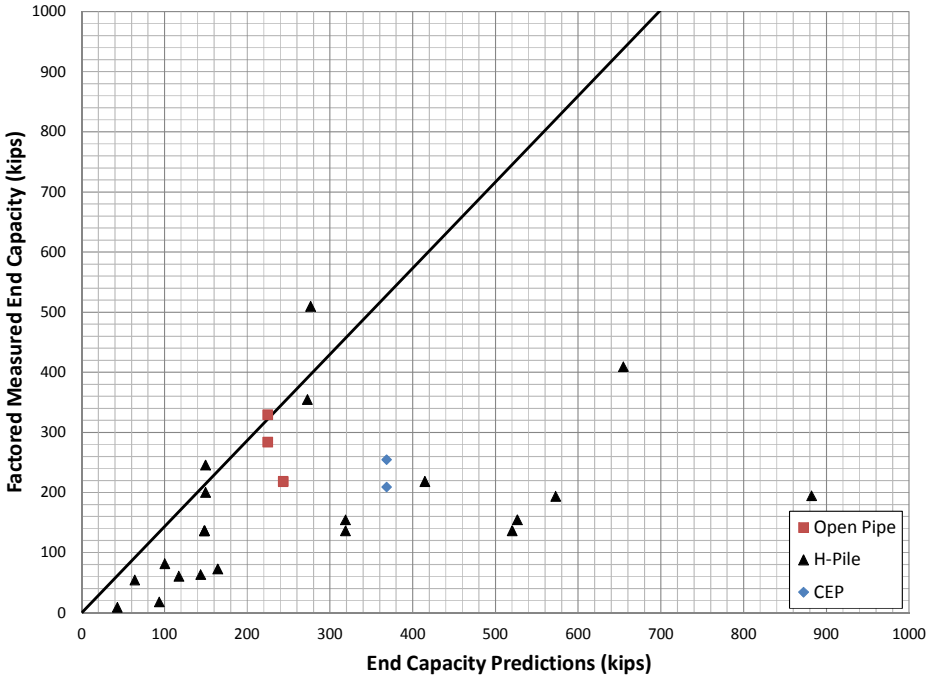

Figure 6-22: Meyerhof SPT Method Bearing Predictions in Till

6.4. Reliability of Selected Methods

The purpose of this section is to present the selected methods which provided the most accurate predictions in a format which allows for the reliability of these methods to be evaluated. Figure 6-23 through Figure 6-26 show the relative and cumulative frequencies of the predicted to factored measured capacity ratios (PFMCR). These figures can be used to pick appropriate PFMCRs for a desired reliability. The combination of Meyerhof method and α-method indicates that approximately 68% of the data falls below a PFMCR of 1.2 with 56% of all data falling within a range of PFMCRs of 0.4 to 1.2. Overall, the data shows a fairly tight distribution centered around a PFMCR of 1.0 which indicates a good fit. It also shows few outliers as approximately only 4% of data exceeds a PFMCR equal to 2.8.

The PFMCRs shown for the proposed IRM in

Figure 6-24 indicate a fairly normal distribution of the data. Approximately 41% of the predictions fall within a range of PFMCRs from 0.8 to 1.2. Additionally, approximately 90% of the data falls below a PFMCR equal to 2.0. The majority of the outliers occur on the over-prediction side of the distribution; however, only less than 1% of the data exceeds a PFMCR of 3.0. When comparing the proposed IRM to the CGS method (Figure 6-25), it is evident the CGS method predictions have a more poorly distributed data set. The CGS method histogram does not show any significant peak in the data shows a significant amount of outliers with approximately 48% of the data falling below a PFMCR of 0.5 or above a ratio of 4.0.

The distribution of PFMCRs with Meyerhof method for end bearing till is shown in Figure 6-26. The distribution indicates the existence of two distinct peaks in the data at PFMCRs from 0.4 to 0.6 and 1.0 to 1.2; however, they are fairly close to one another given the distribution of the remaining data. Approximately 54% of the data falls within the PFMCR range of 0.4 to 1.2. Only 8% of the data lies above a PFMCR of 2.2 while only 4% of the data lies above a PFMCR of 3.0. This indicates that the outliers are fairly well contained, especially when compared to the CGS method results.

A brief statistical analysis of the data which indicates the appropriate PFMCR and the corresponding confidence level for each method is shown in Table 6-7. A PFMCR for each method was selected as the 95^{th} percentile value for each data set i.e. 5% of piles will have a PFMCR greater than the selected value. The 95% confidence interval indicates what percentage of piles is likely to be observed below this PFMCR when used

in the future. It should be noted that a confidence interval could not be generated for the Meyerhof method for bearing capacity in till because of the small sample size of data included in the analysis. The PFMCR observed for this method still has 5% of piles exceeding the value; however, its reliability cannot be confidently reported for future projects. The PFMCR for the CGS method at the 95th percentile is very large indicating the poor predictive ability of this method.

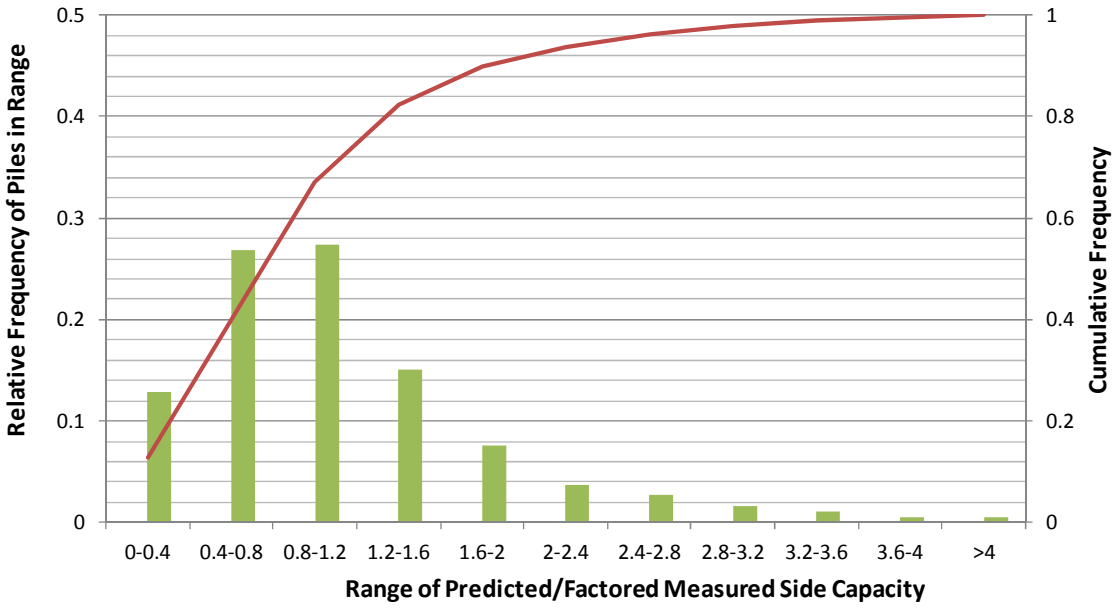

Figure 6-23: Reliability of Meyerhof Method and **α**-Method Combined Predictions for Side Capacity

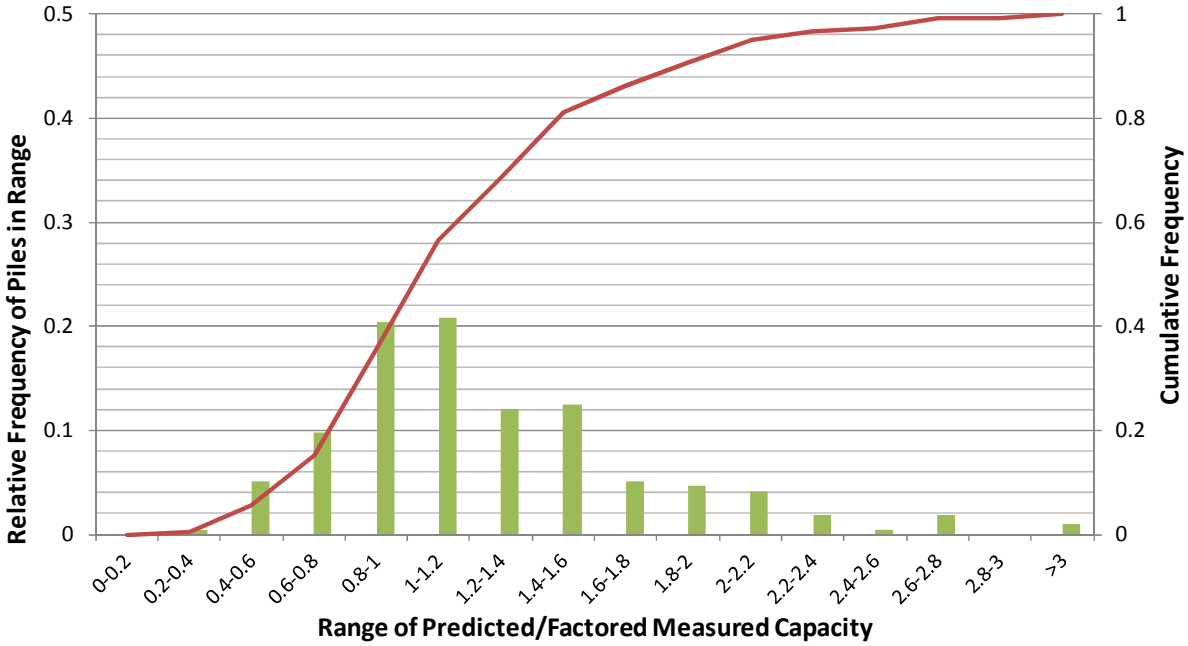

Figure 6-24: Reliability of Proposed Intact Rock Method for Predicting End Capacity on Rock

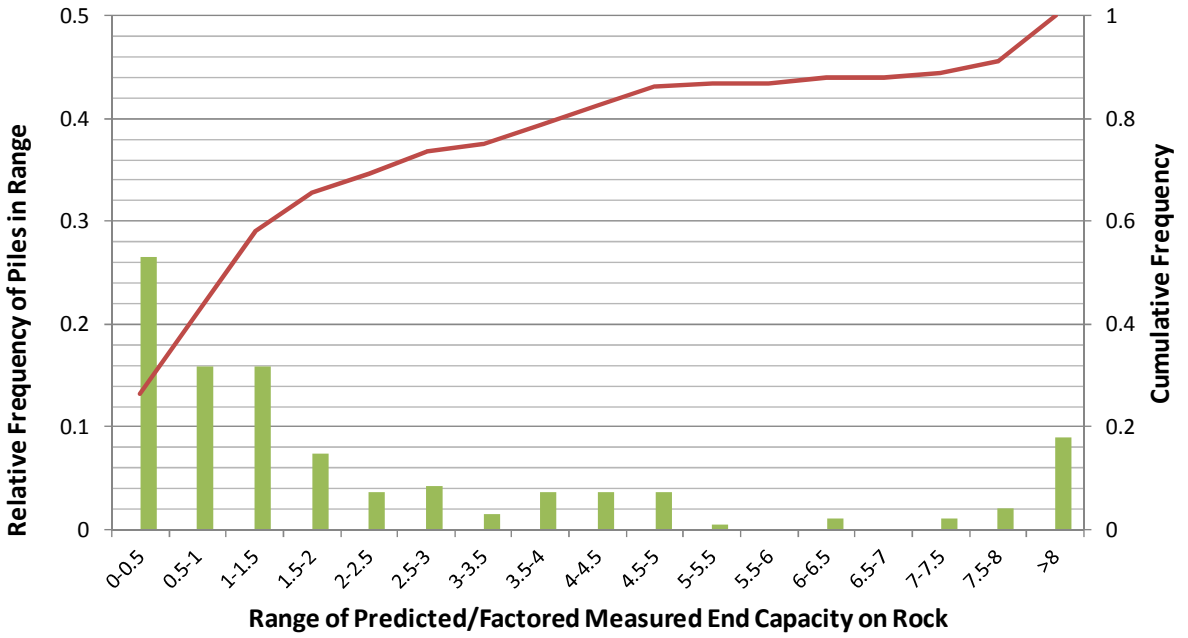

Figure 6-25: Reliability of CGS Method for Predicting End Capacity on Rock

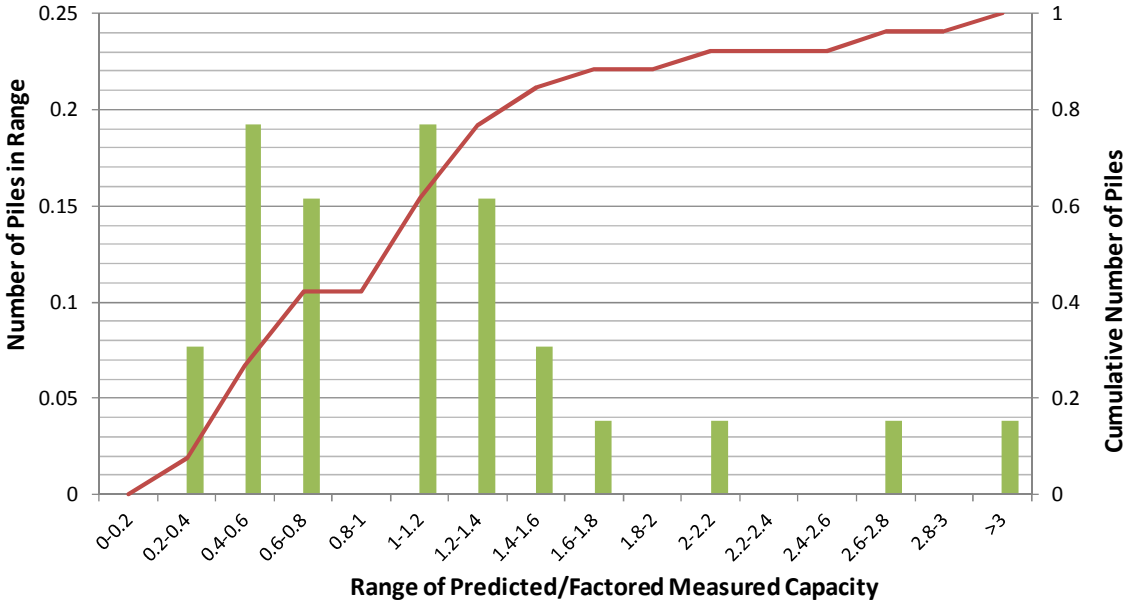

Figure 6-26: Reliability of Meyerhof Method for Predicting End Capacity in Till

Table 6-7: Ratio of Predicted/Factored Measured Capacity at 95th Percentile with Confidence Intervals

		95% Confidence Interval	
Method	**Predicted/Measured**	**Lower Bound**	**Upper Interval**
Meyerhof + α -Method for Side Capacity	2.52	90.7%	97.9%
Meyerhof Method for End Bearing in Till	2.48	N/A	N/A
CGS Method for End Bearing on Rock	10.71	91.5%	98.0%
IRM for End Bearing on Rock	2.21	91.7%	97.8%

Chapter 7:

SUMMARY AND CONCLUSIONS

7.1. Effectiveness of Pile Capacity Calculation Methods

The second phase of this study analyzed the effectiveness of static capacity estimation methods recommended by the American Association of State Highway and Transportation Officials (AASHTO) and Federal Highway Administration (FHWA) at predicting Pile Dynamics, Inc. Case Pile Wave Analysis Program (CAPWAP®) measured dynamic capacities at end of driving (EOD) and in some cases at the beginning of restrike (BOR). For granular soils, the AASHTO recommended Nordlund method was compared to Meyerhof's soil property and Standard Penetration Test (SPT) based methods. Both the α-method and β-methods, which are recognized by the FHWA and AASHTO, were used to analyze cohesive soil layers. The Canadian Geotechnical Society (CGS) method and the proposed Intact Rock method (IRM) were studied for piles bearing on bedrock. For piles bearing in glacial till the Nordlund method was again compared to Meyerhof's soil property and SPT based methods.

7.1.1. Dynamic Measurements

It is important to note that the capacity of piles measured at the EOD will under-estimate the long term capacity as capacity will increase when soil remolded during driving recovers strength (setup). Piles can experience significant capacity increases with time up to approximately one year after driving, especially if the pile is driven through soft cohesive materials of considerable thickness. To compare the effectiveness of each method, setup factors were needed to scale the CAPWAP® measured capacities to the long term strength state (270 days). The setup factors were determined by using the Skov

and Denver (1988) relationship that had been calibrated to project piles that were tested at both EOD and at BOR. The setup factors were found for cohesive and granular soil layers separately. Furthermore, the cohesive factors were categorized by water content while the granular setup factors were determined for low and high displacement piles separately. It was shown in the calibration that the amount of setup in cohesive soil layers increased with water content, while the setup in granular soil increased with the amount of soil displaced by the pile. These setup factors were then applied to the dynamically measured capacities for comparison to capacity estimates by the different methods. It should be noted, however, that the majority of the restrike testing was conducted one day after driving and the calibration found for this restrike was utilized to find setup to the long term state at 270 days. Work by others on consolidation rates was utilized to estimate the time required to achieve the 95% of the long term strength.

7.1.2. Pile Side Capacity

The side capacity predictions by each method were then compared to the factored measured capacity for each pile analyzed. The factored measured capacities were plotted against the prediction methods. All of the methods showed some significant scatter which were often caused by anomalies in the subsurface or driving system. When justified, these measurements were excluded from the side capacity analyses. One cause of these low measurements is believed to be caused by soil arching around the pile in fill material or loose overburden during driving which prevented the layer from contributing to the measured capacity. Although downdrag and lateral squeeze may be present in the soft clay when these granular soils overlay soft clays and may affect the strength of the clay, the CAPWAP® method under the blow of the hammer should not detect downdrag. It is

more likely that the low factored strength of this soft clay may be caused by a low setup factor. There were also some piles which were excluded from the analysis due to apparent errors in the dynamic readings. These errors were evident due to significant and suspected impossible changes in pile capacity from EOD to 1 day BOR. Additionally, some data was excluded from the analysis due to an inadequate hammer to mobilize the full pile capacity along the bottom of the pile. This was especially evident for some of the piles tested at BOR where the setup along the pile caused the initial driving hammer to be inadequate for BOR.

The side capacity comparisons indicated that the α-method predictions produced more reliable estimates in cohesive soils than the β-method. In every case the granular prediction method coupled with the α-method for cohesive resulted in better capacity predictions than the granular prediction method coupled with the β-method for cohesive. The results also indicated that the Meyerhof method was most reliable in predicting the resistance of the granular soil layers. The Nordlund method for granular soils performed the worst of all the prediction methods for granular soils. The comparisons using the Nordlund method showed considerably more scatter than the other methods for granular and had best fit lines for the measured versus predicted data that had significant deviations from the equality line. Meyerhof's method for granular material coupled with the α-method for cohesive soils proved to be the most effective method for predicting side capacity. The best fit line for the measured versus predicted capacities was nearly unity and showed significantly less scatter than the other methods. The Nordlund method for granular soils coupled with the β-method for cohesive soils performed the worst of all side capacity measures. The Nordlund method and β-method predictions had

considerably more scatter than the other methods and significantly over-predicted the measured pile capacities. The over-predictions of the Nordlund method for granular soils were likely caused by the absence of a limiting factor with depth which both the Meyerhof and Meyerhof SPT methods have for granular soils.

There were some limitations in the values of soil property evaluations that may have contributed to the scatter in the side capacity predictions. The horizontal earth pressure coefficients (K_h) used in the Meyerhof method for granular soils were taken from typical published ranges and were not measured. This consideration is especially relevant for the K_h values used in basal till as there are not published values available for highly overconsolidated till. SPT results were corrected for type of hammer, diameter and depth of borehole and the overburden pressure. The resulting STP $(N_1)_{60}$ was used in correlations to obtain the peak drained friction angles for each soil layer. This is also applicable to the Nordlund based methods as the friction angles used in this method were also correlated from SPT N-values. These correlations have scatter and the direct application to the glacial soils in Maine may incur further scatter. The SPT N-value can be affected by large stress in the soil. The Meyerhof SPT method is susceptible to the concerns of consistency in SPT readings since SPT corrections were not used at that time and the N correlations by Meyerhof have large variability. Additionally, the friction angle of 38° for tills found by tests for New Hampshire tills may not be representative for all tills of varying particle size and composition. Shear strength of clay was primarily obtained from vane shears that had a variety of configurations affecting strength. Better estimates of these parameters could help improve side capacity predictions.

7.1.3. Pile End Bearing

7.1.3.1. Rock End Bearing

A new rock bearing method, the Intact Rock method (IRM), is proposed that relates capacity to rock type in Maine. The proposed IRM and Canadian Geotechnical Society (CGS) methods were compared to dynamic test results, and the results indicated that the proposed IRM had significantly better predictions. The proposed IRM had less scatter and had values closer to the line of unity than the CGS predictions. The cause of the CGS method's scatter is likely due to the uncertainty associated with its input parameters. The limitations and causes of scatter for each of the methods are discussed below.

The data available to designers from current subsurface investigations and laboratory testing is too limited for the use of the CGS method. The CGS method requires a detailed description of the entire bedrock mass beneath a project for piles bearing on rock. Most parameters required as inputs for this method are not available from typical subsurface investigations. Unconfined compressive strength (q_u) of the bedrock is rarely tested. Strengths based on a published range of values for each type of bedrock are then utilized for this method. Detailed discontinuity information (e.g. joint spacing and opening) is not directly available for the rock mass and must be interpolated from field descriptions of discrete bedrock cores. Calculations performed by the MaineDOT were included in the study where applicable. When the MaineDOT calculations were unavailable, the input parameters for the CGS method were estimated from the bedrock descriptions from each project's boring logs. When neither was available, the CGS method was not conducted for that pile. Ultimately the CGS method had a much larger

standard deviation and significantly more scatter than the piles analyzed using the proposed IRM.

The proposed IRM uses back-calculated unconfined compressive strength of bedrock to make estimations of end bearing capacity. The unconfined compressive strengths were back-calculated from the measured CAPWAP® end bearing capacities and contain average discontinuity effects and average rock strengths for Maine. The back-calculated q_u values for the proposed IRM were organized by bedrock type. The back-calculated unconfined compressive strengths of sedimentary, igneous, and metamorphic bedrock were 4.4, 5.4, and 5.2 ksi respectively. This process of back calculating strengths was not effective for closed end pipe piles using the closed end area. The resulting q_u for these piles were significantly smaller than those calculated for the other pile types. To account for this, a reduction factor of 9.3 was applied to the closed end pipe pile end area to provide more reasonable predictions. The actual bearing area of the closed end pile varies with the depth of penetration of the pile tip into the bedrock. This cross sectional area is difficult to predict because bedrock hardness, quality, and strength are variable from site to site, but after correction the area appears to be similar to H-piles and open pipe pile steel area.

7.1.3.2. Till End Bearing

The Meyerhof method for estimating end bearing capacity in till resulted in the best predictions. The Nordlund method showed very similar predictions to the Meyerhof method. Both methods used the same assumed friction angle for all till of 38°, and the Nordlund method specified by FHWA uses a Meyerhof limiting stress in its bearing

capacity estimations. The SPT method showed more scatter in its predictions which were likely caused by the use of SPT readings from each subsurface investigation.

7.1.4. Reliability of Selected Static Capacity Methods

The best performing methods for the static capacity analysis of side capacity, end bearing on rock and end bearing in till were the Meyerhof method and α-method combined, the proposed IRM, and Meyerhof method respectively. The relative and cumulative frequencies were plotted for each method and trends in the data were highlighted. Additionally, the CGS method was investigated to highlight the poor distribution and the amount of outliers which existed in the data.

A reliability analysis of each method was conducted which gave the predicted to factored measured capacity ratio (PFMCR) corresponding to the 95^{th} percentile of the data. These PFMCRs were determined to be 2.52, 2.48, 10.72, and 2.21 for the Meyerhof method and α-method combination for side capacity, Meyerhof end bearing in till, CGS method for end bearing on rock and the proposed IRM for end bearing on rock respectively. Additionally, a 95% confidence interval analysis was run for each method to find the reliability of the 95^{th} percentile value. It was found that generally the 95^{th} percentile PFMCR value may actually represent the 90^{th} to 98^{th} percentile value when used in future analysis. The 95^{th} percentile value could not be determined for the Meyerhof method in till due to the small sample size available for analysis.

Chapter 8:

RECOMMENDATIONS

The following recommendations can be drawn from the conclusions of this paper to help improve the pile design process for the MaineDOT.

The comparison of calculation methods to dynamic test capacities using information provided by the subsurface reports and the dynamic test reports led to the following recommendations.

1. The Meyerhof method for granular soils coupled with the α-method for cohesive soils produced the most reliable results and are recommended for determining the side shear resistances along driven piles.
2. The Meyerhof method for piles bearing in glacial till provided the most reliable estimates and is recommended for determining the end bearing capacity of piles not expected to reach bedrock.
3. It is recommended that for driven pile side capacity calculations the full cross sectional area of the steel be used for open and closed end pipe piles and a box area be assumed for H-piles (i.e. plugged flanges). For the end bearing on rock, the enlarged bearing areas from the protective driving tips are recommended in bearing capacity analyses for H-piles and open pipe piles. When calculating end bearing on rock for closed end pipe piles, it is recommended that the full cross sectional area of the pipe is used (a reduction factor of 9.3 is used in the calculations).
4. The back-calculated average unconfined compressive strengths determined by rock type or the use of site-specific unconfined compressive strength test results,

in conjunction with the proposed Intact Rock method (IRM) are recommended for more reliable estimates of end bearing capacity on bedrock.

Most of the dynamic load tests were conducted only at the end of driving (EOD). The EOD tests underestimate the long term capacity of piles. The following recommendations cover the change of pile capacity with time after the EOD tests.

5. Setup factors are recommended to be applied to the EOD measured capacity to determine a more representative pile capacity with time. Hannigan et al (2006) recommend conducting restrike testing 2-6 days after EOD and ASTM D1143 recommends conducting a static load test 3-30 days after EOD. Initially, it is recommended to apply 3 day setup values as determined in this study with a resistance factor appropriate to the EOD measured capacity and with a separate resistance factor appropriate to the added estimated setup capacity of the pile. If it is possible, it is recommended that a restrike test in 3 days be used.
6. It is recommended to conduct beginning of restrike (BOR) tests to confirm the setup of cohesive Maine soils with time. Some of the BOR tests are recommended to be conducted at times when the cohesive soils are anticipated to be 95% consolidated. These should be correlated to field exploration results.

Even the most reliable recommended methods had scatter of results in comparison to dynamic load tests. Estimated subsurface stratigraphy and soil on rock property values can contribute to the scatter. The following recommendations concern improvements in soil/rock property values and stratigraphy that can lead to more reliable calculations.

7. At some abutments, there were significant differences in the measured capacity and length of piles for different piles at the same abutment. Only one boring was conducted at these abutments, but the pile load tests indicated changing stratigraphy at the abutment. It is recommended that another boring be conducted at abutments where the geologic investigations indicated possible stratigraphic variations. The additional boring would improve the reliability of the calculated capacity estimates.
8. Strength testing of glacial till is lacking in the literature. It is recommended that a testing program be conducted to determine the strength characteristics for tills of various compositions. The till should be obtained from at least two sites of ablation till and two sites of basal till with each site having differing grain sizes. Samples should be obtained from a test pit excavated by a backhoe, since boreholes are inadequate to obtain representative till samples. Strength testing should be conducted with triaxial equipment and large scale (to incorporate larger particle sizes) direct shear equipment. This would lead to more reliability of the calculated estimates for side friction and end bearing in the till layers.
9. The coefficient of friction, ϕ, for granular soils has been correlated to Standard Penetration Test (SPT) N-values. Although this is the principal method of obtaining ϕ, there are several correlations and the reliability of the correlations is not known. It is recommended that a field and laboratory investigation be conducted to determine the correlation of SPT N and ϕ values to obtain more reliable estimates of side and end capacity in New England glacial granular materials. This would require 3 borings per site with SPT each 3 ft. Test pits

would be excavated for samples and to obtain in situ densities. Triaxial test equipment would be used to obtain strength values for various relative densities. At least three non-till granular materials, each with a different grain size, as well as one ablation till and one basal till should be sampled and tested.

10. For the Meyerhof method in granular, the lateral earth coefficient value (K_h) has been taken from literature except for basal till where none was found. For basal till where much of the side shear on piles appears to develop, the value of K_h should be quite high as a result of the high over-consolidation. It is recommended that data on the value of K_h, especially in basal till, be obtained by self-boring pressuremeter field testing as an addition to Recommendation 9 to utilize the results of Recommendation 9 sampling and testing. Pressuremeter boreholes would be located in the vicinity of each SPT borehole. More than one basal till location should be tested. This would lead to more reliability for the Meyerhof method.
11. Although the proposed Intact Rock method (IRM) improves reliability compared to the Canadian Geotechnical Society (CGS) method, there is still scatter with the proposed IRM. It is recommended that site-specific uniaxial compressive strength testing of intact rock be conducted for use in the proposed IRM. A LRFD resistance factor of 0.50 is recommended to be applied to the nominal end bearing pile resistance calculated using the proposed IRM.
12. When granular fill is placed over soft clay, then a hole may develop in the fill around the pile during driving. The time for closing of the hole is variable. It is

recommended that no side support for the pile should be considered in the granular fill in design calculations.

13. Once more data is obtained on soil and rock properties and setup; it is recommended that resistance factors reflecting Maine's conditions be formulated for side and end bearing capacity of piles.

REFERENCES

AASHTO (2010). *AASHTO LRFD Bridge Design Specifications*. American Association of State Highway and Transportation Officials, Washington, D.C.

AASHTO. (2002). *Standard Specifications for Highway Bridges*. 17th ed., Washington, D.C.: 2002.

American Petroleum Institute. (1993). "Recommended practice for planning, designing and constructing fixed offshore platforms-working stress design." *API RP 2A*, 20th Ed, American Petroleum Institute, Washington, D.C.

Andrews, David W. (1987). "The Engineering Aspects Of The Presumpscot Formation." *Proceedings of Geologic and Geotechnical Characteristics of the Presumpscot Formation Maine's Glaciomarine "Clay."* Maine Geological Survey, Morrison Geotechnical Engineering, University of Maine Civil Engineering Dept., University of Southern Maine Geosciences Dept., Augusta, ME, 1-15.

Aoki, N., and Velloso, D.A. (1975). "An approximate method to estimate the bearing capacity of piles." *Proc., 5th Pan-American Conference of Soil Mechanics and Foundation Engineering*, Buenos Aires, 367-376.

Associated Pile & Fitting (2012). Request for Information. 27 August 2012. Email.

ASTM. (2008). "ASTM Standard 4945: Standard Test Method for High-Strain Dynamic Testing of Deep Foundations." ASTM International, West Conshohocken, PA.

ASTM . (1996). " ASTM Standard 1143: Standard Test Method for Piles Under Static Axial Compression Load." ASTM International, West Conshohocken, PA.

Attwooll, William J., Holloway, D. Michael, Rollins, Kyle M., Esrig, Melvin I., Sakhai, Si, and Hemenway, Dan. (1999). "Measured Pile Setup During Load Testing and Production Piling: I-15 Corridor Reconstruction Project in Salt Lake City, Utah." *Transportation Research Record,* Transportation Research Board, (1663), 1-7.

Berezantzev, V. G., Khristoforov, V., and Golubkov, V. (1961). "Load Bearing Capacity and Deformation of Piled Foundations." Proc. 5th Int. Conf. S.M. & F.E., vol. 2: 11-15.

Bieniawski, Z.T. (1989). *Engineering Rock Mass Classification*, Wiley, New York, NY.

Bjerrum, L. (1954). "Geotechnical properties of Norwegian marine clays," Geotechnique., vol. IV, no. 2, pp 49-69.

Bowles, J. E. (1977, 1982, 1988), *Foundation Analysis and Design*, McGraw-Hill, 816 pp.

Bradshaw, Aaron S., and Baxter, Christopher D. (2006). "Chapter 4. Dynamic And Static Pile Load Test Data - Design and Construction of Driven Pile Foundations: Lessons Learned on the Central Artery/Tunnel Project." Federal Highway Administration, <http://www.fhwa.dot.gov/engineering/geotech/pubs/05159/chapter4.cfm> (Apr. 29, 2012).

Bullock, Paul J. (2012). *Advantages of Dynamic Pile Testing*. *Full-scale Testing and Foundation Design: Honoring Bengt H. Fellenius*. American Society of Civil Engineers, Reston, VA, 194-709.

Caldwell, D. Q., Hanson, L.S., and Thompson, W.B. (1985). "Styles of Deglaciation in Central Maine." *Late Pleistocene History of Northeastern New England and Adjacent Quebec*. Geological Society of America, Boulder, CO, 45-58.

Camp III, William M., and Parmar, Harpal S. (1999). "Characterization of Pile Capacity with Time in the Cooper Marl Study of Applicability of a Past Approach To Predict Long-Term Capacity." *Transportation Research Record,* Transportation Research Board, (1663), 16-24.

Canadian Foundation Engineering Manual, 2nd ed., Canadian Geotechnical Society, Ottawa, Canada, pp. 456. (1985).

Carter, J.P., and Kulhawy, F.H. (1988) "Analysis and Design of Drilled Shaft Foundations Socketed into Rock," *Report EL-5918*, Electric Power Research Institute, Palo Alto, CA, 188.

Das, Braja M. (2010). *Principles of Foundation Engineering*. Stanford, CT, Cengage Learning.

Davisson, M.T. (1972). "High-Capacity Piles." *Proceedings of Lecture Series on Innovations in Foundation Construction*, Chicago, IL, 81-112.

Dixon, Leif A. (1988). *Effects of Bitumen Coating on the Axial and Lateral Loadings of Abutment Piles Subject to Downdrag.* (Master's Thesis). University of Maine, Orono, ME.

Federal Highway Administration. (1990). *"Dynamic Pile Monitoring and Pile Load Test Report: State Highway 77 Fore River Bridge Replacement."* Federal Highway Administration, Washington, D.C.

Foye, K. C., Abou-Jaoude G. G., and Salgado R. (2004). *Limit States Design (LSD) for Shallow and Deep Foundations*. FHWA/IN/JTRP-2004/21. Joint Transportation Research Program, Indiana Department of Transportation and Purdue University, West Lafayette, Indiana.

Goble, G.G., and Rausche. F. (1976). “Wave Equation Analysis of Pile Driving, WEAP Program.” Federal Highway Administration, Washington, D.C.

Hannigan, P. J., Goble, G. G., Thendean, G., Likins, G. E., and Raushe, F. (2006a). "Design and Construction of Driven Pile Foundations- Volume I." FHWA-HI-97-013, Federal Highway Administration, Washington, D.C.

Hannigan, P. J., Goble, G. G., Thendean, G., Likins, G. E., and Raushe, F., (2006b). "Design and Construction of Driven Pile Foundations- Volume II." FHWA-HI-97-013, Federal Highway Administration, Washington, D.C.

Hoek, E. , Carranza-Torres, C. , and Corkum, B. (2002). “Hoek-Brown failure criterion.” *Proc., 5th North American Rock Mech. Symp. and 17th Tunneling Assoc. of Canada Conf.: NARMS-TAC 2002. Mining Innovation and Tech.*, 2002 Ed., Hammah, eds., Toronto, 267–273.

Holtz, R. D., and William D. Kovacs. (1981). *An Introduction to Geotechnical Engineering*. Prentice-Hall. Upper Saddle River, NJ: Print.

Igoe, D., Gavin, K., and O’Kelly, B. (2011). ”Shaft Capacity of Open-Ended Piles in Sand.” *J. Geotech. Geoenviron. Eng.*, 137(10), 903–913.

Kim, D., Bica, A. V. D., Salgado, R., Prezzi, M., and Lee, W. (2009). “Load testing of a closed-ended pipe pile driven in multilayered soil.” J. Geotech. Geoenviron. Eng., 135(4), 463–473.

Krusinski, Laura. "Questions on Pile Tips and Rock Properties for Canadian Foundation Engr. Manual M." 31 July 2012. E-mail.

Kulhawy, F.H., and Mayne, P.W. (1990). Manual on estimating soil properties. Report EL-6800, Electric Power Res. Inst., Palo Alto.

Lai, Peter, and Kou, Ching L. (1994). “Validity of Predicting Pile Capacity by Pile Drving Analyzer.” *International Conference on Design and Construction of Deep Foundations, Vol II*: Orlando, FL.

Lehane, B. M. , and Randolph, M. F. (2002). “Evaluation of a minimum base resistance for driven pipe piles in siliceous sand.” *Journal of Geotechnical and Geoenvironmental Engineering*, 128(3), 198–205.

Liao, S. S. C. and Whitman, R. V. (1986). “Overburden Correction Factors for SPT in Sand.” *Journal of Geotechnical Engineering*, American Society of Civil Engineers, 112(3), 373-377.

Linell, Kenneth A., and Shea, H. F. (1960). "Strength and Deformation Characteristics of Various Glacial Tills in New England." *Research Conference on Shear Strength of Cohesive Soils*, American Society of Civil Engineers, Boulder, CO, 275-314.

Long, James H., Bozkurt, Diyar, Kerrigan, John A., and Wysockey, Michael H. (1999). "Value of Methods for Predicting Axial Pile Capacity." *Transportation Research Record,* Transportation Research Board, (1663), 57-63.

Long, J., Kerrigan, J., and Wysockey, M. (1999). "Measured Time Effects for Axial Capacity of Driven Piling." *Transportation Research Record,* Transportation Research Board, (1663), 8-15.

Maine Department of Conservation. (2005). "Surficial Geologic History of Maine." *Maine Geological Survey: Surficial Geology of Maine*. <http://www.maine.gov/doc/nrimc/mgs/explore/surficial/facts/surficial.htm> (Sept., 13 2012).

Maine Department of Conservation. (2005). "Maine Geological Survey: Fossils Preserved in Maine Sediments - Marine Limit." *Maine Geological Survey: Fossils Preserved in Maine Sediments - Marine Limit*. <http://www.maine.gov/doc/nrimc/mgs/explore/fossils/sediment/marine-limit.htm>. (Sept., 13 2012).

Meyerhof, G.G. (1957). "Discussion on Research on Determining the Density of Sands by Spoon Penetration Testing." *Proceedings, Fourth International Conference on Soil Mechanics and Foundation Engineering*, London, 3, 110.

Meyerhof, G.G. (1976). "Bearing Capacity and Settlement of Pile Foundations." *Journal of the Geotechnical Engineering Division*, American Society of Civil Engineers, 102 (GT3), 195-228.

Navfac. (1986). *DM-7.01 Soil Mechanics*, Dept of Navy.

Navfac. (1986). *DM-7.02 Foundations & Earth Structures*, Dept of Navy.

Nordlund, R.L. (1963). "Bearing Capacity of Piles in Cohesionless Soils." *Journal of the Soil Mechanics and Foundations Division*, ASCE, SM3, 1-35.

Orrje, O. and Broms, B. B. (1967), "Effects of Pile Driving on Soil Properties." *Journal of Soil Mechanics and Foundations Division*, ASCE, 93 (SM5), 59-73.

Paik, K. H. , and Salgado, R. (2003). "Determination of the bearing capacity of open-ended piles in sand." *J. Geotech. Geoenviron. Eng.*, 129 (1), 46-57.

Paik, K. , Salgado, R. , Lee, J. , and Kim, B. (2003). "Behavior of open- and closed-ended piles driven into sands." *J. Geotech. Geoenviron. Eng.*, 129 (4), 296–306.

Poulos, H. G., and E. H. Davis. (1980).*Pile Foundation Analysis and Design*. Wiley, New York.

Raushe, F., Thendean, G., Abou-Matar, H., Likens, G. E., and Goble, G. G. (1997). "Determination of Pile Driveability and Capacity From Penetration Tests, Volume I: Final Report." FHWA-RD-96-179, Federal Highway Administration, McLean, VA.

Raushe, F., Thendean, G., Abou-Matar, H., Likens, G. E., and Goble, G. G. (1997). "Determination of Pile Driveability and Capacity From Penetration Tests, Volume II: Appendixes." FHWA-RD-96-180, Federal Highway Administration, McLean, VA.

Raushe, F., Thendean, G., Abou-Matar, H., Likens, G. E., and Goble, G. G. (1997). "Determination of Pile Driveability and Capacity From Penetration Tests, Volume III: Literature Review, Data Base, and Appendixes." FHWA-RD-96-181, Federal Highway Administration, McLean, VA.

Rowe, R.K., and Armitage, H.H. (1987). "A Design Method for Drilled Piers in Soft Rock," *Canadian Geotechnical Journal*, Vol. 24, pp. 126-142.

R.W. Conklin Steel Supply. "HPile_Points." *RW Conklin Steel*, <http://www.conklinsteel.com/images/HPile_Points.pdf> (Mar. 11, 2013).

Sandford, Thomas C. (1989). "Evaluation of Dragdown on Pile," University of Maine Civil Engineering Department, Report GT 89-2, April 1989, pp. 55.

Sandford, Thomas C, and Amos, Jeannine. (1987). "Engineering Analysis of Gorham Landslide." *Proceedings of Geologic and Geotechnical Characteristics of the Presumpscot Formation Maine's Glaciomarine "Clay."* Maine Geological Survey, Morrison Geotechnical Engineering, University of Maine Civil Engineering Dept., University of Southern Maine Geosciences Dept., Augusta, ME, 1-28.

Schnitker, D., and Borns, H. W. (1987). "Depositional Environmental and Composition of the Presumpscot Formation." *Proceedings of Geologic and Geotechnical Characteristics of the Presumpscot Formation Maine's Glaciomarine "Clay."* Maine Geological Survey, Morrison Geotechnical Engineering, University of Maine Civil Engineering Dept., University of Southern Maine Geosciences Dept., Augusta, ME, 1-13.

Seo, H., Irem, Z.Y., and Prezzi, M. (2009). "Assessment of the axial load response of an H pile driven in multilayered soil." J. Geotech. Geoenviron. Eng., 135(12), 1789-1804.

Skov R, and Denver H. (1988). "Time-Dependence of Bearing Capacity of Piles." *Proceedings 3rd International Conference on Application of Stress-Waves to Piles,* 1-10.

Smith, Geoffrey W. (1985). "Chronology of Late Wisconsinan Deglaciation of Coastal Maine." *Late Pleistocene History of Northeastern New England and Adjacent Quebec*. Geological Society of America, Boulder, CO, 29-44.

Sowers, G. F. (1979). "Chapter 11, Deep Foundations." *Introductory Soil Mechanics and Foundations,* Macmillan, 505-568.

Svinkin, M.R., and Skov, R. (2002). “Setup effect of cohesive soils in pile capacity.” Vulcan Hammer.net, <http://www.vulcanhammer.net/svinkin/set.php> (Mar. 4, 2013)

Terzaghi, Karl, Ralph B. Peck, and Gholamreza Mesri. (1996). *Soil Mechanics in Engineering Practice*. Wiley, New York. Print.

Thompson, Woodrow B. (1987)."The Presumpscot Formation in Southwestern Maine." *Proceedings of Geologic and Geotechnical Characteristics of the Presumpscot Formation Maine's Glaciomarine "Clay,"* Maine Geological Survey, Morrison Geotechnical Engineering, University of Maine Civil Engineering Dept., University of Southern Maine Geosciences Dept., Augusta, ME, 1-22.

Thurman, A.G. (1964). “Discussion of Bearing Capacity of Piles in Cohesionless Soils.” *Journal of the Soil Mechanics and Foundations Division*, American Society of Civil Engineers, SM1, 127-129.

Tomlinson, M. J. (1957). "The Adhesion of Piles Driven in Clay Soils," Proc 4th Int Conf on Soil Mech and Found Eng, v 2, pp.66-71.

Turner, John P. (2006). “Rock-socketed Shafts for Highway Structure Foundations.” *NCHRP Synthesis 360*, Transportation Research Board, Washington, D.C.

Vesic, A. S. (1967). "A Study of Bearing Capacity of Deep Foundations," Final Rep., Proj. B-189,School of Civil Eng, Georgia Inst Tech.,Atlanta, Ga.

Vijayvergiya, V.N., and Focht, J.A., Jr. (1972). *A New Way to Predict Capacity of Piles in Clay*, Offshore Technology Conference Paper 1718, Fourth Offshore Technology Conference, Houston.

Wyllie, D.C. (1999). *Foundations on Rock*, 2nd ed., E&FN Spon, New York, N.Y., 401.

APPENDIX A: PILE TIP PROTECTION

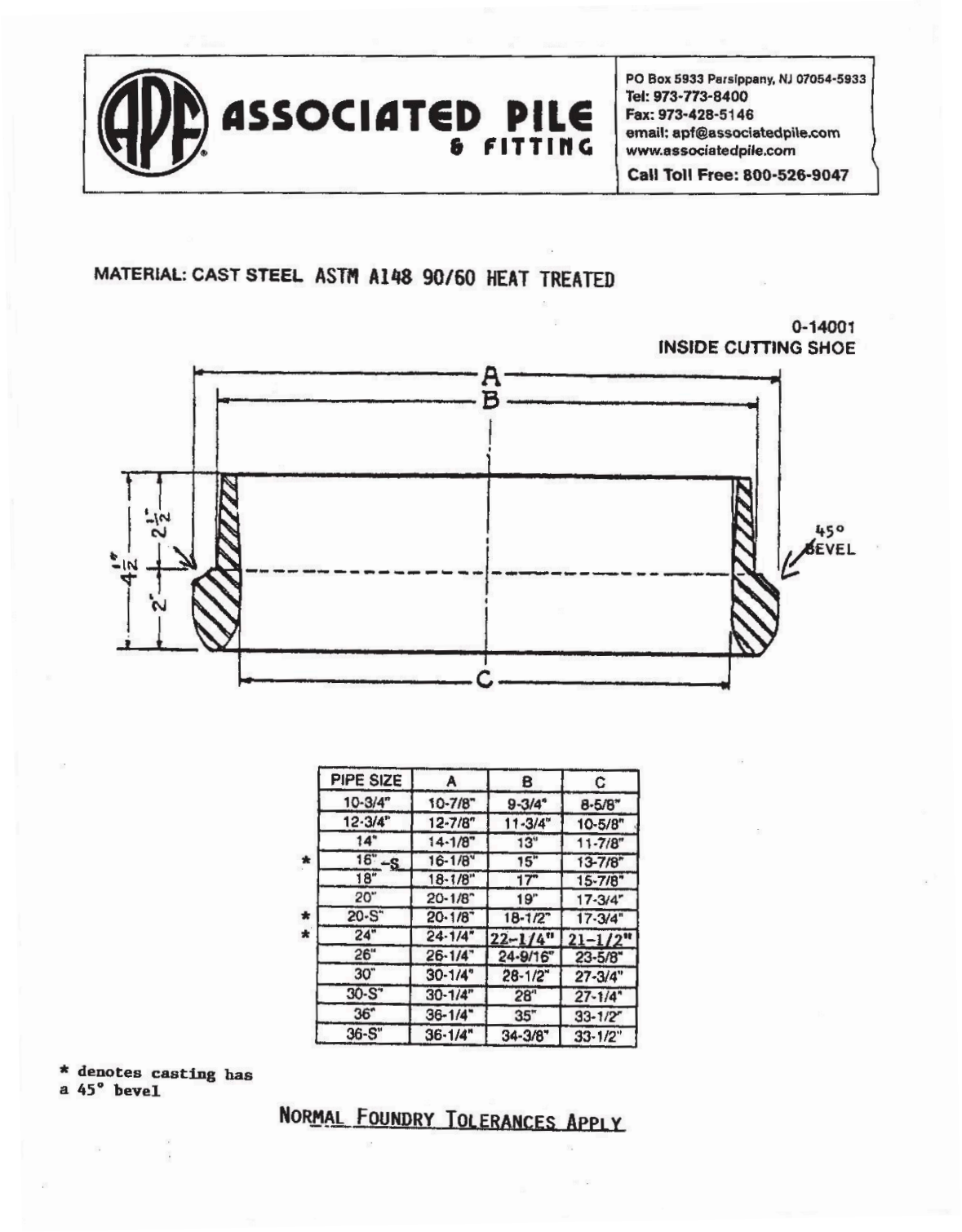

ASSOCIATED PILE & FITTING

PO Box 5933 Parsippany, NJ 07054-5933
Tel: 973-773-8400
Fax: 973-428-5146
email: apf@associatedpile.com
www.associatedpile.com
Call Toll Free: 800-526-9047

MATERIAL: CAST STEEL ASTM A148 90/60 HEAT TREATED

0-14001
INSIDE CUTTING SHOE

	PIPE SIZE	A	B	C
	10-3/4"	10-7/8"	9-3/4"	8-5/8"
	12-3/4"	12-7/8"	11-3/4"	10-5/8"
	14"	14-1/8"	13"	11-7/8"
*	16" -S	16-1/8"	15"	13-7/8"
	18"	18-1/8"	17"	15-7/8"
	20"	20-1/8"	19"	17-3/4"
*	20-S"	20-1/8"	18-1/2"	17-3/4"
*	24"	24-1/4"	22-1/4"	21-1/2"
	26"	26-1/4"	24-9/16"	23-5/8"
	30"	30-1/4"	28-1/2"	27-3/4"
	30-S"	30-1/4"	28"	27-1/4"
	36"	36-1/4"	35"	33-1/2"
	36-S"	36-1/4"	34-3/8"	33-1/2"

* denotes casting has a 45° bevel

NORMAL FOUNDRY TOLERANCES APPLY

Figure A-1: Pile Tip Protection for Open End Pipe Piles (APF 2012)

ASSOCIATED PILE & FITTING
PO Box 5933 Parsippany, NJ 07054-5933
Tel: 973-773-8400
Fax: 973-428-5146
email: apf@associatedpile.com
www.associatedpile.com
Call Toll Free: 800-526-9047

MATERIAL: CAST STEEL

P-13006
Inside Flange
Ribbed 60° Point

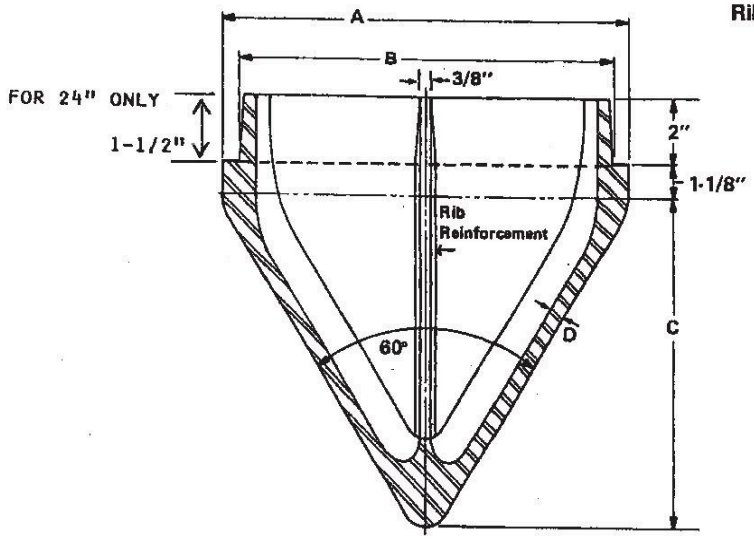

PIPE O.D.	A	B	C	D
8-5/8	8-3/4	7-1/2	7-1/8	1/2
9-5/8	9-3/4	7-1/2	7-1/8	1/2
10-3/4	10-7/8	9-3/4	9	1/2
12	12-1/8	11	10-3/8	1/2
12-3/4	12-7/8	11-3/4	10-3/4	1/2
13-3/8	13-1/2	11-11/16	11-3/8	1/2
14	14-1/8	13	11-13/16	9/16
16	16-1/8	15	13-1/2	9/16
18	18-1/8	17	15-1/4	5/8
20	20-1/8	19	17	5/8
22	22-1/8	21	18-7/8	5/8
24	24-1/8	22-3/8	20-3/8	5/8

Figure A-2: Driving Tip Dimensions for Closed End Pipe Piles (APF 2012)

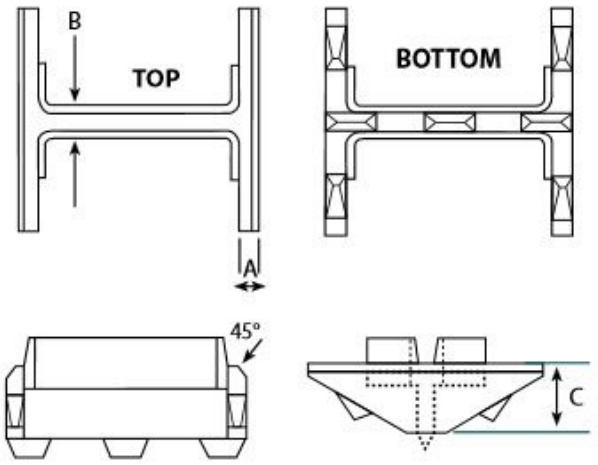

H-PILE POINT MODEL	A	B	C
14" HP			
77750-B	1"	1-1/4"	2-3/4"
12" HP			
77750-B	1"	1-5/16"	3"
7780-B	3/4"	3/4"	3-1/2"
10" HP			
77750-B	1"	1"	2-1/16"

Figure A-3: Driving Tip Dimensions for H-Piles (R.W. Conklin Steel Supply 2013)

APPENDIX B: PRESENTATION OF DYNAMIC TEST DATA

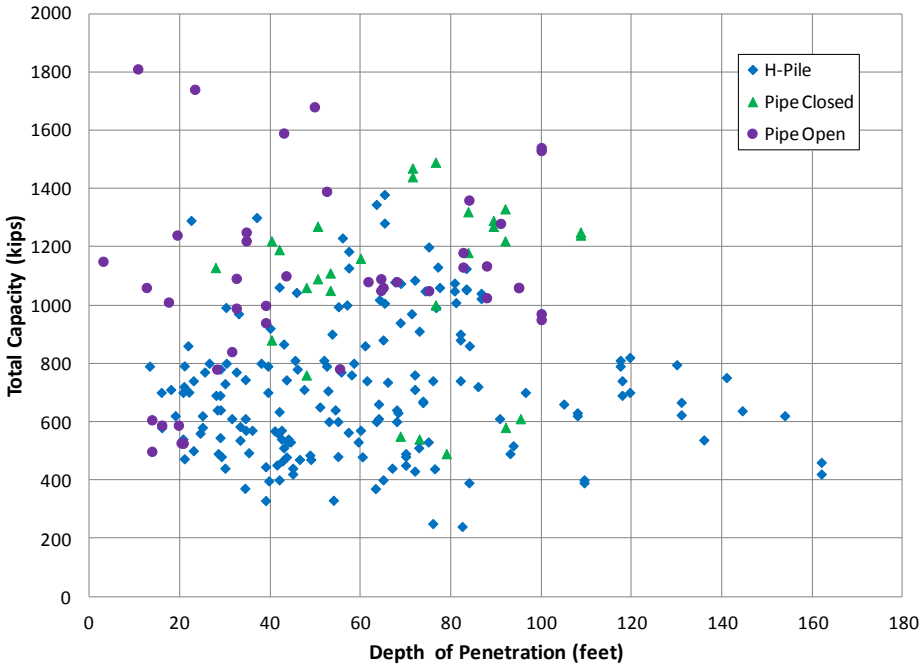

Figure B-1: Total Capacity of Piles on Bedrock

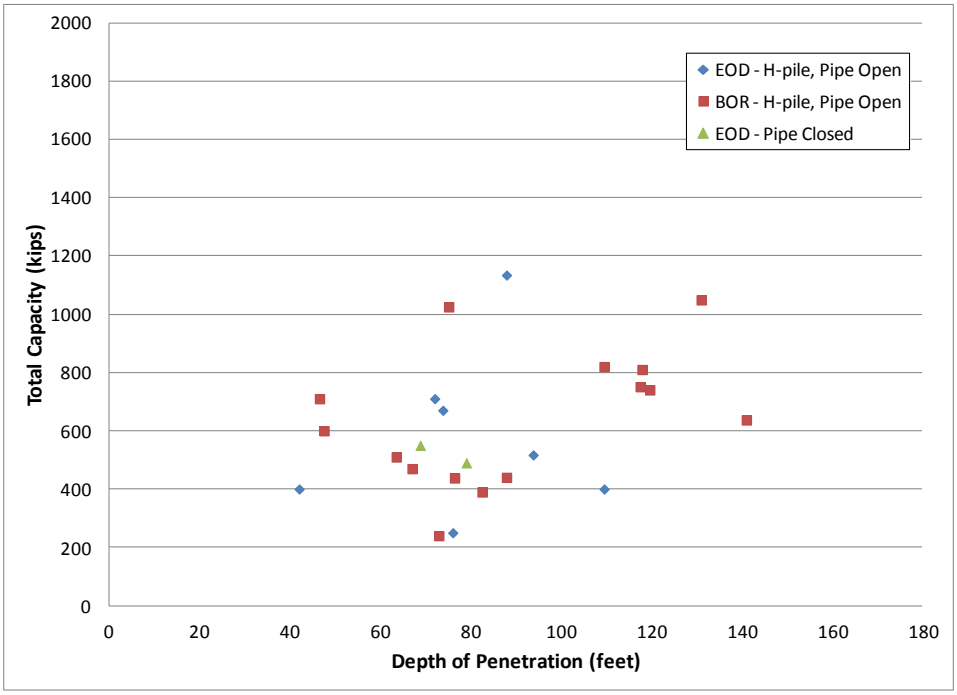

Figure B-2: Total Capacity for Piles Bearing in Till

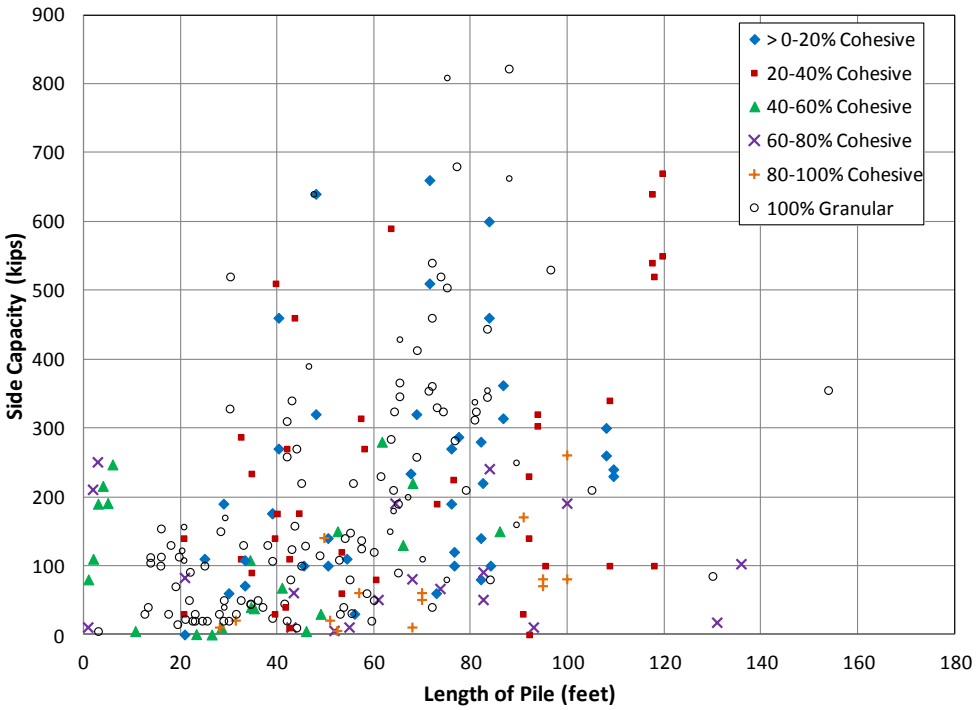

Figure B-3: Side Capacity of Piles within Cohesive Soil vs. Depth

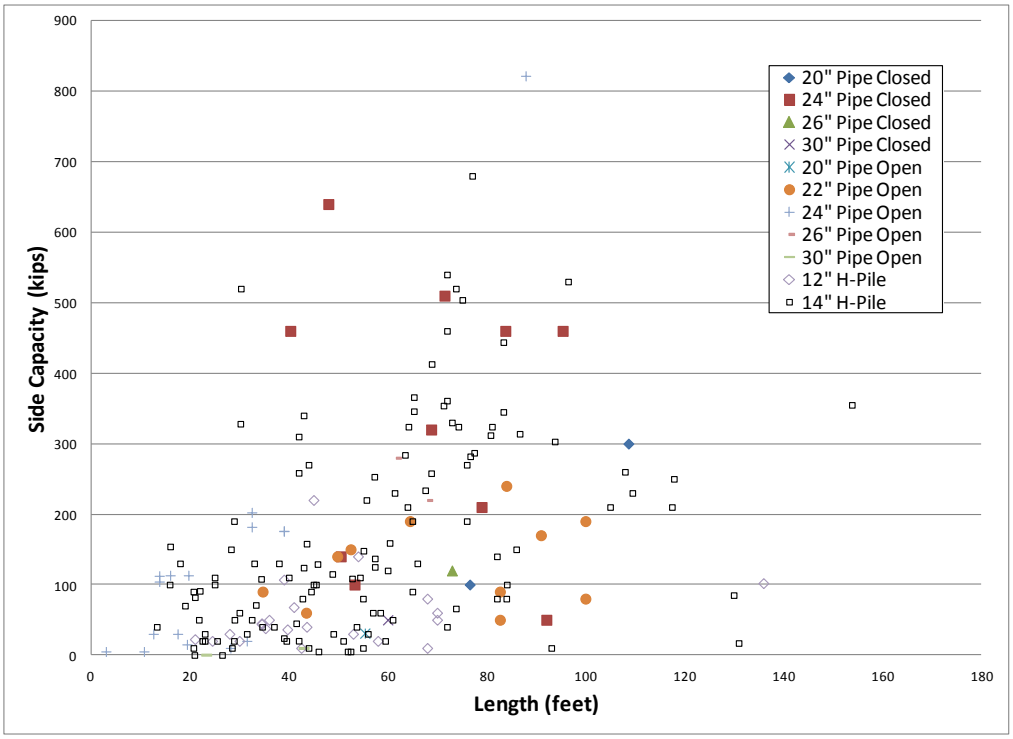

Figure B-4: Side Capacity of Piles by Pile Type vs. Depth

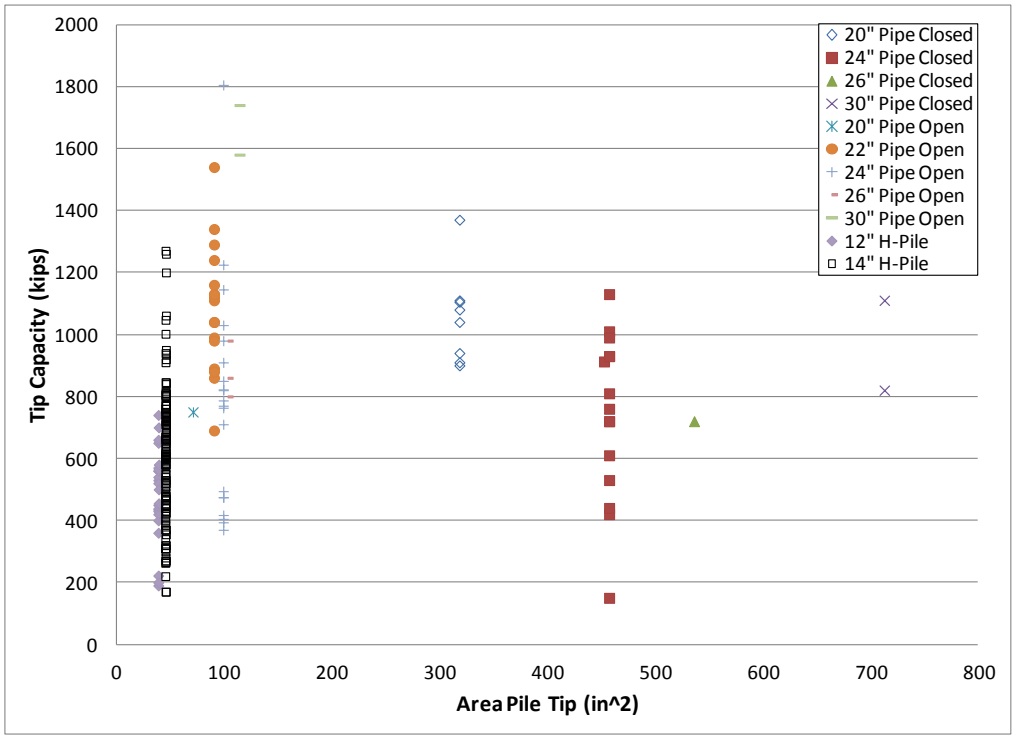

Figure B-5: Effects of Pile Tip Area on Bearing Capacity in Bedrock

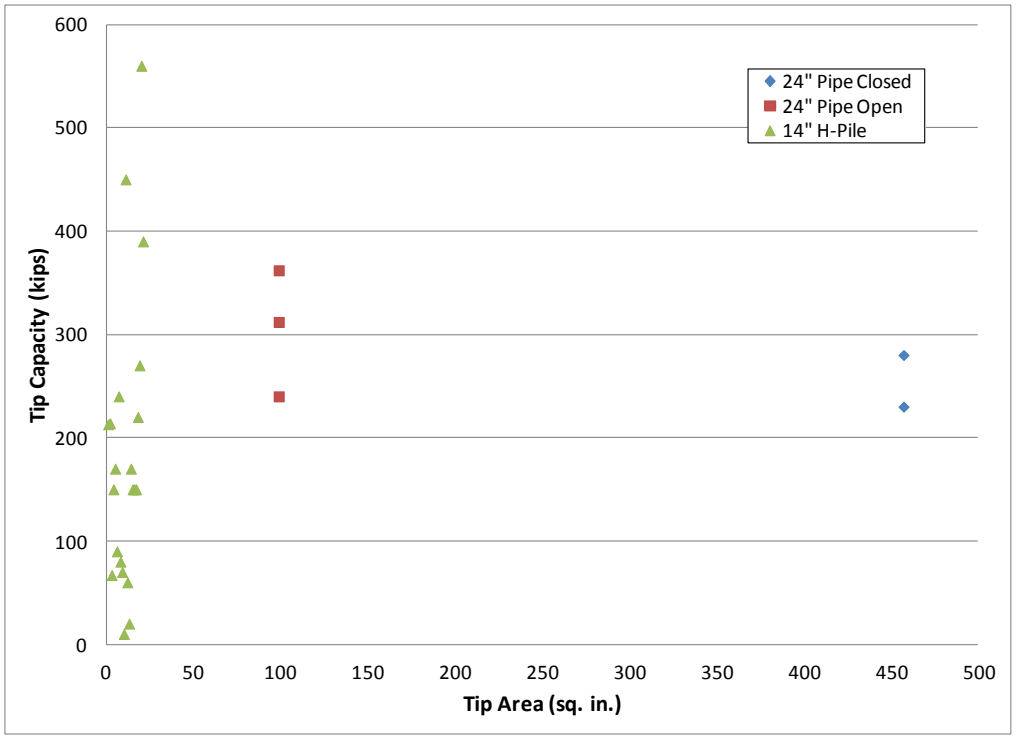

Figure B-6: Effects of Pile Tip Area on Bearing Capacity in Till

APPENDIX C: SAMPLE CALCULATIONS

Sample calculation shown below. The rest of the calculations are found in the disk jacket.

16716.00 Monmouth - Abutment 1- Pile 5

$P := 13.84in \cdot 2 + 14.7in \cdot 2 = 4.757ft$ Perimeter for HP14x89 pile

$V\_disp := 26.1in^2 \cdot \frac{1ft^2}{144in^2} = 0.181 \cdot \frac{ft^3}{ft}$ Volume of soil displaced per foot of pile

$R\_\delta\_\phi := .8$ Ratio of δ to Φ from Fig 9.10 (Hannigan et al, 2006a)

$\delta_{pm} := 20deg$ Soil-Pile friction angle (NAVFAC 1986)

$\omega := 0deg$ Pile taper from vertical

LAYER 1: Clay 0-67.9 feet (silty stiff clay)

$L\_1 := 67.9ft$ Thickness of Layer

$\sigma'_{v\_L1} := 2.120ksf$ Vertical effective stress

$S_{u\_L1} := .463ksf$

$S_{u\_L1rm} := .055ksf$ Remolded shear strength est. from (Andrews 1987)

$\phi_{f\_L1} := 35.6deg$ Friction angle at failure (Amos and Sandford 1987)

$\alpha\_L1 := 1$ α - method coefficient

$\alpha\_L1rm := 1$ α - method coefficient REMOLDED

$\beta\_L1 := .51$ β - method coefficient From Fig. 9.20 (Hannigan et al, 2006a)

$\lambda\_L1 := .18$ λ - method coefficient

$\alpha\_Qp\_L1 := (\alpha\_L1) \cdot S_{u\_L1} \cdot P \cdot L\_1 = 149.539kip$

$\alpha\_Qp\_L1rm := (\alpha\_L1rm) \cdot S_{u\_L1rm} \cdot P \cdot L\_1 = 17.764kip$

$\beta\_Qp\_L1 := (\beta\_L1) \cdot \left(\sigma'_{v\_L1}\right) \cdot P \cdot L\_1 = 349.203kip$

$\lambda\_Qp\_L1 := (\lambda\_L1) \cdot \left[\sigma'_{v\_L1} + 2 \cdot \left(S_{u\_L1}\right)\right] \cdot P \cdot L\_1 = 177.082kip$

$\lambda\_Qp\_L1rm := (\lambda\_L1) \cdot \left[\sigma'_{v\_L1} + 2 \cdot \left(S_{u\_L1rm}\right)\right] \cdot P \cdot L\_1 = 129.643kip$

LAYER 2: Granular Layer 67.9-105 feet

$L\_2 := 105ft - 67.9ft = 37.1 \cdot ft$ Thickness of Layer

$N1\_60\_L2 := 7.9$ Corrected SPT value for granular material

$\phi_{f\_L2} := 30.5deg$ Friction angle at failure

$\delta_p := (R\_\delta\_\phi) \cdot (\phi_{f\_L2}) = 24.4 \cdot deg$ Friction angle between soil and pile

$\sigma'_{v\_L2} := 5.327ksf$ Vertical effective stress

$L' := 10 \cdot \frac{14}{12} ft = 11.667ft$ Meyerhof Limiting depth for Dr<30

$\sigma'_{v\_L'} := .729ksf$ Vertical effective stress when L>L'

$CF\_L2 := .9$ Correction factor when δ does not equal φf

$K_{\delta\_L2} := 10^{-\left[\frac{\log(.88)-\log(1.135)}{\log(.1)-\log(.2)} \cdot (\log(.1)-\log(.181))-\log(.88)\right]} = 1.094$ log linear interpolation for Kδ factor in Nordlund method from Table 9-4a (Hanniganet al, 2006a)

$K_{o\_L2} := .495 \cdot 1.75 = 0.866$ K value for Meyerhof's Eq. from Kulhawy and Mayne (1990)

$Nordlund\_Qp\_L2 := (K_{\delta\_L2}) \cdot (CF\_L2) \cdot (\sigma'_{v\_L2}) \cdot \frac{\sin(\delta_p + \omega)}{\cos(\omega)} \cdot P \cdot L\_2 = 382.422kip$

$Meyerhof\_SPT\_qp\_L2 := (N1\_60\_L2) = 7.9$ kPa

calculated is less than limiting value of 100 kPa (Hannigan et al, 2006a) so use calculated

$Meyerhof\_SPT\_QP\_L2 := Meyerhof\_SPT\_qp\_L2 \cdot .029ksf \cdot P \cdot L\_2 = 40.43kip$

$Meyerhof\_Prop\_Qp\_L2 := (K_{o\_L2}) \cdot (\sigma'_{v\_L'}) \cdot \tan(\delta_{pm}) \cdot P \cdot L\_2 = 40.561kip$

LAYER 3: Till Layer 105-141 feet

$L\_3 := 141ft - 105ft = 36 \cdot ft$ Thickness of Layer

N1_60_L3 not provided for till layer Corrected SPT value for granular material

$\phi_{f\_L3} := 38deg$ Friction angle at failure

$\delta_p := (R\_\delta\_\phi) \cdot (\phi_{f\_L3}) = 30.4 \cdot deg$ Friction angle between soil and pile

$\sigma'_{v\_L3} := 7.756ksf$ Vertical effective stress

$L' := 10 \cdot \frac{14}{12} ft = 11.667ft$ Limiting depth for Dr<30

$\sigma'_{v\_L'} := .729\text{ksf}$ Vertical effective stress when L>L'

$CF\_L3 := .9$ Correction factor when δ does not equal φf

$K_{\delta\_L3} := 10^{-\left[\frac{\log(1.48)-\log(1.79)}{\log(.1)-\log(.2)}\cdot(\log(.1)-\log(.181))-\log(1.48)\right]} = 1.742$ log linear interpolation for Kδ factor in Nordlund method from Table 9-4a (Hannigan et al, 2006a)

$K_{o\_L3} := 1.55\cdot 1.75 = 2.712$ K value for Meyerhof's Eq. from Kulhawy and Mayne (1990)

$Nordlund\_Qp\_L3 := (K_{\delta\_L3})\cdot(CF\_L3)\cdot(\sigma'_{v\_L3})\cdot\frac{\sin(\delta_p+\omega)}{\cos(\omega)}\cdot P\cdot L\_3 = 1.053\times 10^{3}\cdot\text{kip}$

$Meyerhof\_Prop\_Qp\_L3 := (K_{o\_L3})\cdot(\sigma'_{v\_L'})\cdot\tan(\delta_{pm})\cdot P\cdot L\_3 = 123.245\text{kip}$

END BEARING CALCULATIONS

Meyerhof General:

$At := 14\text{in}\cdot 14\text{in} = 196\cdot\text{in}^2$ Area of pile toe

$\gamma_{toe} := 135\text{pcf}$ Unit weight at pile toe

$L\_Bcrit := 1($ Critical Length to depth

$Ltot := 141\text{ft}$ Length of Pile

$B := 14\text{in}$ Width of pile

$cc := \frac{Ltot}{B} = 120.857$ Length to width ratio

$\phi_{bott} := 38\text{deg}$ Friction angle at bottom

since cc>L_Bcrit use Meyerhof limiting surcharge

$\sigma'_{bot} := \tan(\phi_{bott})\cdot\text{ksf} = 0.781\cdot\text{ksf}$

$Nq' := 23($ $N\gamma' := 26($

$Qt := At\cdot(\sigma'_{bot}\cdot Nq' + 0.5\cdot\gamma_{toe}\cdot B\cdot N\gamma') = 272.455\text{kip}$

Nordlund Method

$\alpha_t := 0.72$ coefficient

$Nq'_{nord} := 110$

$\sigma'_{v\_bott} := 7.756\,ksf$

since calculated stress is > limiting stress of 3.2 ksf use:

$\sigma'_{v\_bott\_lim} := 3.2\,ksf$

$Qp := \alpha_t \cdot Nq'_{nord} \cdot \sigma'_{v\_bott\_lim} \cdot At = 344.96\,kip$

$qL := 265\,ksf$

$Qp\_limit := qL \cdot At = 360.694\,kip$

use Qp

Meyerhof SPT

$N60 := 50$ from boring log

$CN := \left[\frac{1}{\left(\frac{\sigma'_{v\_bott}}{2000\,psf}\right)}\right]^{0.5} = 0.508$ correction factor

$N_{1\_60} := N60 \cdot CN = 25.39$

$Qpspt := At \cdot \left[\frac{0.8 \cdot N_{1\_60} \cdot (L\_3)}{B} \cdot ksf\right] = 853.111\,kip$

$QL := \left(8 \cdot N_{1\_60} \cdot ksf\right) \cdot At = 276.471\,kip$ Limiting value for sands